NATIONAL ADVISORY COMMITTEE FOR AERONAUTICS

WARTIME REPORT

ORIGINALLY ISSUED

July 1945 as
Memorandum Report L5F20

WIND-TUNNEL TESTS OF THE 0.15-SCALE POWERED MODEL OF THE FLEETWINGS XBTK-1 AIRPLANE LATERAL STABILITY AND CONTROL

By Kenneth W. Goodson and H. Norman Silvers

Langley Memorial Aeronautical Laboratory
Langley Field, Va.

NACA

WASHINGTON

NACA WARTIME REPORTS are reprints of papers originally issued to provide rapid distribution of advance research results to an authorized group requiring them for the war effort. They were previously held under a security status but are now unclassified. Some of these reports were not technically edited. All have been reproduced without change in order to expedite general distribution.

3 1176 01354 4375

MR No. L5F20

NATIONAL ADVISORY COMMITTEE FOR AERONAUTICS

MEMORANDUM REPORT

for the

Bureau of Aeronautics, Navy Department

WIND-TUNNEL TESTS OF THE 0.15-SCALE POWERED MODEL OF THE FLEETWINGS XBTK-1 AIRPLANE LATERAL STABILITY AND CONTROL

By Kenneth W. Goodson and H. Norman Silvers

SUMMARY

Tests were conducted in the Langley 7- by 10-foot tunnel on the 0.15-scale powered model of the Fleetwings XBTK-1 airplane to investigate the lateral stability characteristics.

The results of this investigation indicated that the effective dihedral, with a geometric dihedral of $8\frac{1}{4}^{\circ}$, was positive for all conditions except wave-off. In this condition, the model had negative effective dihedral at lift coefficients above 2.10. The negative values of effective dihedral were not decreased when the geometric dihedral was changed to 11°.

The directional stability was satisfactory for all conditions. Increasing the geometric dihedral generally decreased the directional stability.

The tests indicated that the airplane will probably not experience rudder lock.

Results of the rudder modification tests indicate that the positive variation of rudder hinge-moment coefficient with yaw, which may result in snaking of the airplane, may be reduced by either unsealing the rounded horn or removing the horn and sealing the gap.

The rudder effectiveness will probably be sufficient to trim the airplane with the wings level in any condition. In the wave-off condition, the rudder-tab deflection would be insufficient to trim the pedal force to zero at zero bank.

The aileron effectiveness will probably be satisfactory throughout the angle-of-attack range.

INTRODUCTION

At the request of the Bureau of Aeronautics, Navy Department, a series of tests was made in the Langley 7- by 10-foot tunnel of a 0.15-scale powered model of the Fleetwings XBTK-1 airplane. The investigation was conducted to provide data on the stability and control characteristics of the model. The longitudinal stability and control results of this investigation are presented in reference 1. The present report includes the results of tests made to determine the lateral stability and control characteristics of the model. From the results of these tests the probable flying qualities of the airplane may be estimated.

COEFFICIENTS AND SYMBOLS

The results of the tests are presented as standard NACA coefficients of forces and moments. Rolling-, yawing-, and pitching-moment coefficients are given about the center-of-gravity location shown in figure 1 (25.6 percent of the mean aerodynamic chord). The data are referred to a system of axes in which the Z-axis is in the plane of symmetry and perpendicular to the relative wind, the X-axis is in the plane of symmetry and perpendicular to the Z-axis, and the Y-axis is perpendicular to the plane of symmetry.

The coefficients and symbols are defined as follows:

C_L lift coefficient (Z/qS)

C_{D_R} resultant-drag coefficient (X/qS)

C_Y lateral-force coefficient (Y/qS)

C_l rolling-moment coefficient (L/qSb_w)

C_m pitching-moment coefficient (M/qSc)

C_n yawing-moment coefficient (N/qSb_w)

C_h hinge-moment coefficient $(H/qb\bar{c}^2)$

T_c' effective thrust coefficient (T_e/qS)

nD/V propeller diameter-advance ratio

η propulsive efficiency $(T_eV/2\pi nQ)$

Q_c torque coefficient $(Q/\rho V^2D^3)$

where the quantities are defined below and in figure 2

$\left.\begin{matrix}X\\Y\\Z\end{matrix}\right\}$ forces along axes, pounds

$\left.\begin{matrix}L\\M\\N\end{matrix}\right\}$ moments about axes, pound-feet

H hinge moment of a control surface, pound-feet

Q torque, pound-feet

T_e effective thrust, pounds

q dynamic pressure $(\rho V^2/2)$, pounds per square feet

S wing area (8.55 sq ft on model)

c wing mean aerodynamic chord (1.22 ft on model)

$\bar{c}$ root mean square chord of a control surface back of hinge line, feet

b_w wing span (7.33 ft on model)

b span of control surface, feet

V air velocity, feet per second

D propeller diameter (2.04 ft on model)

n revolutions per second

W weight of the airplane, pounds

and

ρ mass density of air, slugs per cubic foot

α angle of attack of thrust line, degrees

i_w wing setting with respect to thrust line (2° on model)

ψ angle of yaw, degrees

δ control surface deflection, degrees

β propeller blade angle at 0.75 radius (18°)

Γ_e effective dihedral, degrees

Γ_o geometric dihedral, degrees

Subscripts:

a aileron (a_r, a_l, right and left aileron)

w wing

r rudder

f flap

t tab

ψ denotes partial derivative of a coefficient with respect to yaw $\left(\text{example: } C_{l_\psi} = \frac{\partial C_l}{\partial \psi}\right)$

MODEL AND APPARATUS

The XBTK-1 airplane is a single-place single-engine, carrier-based, dive and torpedo bomber with a full cantilever low wing. It has partial-span, extensible slotted flaps, "picket-fence" dive brakes, adjustable

stabilizer, and a fully retractable conventional landing gear. At the design gross weight, the airplane carries a radar unit under the right wing panel and an auxiliary droppable fuel tank under the left wing panel in addition to one 1000-pound bomb under the fuselage. The rudder is aerodynamically balanced by a combination of an overhang balance, a horn, and a tab. The balance tab has a deflection rate of 0.51 of the rudder deflection and may also be hand-cranked to a maximum deflection of ±5° for trimming. Each aileron is aerodynamically balanced by an internal sealed balance and a spring tab. The balance area is 41 percent of the aileron area. A summary of the physical characteristics of the airplane is presented in tables I, II, and III.

The model was furnished by the Fleetwings Division of the Kaiser Cargo Corporation. A three-view drawing of the 0.15-scale model is shown in figure 1 and photographs of the model are given in figures 3(a), 3(b), and 3(c). Small wooden dowels were placed in the leading edge of the wing (18.09 in. from the center line) to simulate cannon on the airplane.

The model was equipped with a slotted extensible type of landing flap which extends across the fuselage (figs. 3 and 4(a)) with a 22.5-percent chord and a 43.1-percent span. The center and the outer flaps can be operated separately. Special fittings were supplied for changing the geometric dihedral.

The dive brakes (figs. 3(c) and 4(b)), which are of the picket-fence type, are mounted on the upper and lower surfaces of the center wing panel near the trailing edge. The hinge line of the upper surface brake is located at the trailing edge. The hinge line of the lower dive brake is, however, located at the leading edge of the lower brake in the conventional manner. The dive brakes on the airplane are linked together in such a manner as to reduce the total hinge moment of the system.

The vertical tail has a modified NACA 66,2-015 root section and a modified NACA 65,2-009 theoretical tip section. The modification consisted of replacing the cusp trailing edge with a straight line fairing tangent to the airfoil contour at the 0.70-chord section. The rudder had an area of 30.5 percent of the vertical tail and was mass-balanced. The model was tested with several

modifications of the vertical tail as shown in figure 5. The rudder was first modified by rounding the lower surface of the horn balance. It was further modified by making hinge cut-outs in the balance and in the seal (modification 3). The rudder was sealed up to the horn. The data presented herein are based upon the above modifications (fig. 6) since these modifications represent the prototype airplane. A further modification was made by removing the horn.

The aileron on the model, which was located outboard of the center wing panel, had a span 54 percent of the wing semispan. The aileron was of constant percentage chord $\left(\frac{c_a}{c_w} = 0.20\right)$. All tests reported herein were made with an aileron seal of cellulose tape. No provisions were made on this model for the measurement of aileron hinge moments.

The model was equipped with a 2.04-foot-diameter propeller with blades set at 18° and was powered by a 56-horsepower induction motor. The propeller speeds were determined by a small alternator tachometer and a cathode-ray oscillograph combination.

The model configurations referred to in the text and on the figures are as follows:

1. Cruising configuration
   - Flaps neutral
   - Landing gear retracted
   - Fuel tank on left wing
   - Radar on right wing

2. Landing configuration
   - Flaps deflected (45°)
   - Landing gear extended
     - (a) Main wheels down
     - (b) Wheel-well cut-outs in wing open
     - (c) Tail wheel down
     - (d) Tail-wheel door open
     - (e) Arresting hook extended
   - Fuel tank on left wing
   - Radar on right wing

3. Diving configuration
   Upper dive flaps deflected (73°)
   Lower dive flaps deflected (80°)
   Center flap deflected (45°)
   Landing gear retracted
   Radar on right wing

The rudder, rudder-tab, and aileron deflections were set by means of templets to ±0° 30'. Flap and dihedral fittings were supplied by the manufacturer. Strain gages and strain-gage fittings were constructed and installed by the Langley Laboratory.

TESTS AND RESULTS

Test conditions.- The tests were made at dynamic pressures of 9.21 and 16.37 pounds per square foot, corresponding to airspeeds of about 60 and 80 miles per hour. The test Reynolds numbers were about 685,000 and 910,000 based on the wing mean aerodynamic chord of 1.22 feet. Because of the turbulence factor of 1.6 for the tunnel, effective Reynolds numbers (for maximum lift coefficient) were about 1,100,000 and 1,460,000.

Test procedure.- The model propeller was calibrated by measuring the resultant drag of the model in the cruising condition at zero angle of attack for a range of propeller speeds. The thrust coefficients were determined from the relation

$$T_c' = C_D - C_{D_R}$$

where C_D is the drag of the model with the propeller removed. The torque coefficient Q_c was computed from the motor calibration chart (torque as a function of minimum current) using the minimum current of the motor for each propeller speed. The propeller calibration is presented as a function of nD/V (fig. 7). The variation of lift coefficient with thrust coefficient for the airplane is presented in figure 8(a). With the aid of these two figures, a propeller speed required to simulate the specified power condition may be determined for a particular tunnel speed. All tests reported herein were made at thrust coefficients simulating take-off power on the prototype airplane. The torque coefficient

of the model, as a function of lift coefficient, was in good agreement with the torque coefficient of the airplane (fig. 8(b)). All tests simulating windmilling power were made at a thrust coefficient of -0.010.

Corrections.- All data have been corrected for tares caused by the model support strut. Jet-boundary corrections have been applied to the angles of attack, the drag coefficient, and the tail-on pitching-moment coefficients.

Presentation of data.- The results of the lateral stability investigation made on the 0.15-scale model of the XBTK-1 airplane are presented in the following figures:

	Figure no.
A. Rudder-fixed stability:	
1. Lateral stability parameters	9
2. Lateral stability characteristics in yaw . .	10
B. Rudder-free stability	11
C. Control characteristics:	
1. Effect of rudder modification on the aerodynamic characteristics in yaw	12
2. Effect of rudder deflection on the aerodynamic characteristics in	
(a) Yaw	13 and 14
(b) Pitch	15
3. Effect of rudder-tab deflection on the aerodynamic characteristics in yaw	16
D. Aileron characteristics in pitch	17 and 18

DISCUSSION

Rudder-Fixed Stability

Effective dihedral.- The effective dihedral with the original geometric dihedral angle of $8\frac{1}{4}^{\circ}$ was positive for all conditions except for the take-off power, landing configuration where it becomes negative above a lift

coefficient of about 2.1. The effective dihedral for the high-speed condition was fairly high (8.7°). This value was obtained from figure 9 by using the theoretical value for $\partial C_l/\partial\psi$ of 0.00023 per degree of effective dihedral (reference 2). A comparison of tail-off and tail-on data shows that the vertical tail has a large positive effect on the effective dihedral for all configurations and powers. Because of the large incremental change in rolling moment with rudder deflection (fig. 13), the slope of the rolling-moment curve will become less positive or more negative when the model is trimmed in yaw; therefore, the effective dihedral will be decreased. The effective dihedral for the trimmed wave-off condition (take-off power, landing configuration) is about -3.5° to -4.0° at a lift coefficient of about 2.06 (fig. 13(e)); however, figure 9(d) indicates that the effective dihedral will probably be decreased at higher lift coefficients. In an effort to increase the effective dihedral in the wave-off condition, it was decided to increase the geometric dihedral angle to 11°. Calculations by the method of reference 2 indicated that C_{l_ψ} should be increased by 0.00048 when the geometric dihedral of the outer panels was changed from $8\frac{1}{4}°$ to 11°. The measured positive increase in C_{l_ψ} corresponded very closely to the calculated value in all conditions except for the wave-off condition at lift coefficients above 2.28 for which case the effective dihedral was actually reduced (fig. 9(d)). The explanation for this negative increase in effective dihedral is not known at present; however, similar results have been observed on another model tested in the Langley 7- by 10-foot tunnel. Good agreement in C_{l_ψ} was obtained between the data from yaw-range tests (fig. 13) and those from pitch tests made at $\psi = \pm 5°$ (fig. 9).

Directional stability.- The test data indicated that the model was very stable directionally for all conditions; the value of C_{n_ψ} was always greater than -0.0015. Lowering the flaps (fig. 9(c) and 9(d)) generally increased the directional stability throughout the lift range. The directional stability did, however, decrease somewhat as the lift increased in the landing condition. The directional stability increases in all conditions when power is applied (fig. 9). This increase is most pronounced in the wave-off condition (take-off power, landing configuration). The

parameter C_{n_ψ} determined from tests made through the yaw range agree well with the C_{n_ψ} of lateral stability parameter tests. The directional stability parameter obtained from yaw tests is tabulated below for the sake of comparison for various model configurations and power conditions.

Figure no.	Model configuration	α	C_L	Power	$\partial C_n / \partial \psi$ $\delta_r = 0$	
					Tail-on	Tail-off
13(a)	Cruising	11.0	1.14	Windmilling	-0.00187	0.00080
13(b)	Cruising	-.5	.23	Take-off	-.00208	.00068
13(c)	Cruising	7.7	1.03	Take-off	-.00280	.00112
13(d)	Landing	10.5	1.63	Windmilling	-.00220	.00080
13(e)	Landing	10.0	2.06	Take-off	-.00590	.00049
14	Dive	1.0	.15	Windmilling	-.00212	--------

Increasing the geometric dihedral angle to 11°, in general, decreased the directional stability. For the wave-off conditions, C_{n_ψ} was increased slightly at lift coefficients above 2.22 when the geometric dihedral was increased.

Lateral force.- The positive values of C_{Y_ψ} for all conditions indicate that the airplane will have right sideslip with right bank and vice versa. The tail increases the positive value of C_{Y_ψ} as shown by comparing tail-on and tail-off data.

Pitching moment due to yaw.- The data of figure 13 indicate substantial changes in pitching moment with yaw for the power-on conditions. However, estimations indicate that less than 1° change in elevator deflection would be sufficient to trim the pitching moments resulting from a change in rudder deflection of ±5°

Rudder-Free Stability

Rudder-free characteristics.- The rudder-free characteristics for the most critical conditions were obtained from data of figures 13 and 16. These rudder-free data were obtained by taking into consideration the balance-tab deflection and a trim-tab deflection of 5°. Curves are presented also considering only a trim-tab deflection of 5°. From preliminary calculations, trim-tab deflections of 5° and 15° were required for the take-off power cruising configuration and the take-off power landing configuration, respectively; however, since only ±5° of trim-tab deflection was provided for on the prototype airplane, the rudder-free curves were determined for this value. The results (fig. 11) indicate that the airplane will probably not have rudder lock; however, there is a tendency for rudder lock at both negative and positive yaw values of about 10° to 15°. A comparison of the results obtained with the balance tab locked and operating indicates that the rudder-lock tendency is aggravated by balance-tab deflection. The rudder-free characteristics with the balance tab locked are comparable to those of a spring tab. It is thought that by using a spring tab to obtain aerodynamic balance of the rudder the trend toward rudder lock may be reduced.

CONTROL CHARACTERISTICS

Rudder modifications.- The original rudder horn had a flat under surface. It was thought that this might lead to early compressibility effects. Also, it was noted from preliminary tests that with the original rudder C_{h_ψ} was positive. Since snaking of the airplane may result from this aerodynamic characteristics of the rudder, it was desired to determine the effect of various modifications (fig. 4(a)) in reducing the positive value of C_{h_ψ}. Results of rudder tests conducted through the yaw range (fig. 12) indicate that C_{h_ψ} may be appreciably reduced by either unsealing the rounded horn or removing the horn and sealing the rudder gap. The latter modification reduces C_{h_ψ} to approximately zero. The effectiveness of the rudder was increased by rounding the under surface of the horn (modification 1). The other modifications decreased the effectiveness.

A comparison of the results of the rudder modifications at small rudder deflections is presented in the following table.

Rudder modification	$\partial C_n/\partial \delta_r$	$\partial C_h/\partial \psi$	$\partial C_h/\partial \delta_r$
Original	-0.00156	0.0031	-0.0024
1	-.00185	.0027	-.0024
2	-.00105	.0018	-.0016
3	-.00163	.0027	-.0030
4	-.00142	.0009	-.0025
5	-.00138	0	-.0035

The increment of C_{h_ψ} obtained when the horn was removed (approximately -0.0027) (figs. 12(d) and 12(f)) checked closely with the estimated value (-0.0021) using data of reference 3.

The rudder modifications have very little effect on the cross-wind and rolling-moment coefficients.

Rudder and rudder-tab characteristics.- The rudder (modification 3) and rudder-tab effectiveness as determined from figures 13, 14, and 16 are presented in the following table:

Model configuration	α	C_L	Power	$\partial C_n/\partial \delta_r$ $\psi = 0$	$\partial C_{h_r}/\partial \delta_t$ $\psi = 0$
Cruising	11.0	1.14	Windmilling	-0.00153	-0.00265
Cruising	-.5	.23	Take-off	-.00163	-.00340
Cruising	7.7	1.03	Take-off	-.00231	-.00600
Landing	10.5	1.63	Windmilling	-.00155	-.00334
Landing	10.0	2.06	Take-off	-.00311	-.00950
Dive	1.0	.15	Windmilling	-.00142	--------

The rudder and rudder-tab effectiveness are greatly increased with take-off power in the landing configuration.

Preliminary calculations indicate that there will probably be sufficient rudder effectiveness to trim the airplane in yaw with the wings level for any condition. Further estimations indicate that there is sufficient trim-tab deflection to trim the pedal force to zero with the wings level except for the wave-off condition.

The rudder hinge-moment coefficient does not show an appreciable change in the dive configuration as compared with that of the cruising configuration.

A positive rudder-tab deflection of 10° (fig. 15) has a small constant effect (-0.003) on the yawing moment throughout the lift range for the take-off power, cruising configuration. The rudder hinge moment resulting from a 10° tab deflection (zero rudder) will overbalance the hinge moment caused by 10° of rudder deflection (zero tab). The lateral force is reasonably constant throughout the pitch range.

Aileron characteristics.- The aileron characteristics were obtained from tail-off tests for two model configurations (cruising and landing). The results of these tests (figs. 17 and 18) indicate that the effectiveness of the control surface is very good throughout the angle-of-attack range. Flap deflection has no appreciable effect upon this condition. Preliminary calculations from unpublished data indicate that the required helix angle of 0.08 may be obtained by the airplane in either the landing or high-speed conditions.

The adverse yaw resulting from aileron deflection is increased when the flap is deflected.

CONCLUSIONS

The results of wind-tunnel tests to determine the lateral stability and control characteristics of the XBTK-1 airplane indicate that the following conclusions may be drawn:

1. The effective dihedral was positive for all conditions except wave-off where it was negative at lift coefficients above 2.10. The negative effective dihedral for this condition was greater when the geometric dihedral angle of the outer panel was changed from $8\frac{1}{4}^{\circ}$ to 11°.

2. The directional stability should be satisfactory for all flight conditions. Increasing the geometric dihedral angle generally decreased the directional stability.

3. The positive values of C_{Y_ψ} for all conditions indicate that the airplane will have right sideslip with right bank, and vice versa.

4. The estimated rudder-free characteristics indicate that there will probably be no rudder lock although snaking of the airplane may result from the positive variation of rudder hinge moment with angle of yaw with the horn balance in place.

5. The variation of rudder hinge moment with angle of yaw was reduced to approximately zero when the horn was removed. The rudder effectiveness was increased when the horn was rounded but was decreased when the gap was unsealed, when hinge cut-outs were made in the seal and balance, and when the horn was removed.

6. Estimations indicate that there is probably sufficient rudder effectiveness to trim the airplane with wings level and, except for the wave-off condition, there is sufficient tab deflection to trim the pedal force to zero with wings level.

7. The effectiveness of the aileron should be satisfactory through the angle-of-attack range. The adverse yaw resulting from aileron deflection is increased when the flap is deflected.

Langley Memorial Aeronautical Laboratory
National Advisory Committee for Aeronautics
Langley Field, Va.

REFERENCES

1. Weil, Joseph, and Boykin, Rebecca I.: Wind-Tunnel Tests of the 0.15-Scale Powered Model of the Fleetwings XBTK-1 Airplane. Longitudinal Stability and Control. NACA MR No. L5D27a, 1945.

2. Pearson, Henry A., and Jones, Robert T.: Theoretical Stability and Control Characteristics of Wings with Various Amounts of Taper and Twist. NACA Rep. No. 635, 1938.

3. Lowry, John G., Maloney, James A., and Garner, I. Elizabeth: Wind-Tunnel Investigation of Shielded Horn Balances and Tabs on a 0.7-Scale Model of XF6F Vertical Tail Surface. NACA ACR No. 4C11, 1944.

TABLE I

DESCRIPTION OF FLEETWINGS XBTK-1 AIRPLANE

Name and type	XBTK-1 (Navy dive-torpedo bomber)
Engine	Pratt & Whitney R-2800-22W
Ratings:	
Normal power	1700 bhp at 2600 rpm at sea level 1700 bhp at 2600 rpm at 7000 ft 1450 bhp at 2600 rpm at 18,500 ft
Take-off power . .	2100 bhp at 2800 rpm at sea level
Military power . .	2100 bhp at 2800 rpm at 1000 ft 1600 bhp at 2800 rpm at 16,000 ft
Propeller	Hamilton Standard
Diameter, ft	13.58
Blades (number and designation)	four, 2C15B1
Gear ratio	0.45
Activity factor	95.6
Blade thickness $(h/b)_{0.75R}$	0.060
Normal gross weight, lb	14,850
Over-all length, ft	39.0
Over-all height, ft	11.86
Wing span, ft	48.67

NATIONAL ADVISORY
COMMITTEE FOR AERONAUTICS

TABLE II

AIRPLANE WING AND TAIL-SURFACE DATA

	Wing	Horizontal tail	Vertical tail
Area, sq ft	380	80	[a]51.25
Span, ft	48.67	18.5	8.54
Aspect ratio	6.23	4.26	1.42
Taper ratio	.50	.59	----------
Dihedral, deg	8.25	0	----------
Incidence, deg	2	2 to -7	0
Geometric twist, deg	-2.2	0	0
Root section	NACA 2416	NACA 66,2-015 Modified	NACA 66,2-015 Modified
Tip section	NACA 4412	NACA 66,2-009 Modified	NACA 65,2-009 Modified
Mean aerodynamic chord, ft	8.17	----------	----------
Root chord, ft	9.17	5.45	6.89
Theoretical tip chord, ft	4.585	3.20	2.67

[a]Includes dorsal fin.

NATIONAL ADVISORY
COMMITTEE FOR AERONAUTICS

TABLE III

AIRPLANE CONTROL-SURFACE DATA

	Ailerons	Elevators	Rudder	Flaps	Dive brakes
Percent span	54.0	95.0	100	43.1	Upper 31.4 Lower 35.1
Area, aft of hinge line, sq ft	36.86	22.50	15.66	42.0	
Balance area, sq ft	15.11	2.96	[a]5.02	-----	----------
Trim-tab area, sq ft	[b].52	None	1.00	-----	----------
Percent span	2.8	----------	23.0	-----	----------
Tab travel, deg	±15	----------	±5	-----	----------
Balance tab area, sq ft	2.76	3.36	1.00	-----	----------
Percent span	13.3	35.7	23.0	-----	----------
Tab travel, deg	±15(±30 lb)	±15(±55 lb)	±15(δ_t=-0.51δ_r)	-----	----------
Control travel, deg	±15	15, -25	±30	45	[c]Upper 73 Lower 80
Root mean square chord, ft	1.37	1.27	1.90	2.06	Upper 1.45 Lower 1.55
Distance to hinge line from normal c.g. (25.6), ft	----------	22.00	23.67	-----	----------

[a]1.20 sq ft horn.
[b]Left aileron only.
[c]Measured from aileron contour.

Flap deflections (corresponding powers)	
Landing, deg	45 (power off)
Cruising, deg	flaps retracted
Diving, deg . .	(center flap) 45

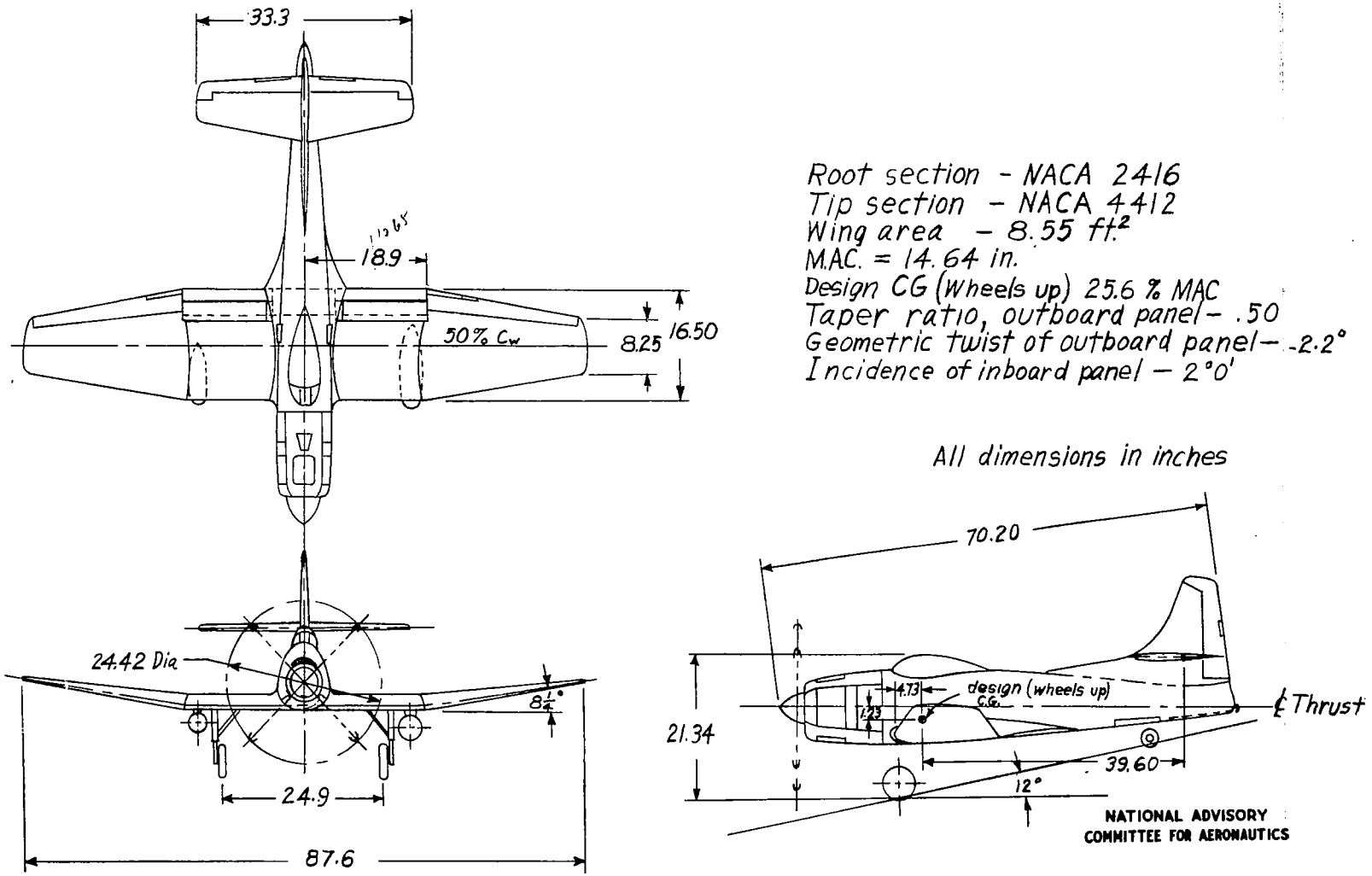

Figure 1 .- Three view drawing of 0.15-scale model of Fleetwings XBTK-1 airplane.

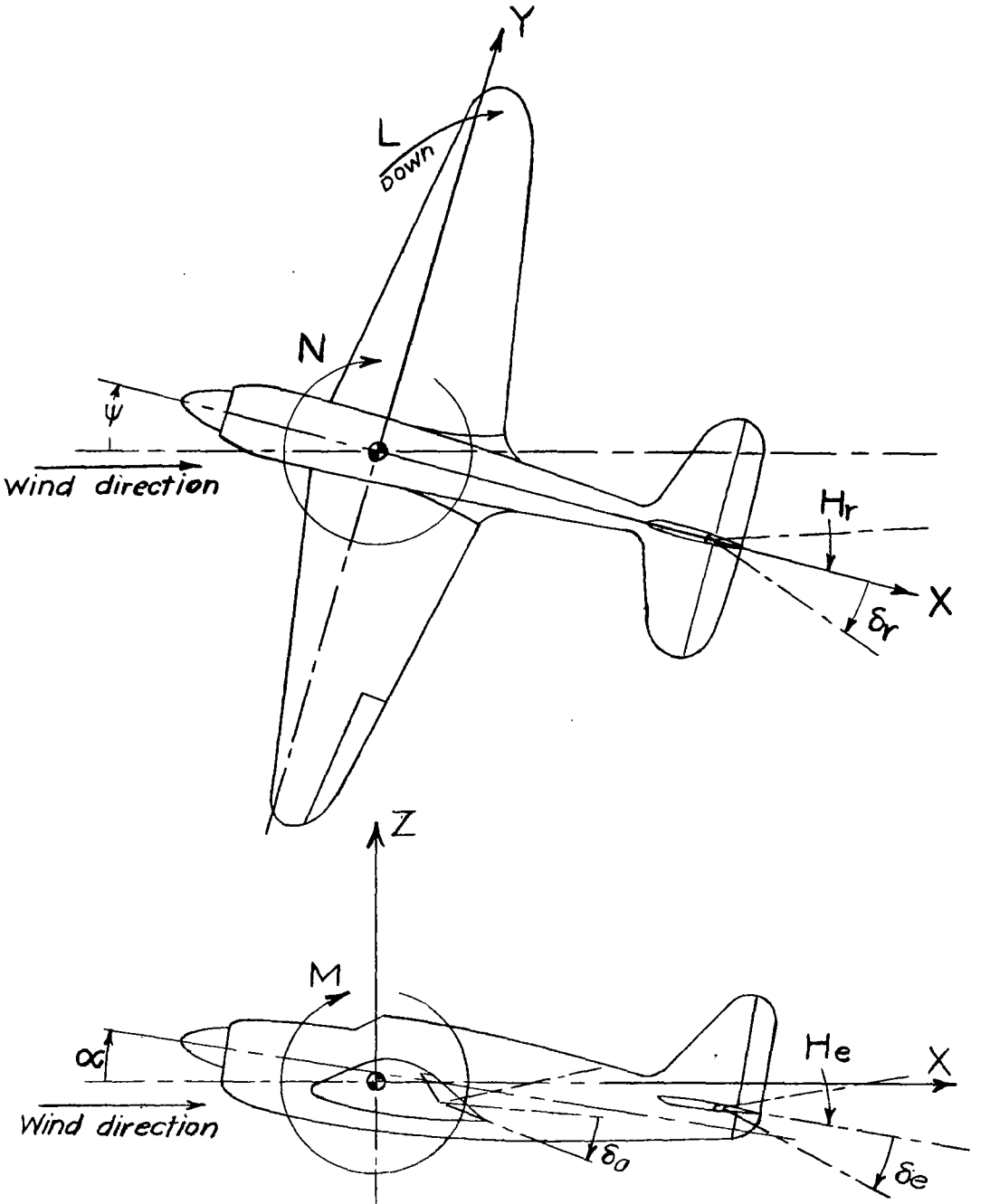

NATIONAL ADVISORY
COMMITTEE FOR AERONAUTICS

Figure 2.- Notation of the system of axes and the control-surface hinge moments and deflections. (Arrows indicate positive values.)

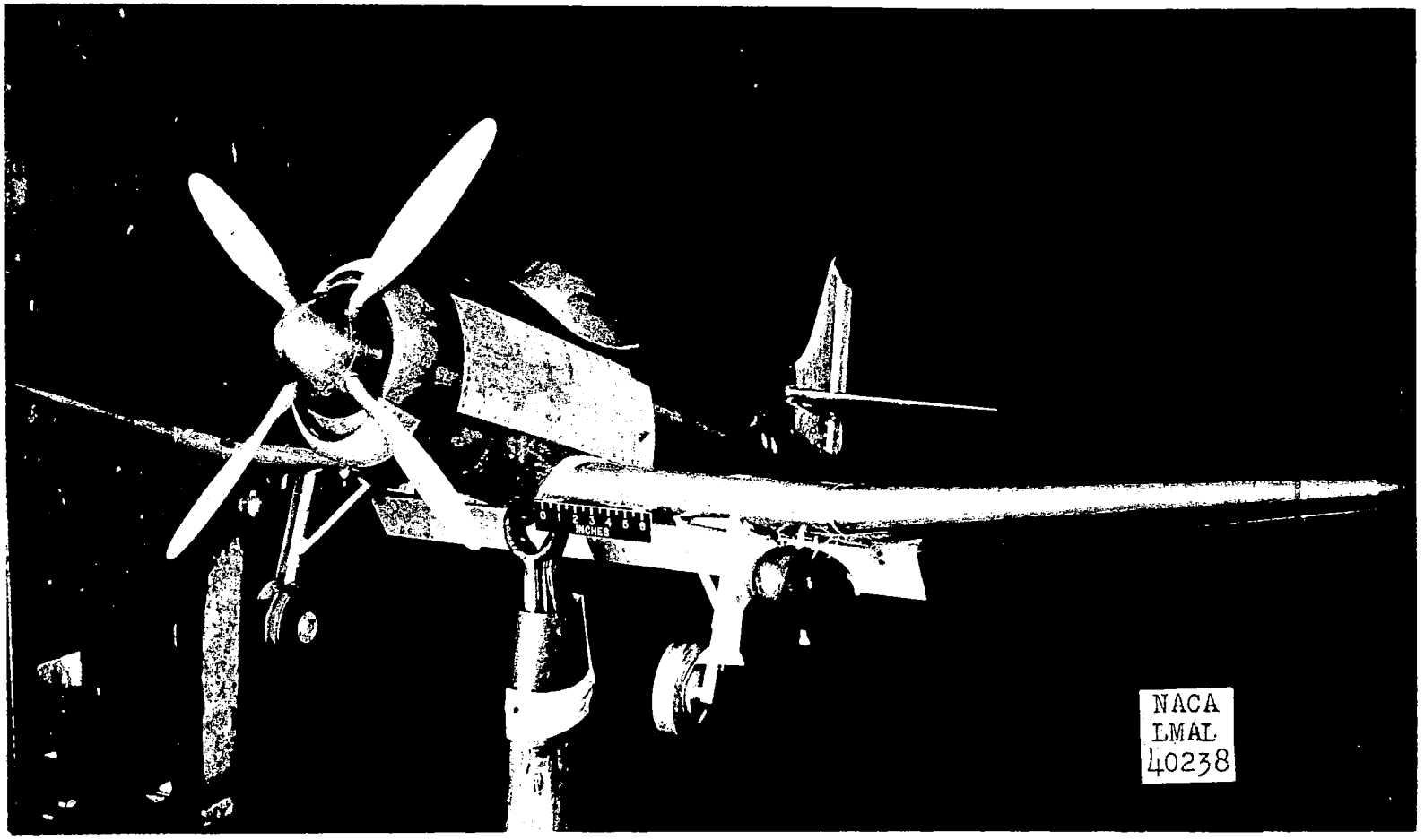

Figure 3(a).- Three-quarter front view of a 0.15-scale model of the XBTK-1 airplane.

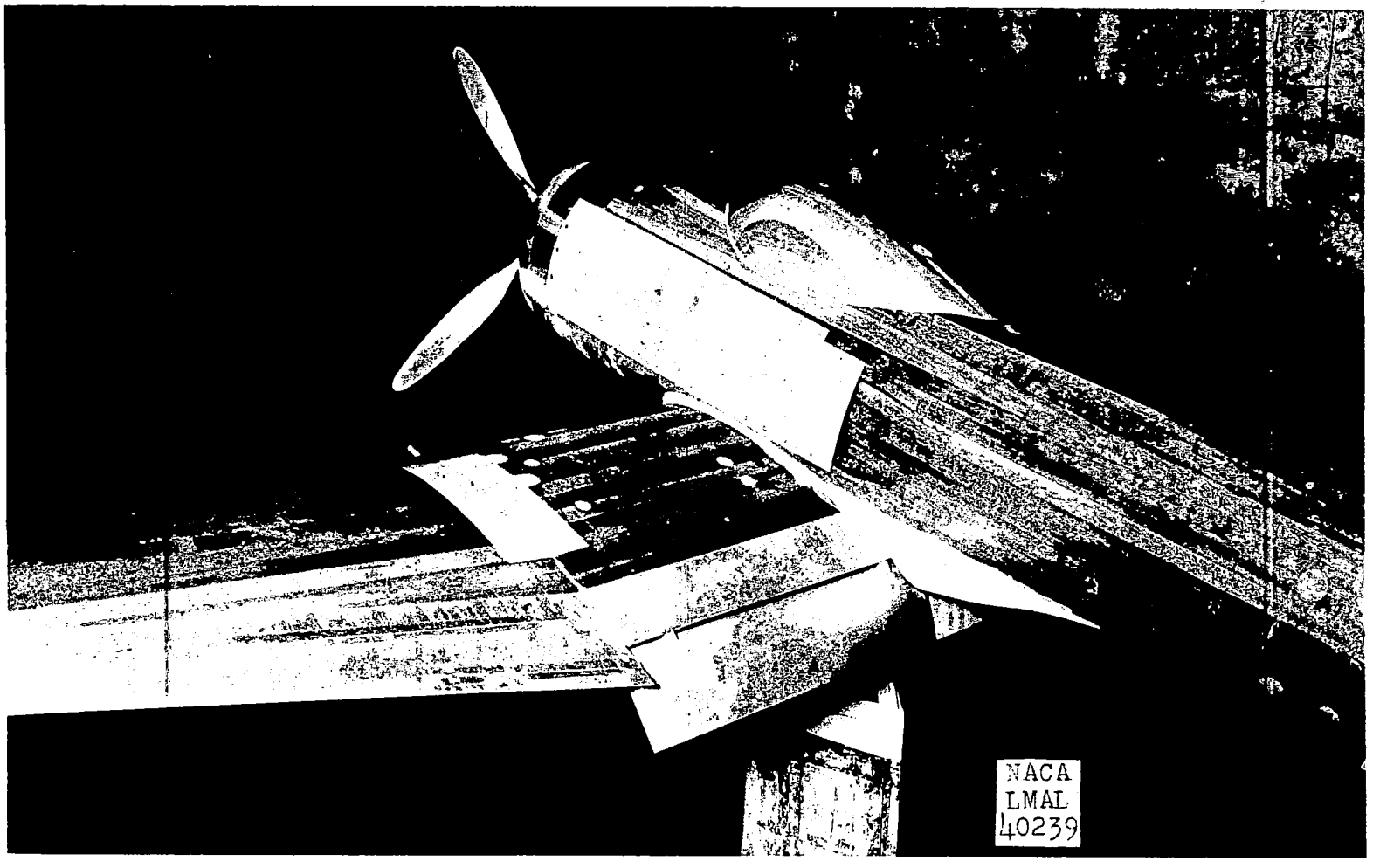

Figure 3(b).- Three-quarter rear view of a 0.15-scale model of the XBTK-1 airplane.

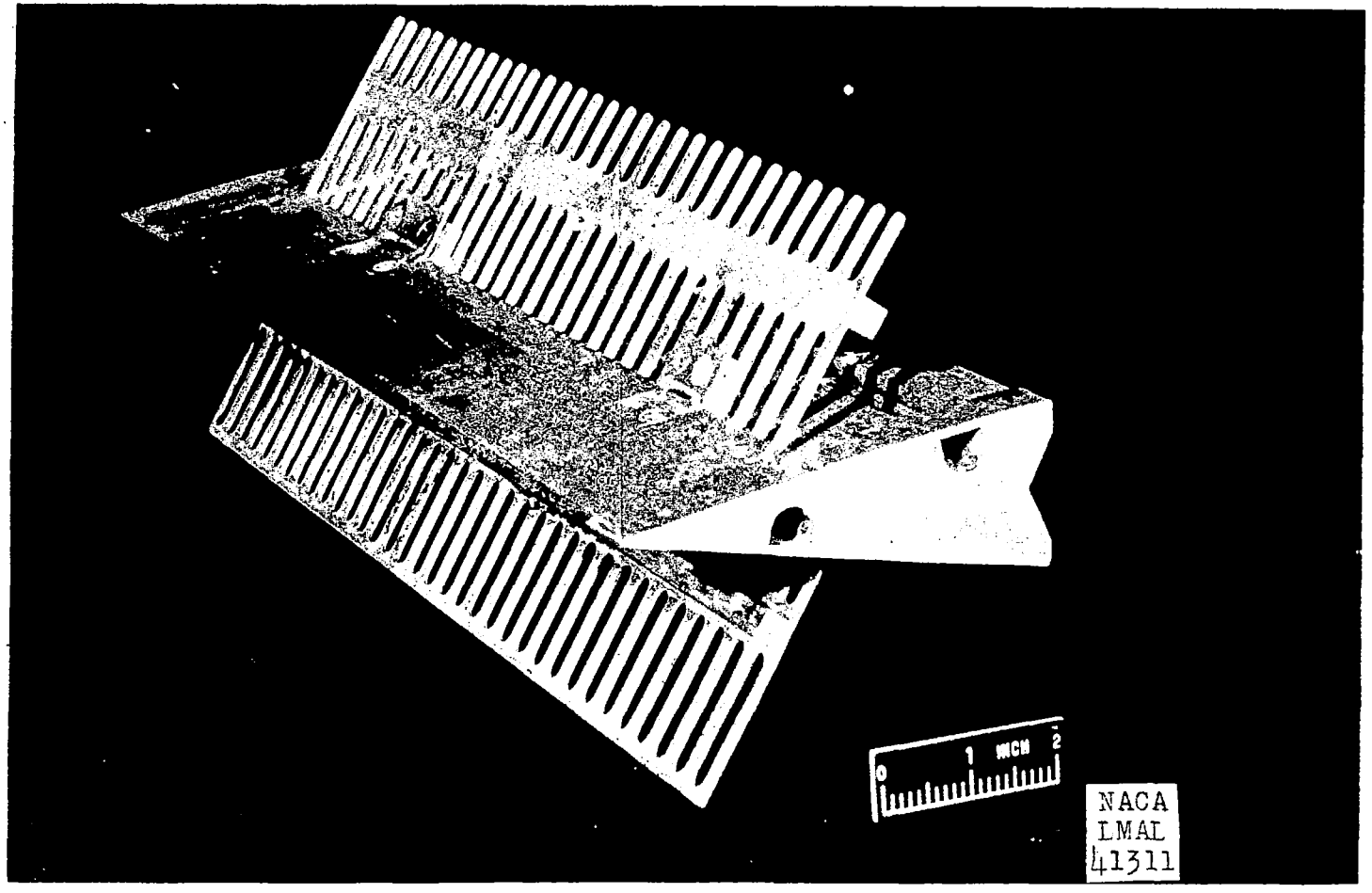

Figure 3(c).- Three-quarter rear view of the dive brakes tested on the 0.15-scale model of the XBTK-1 airplane.

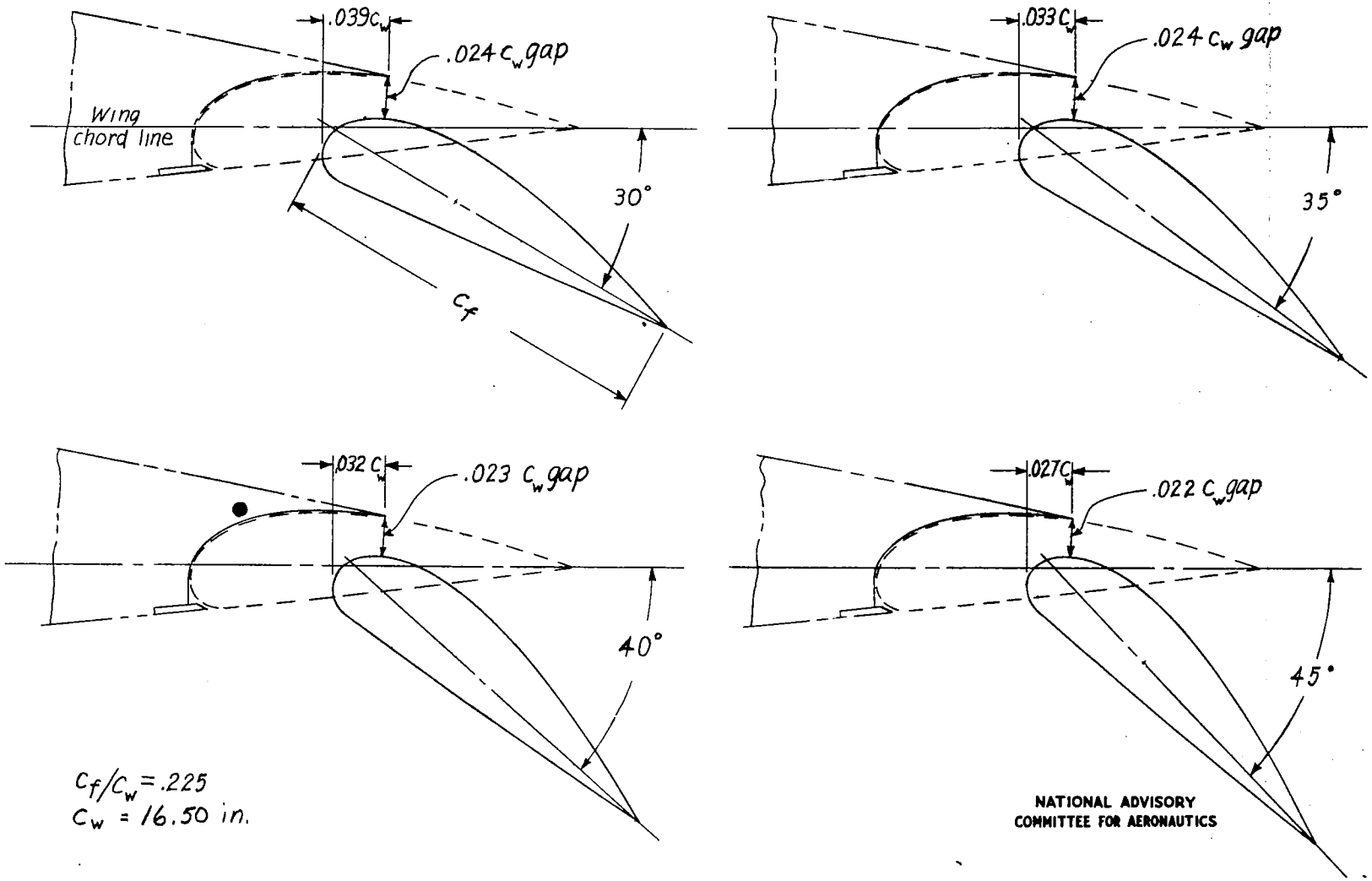

Figure 4(a).-Details of slotted flap positions for various deflections tested on the 0.15 scale model of the XBTK-1 airplane.

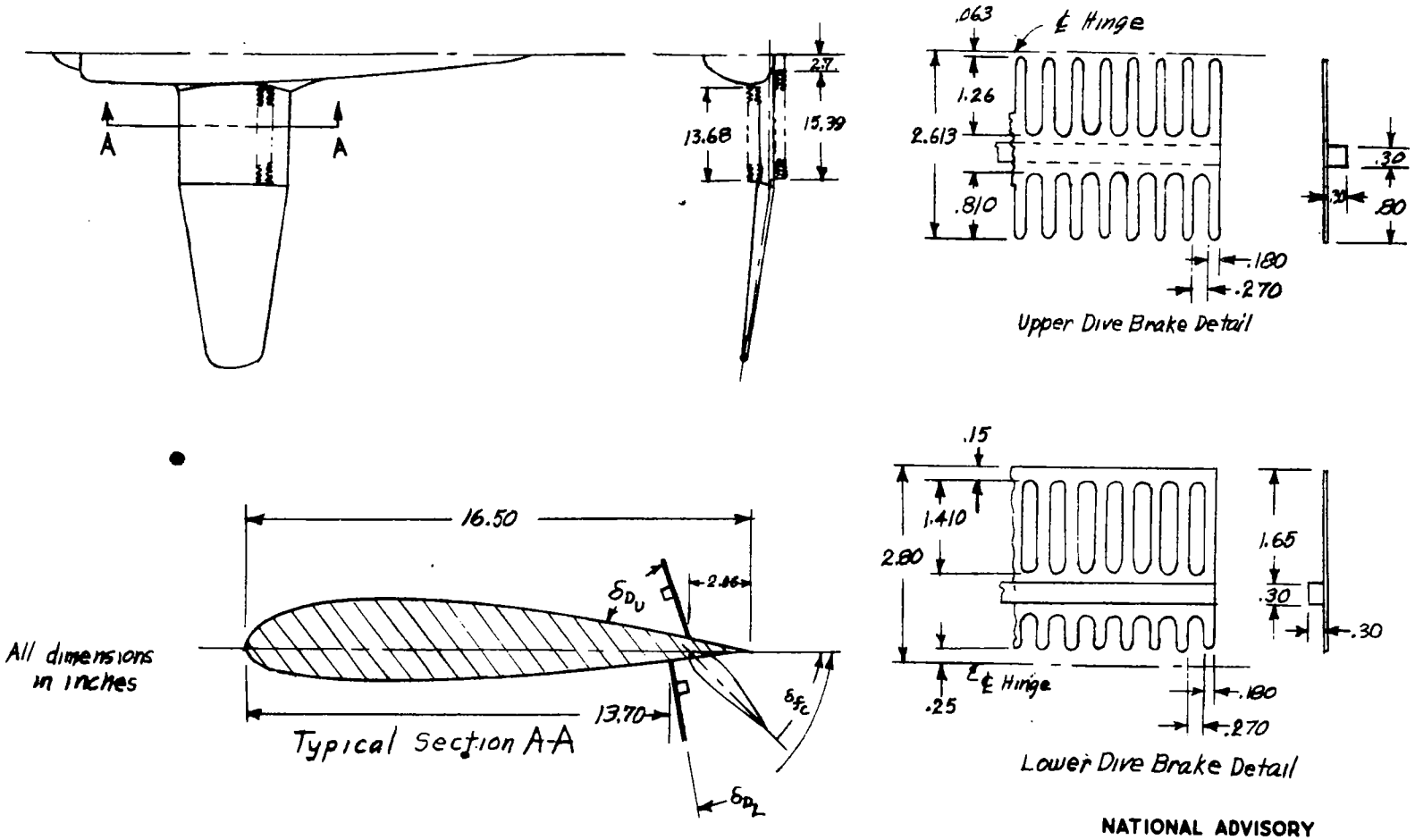

NATIONAL ADVISORY COMMITTEE FOR AERONAUTICS

Figure 4(b).-Detail of dive brakes on the 0.15 scale model of the XBTK-1 airplane.

All dimensions in inches

Total vertical tail area - - - - - - - - - 1.15 sq. ft.*
Rudder area aft of hinge - - - - - - - - - .352 sq. ft
Root mean square chord aft of hinge - - 34.2 in.
Unshielded area of rudder horn - - - - - - - - .016 sq. ft
Shielded area of rudder horn - - - - - - - - .011 sq. ft

* includes dorsal fin

Not to scale

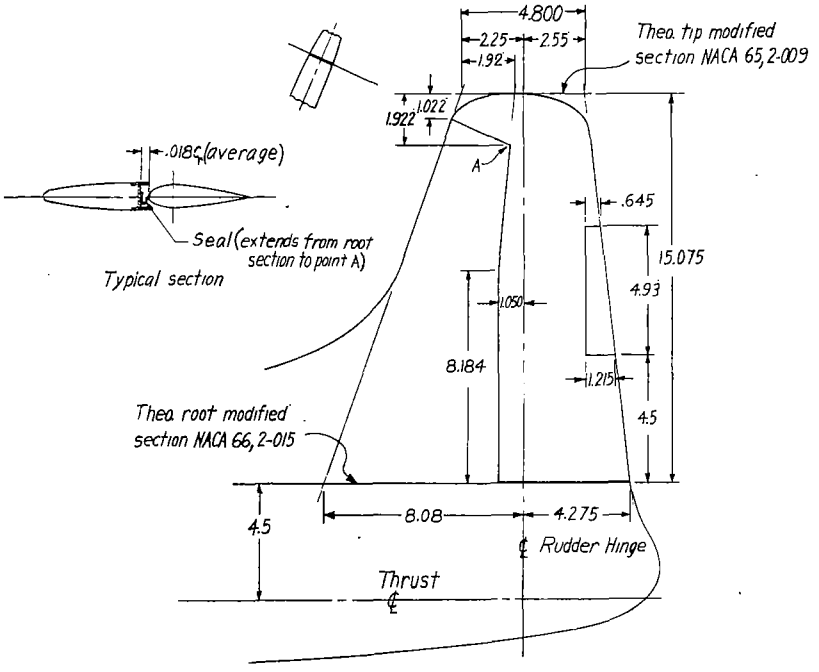

Original vertical tail

Rudder Modifications	Details
1 - Horn rounded	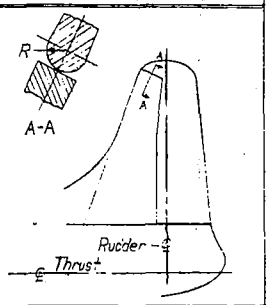
2 - Horn rounded Unsealed	
3 - Horn rounded and two dummy hinge cutouts in balance Rudder sealed up to horn with two dummy hinge cutouts in the seal of dimensions $\frac{1}{8}$" & $\frac{13}{64}$" width for the 7" and 5.5" location of hinge cutouts respectively	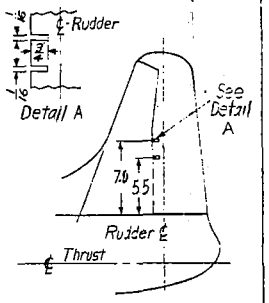
4 - Horn removed and completely sealed up to tip except for dummy hinge cutouts in seal and balance	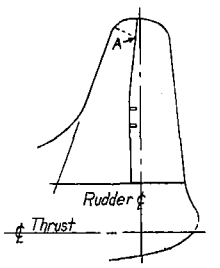
5 - Horn removed and sealed up to point "A" with cutouts same as in modification 4	

NATIONAL ADVISORY COMMITTEE FOR AERONAUTICS

Figure 5.- Comparison of rudder modifications as tested on the 0.15 scale model of the XBTK-1 airplane.

Total vertical tail area -------*1.15 sq ft
Rudder area aft of hinge---0.352 sq ft
Root mean square chord
aft of hinge----------3.42 in
Cutouts in seal $\frac{1}{8}$ and $\frac{13}{64}$ wide
for hinge cutouts at 7.0 and
5.5, respectively.
Average trailing edge angle---20°45'

*Includes dorsal fin

Note-Not to scale, all dimensions inches

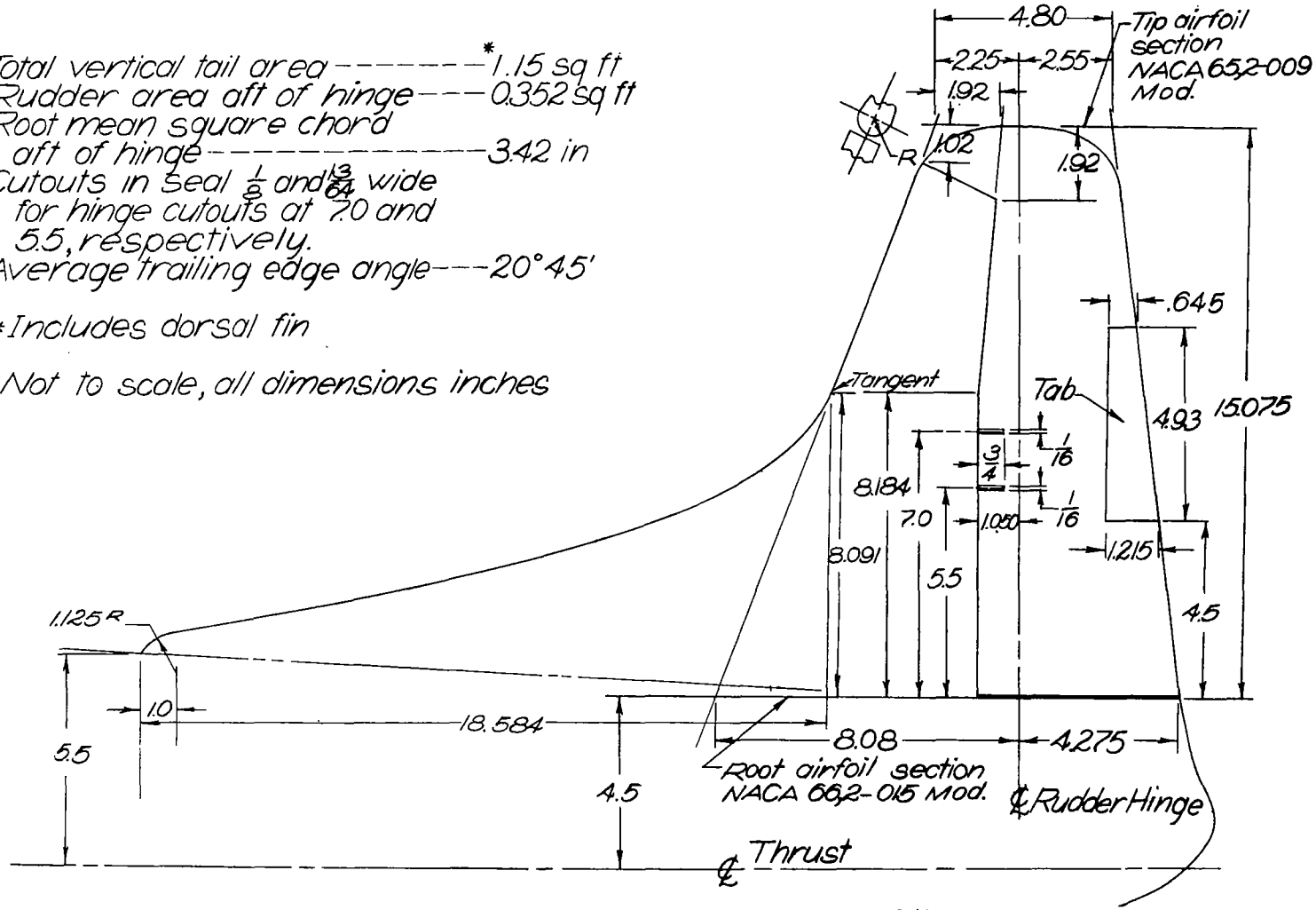

Figure 6.-Drawing of the vertical tail of the 0.15 scale model of the XBTK-1 airplane (modification 3).

NATIONAL ADVISORY COMMITTEE FOR AERONAUTICS

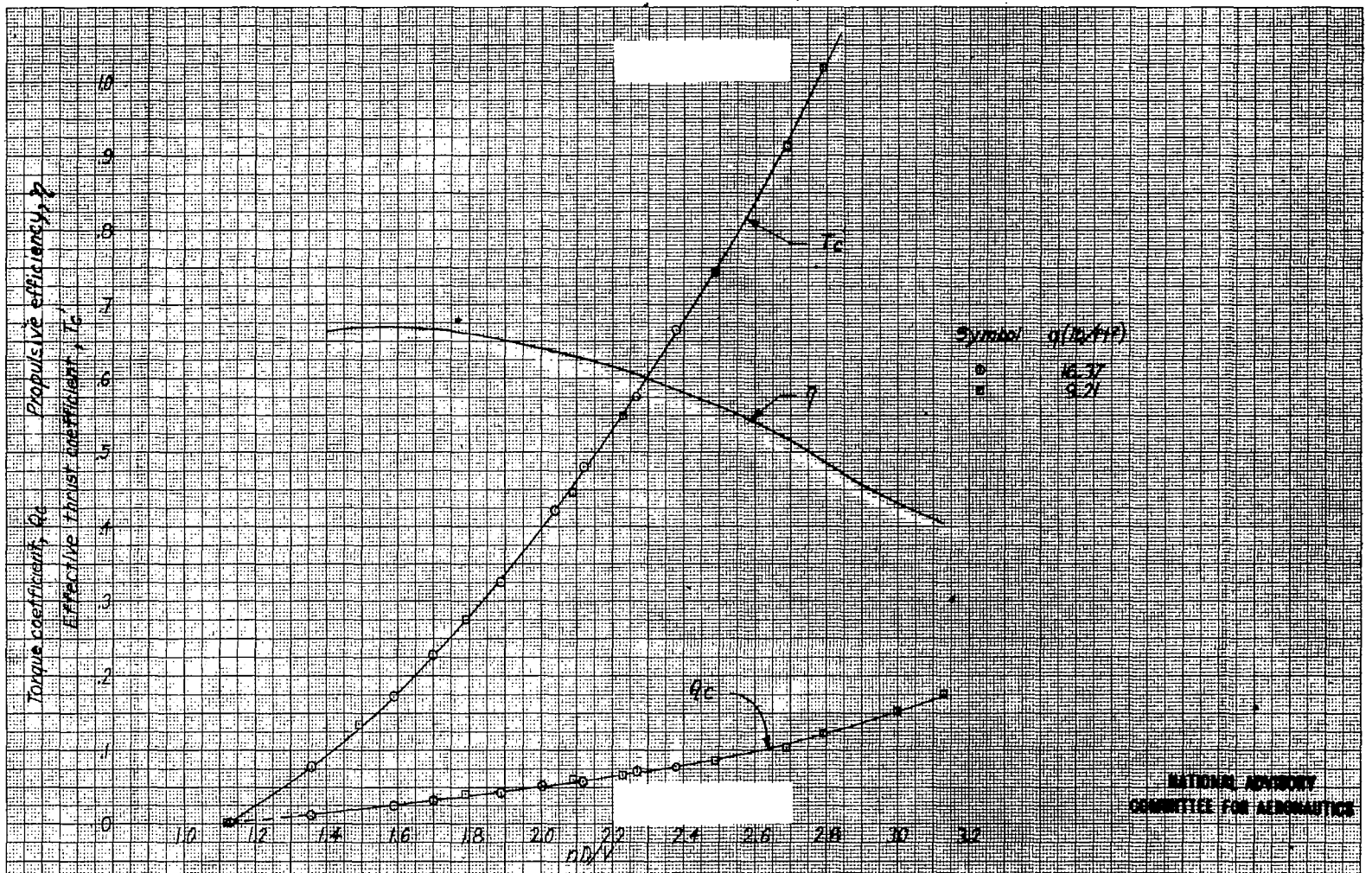

Figure 7.- Characteristics of a 2.04-ft. diameter four-bladed propeller on 0.15 scale model of XB-14 airplane. $\alpha = 0°$, $\beta = 18°$.

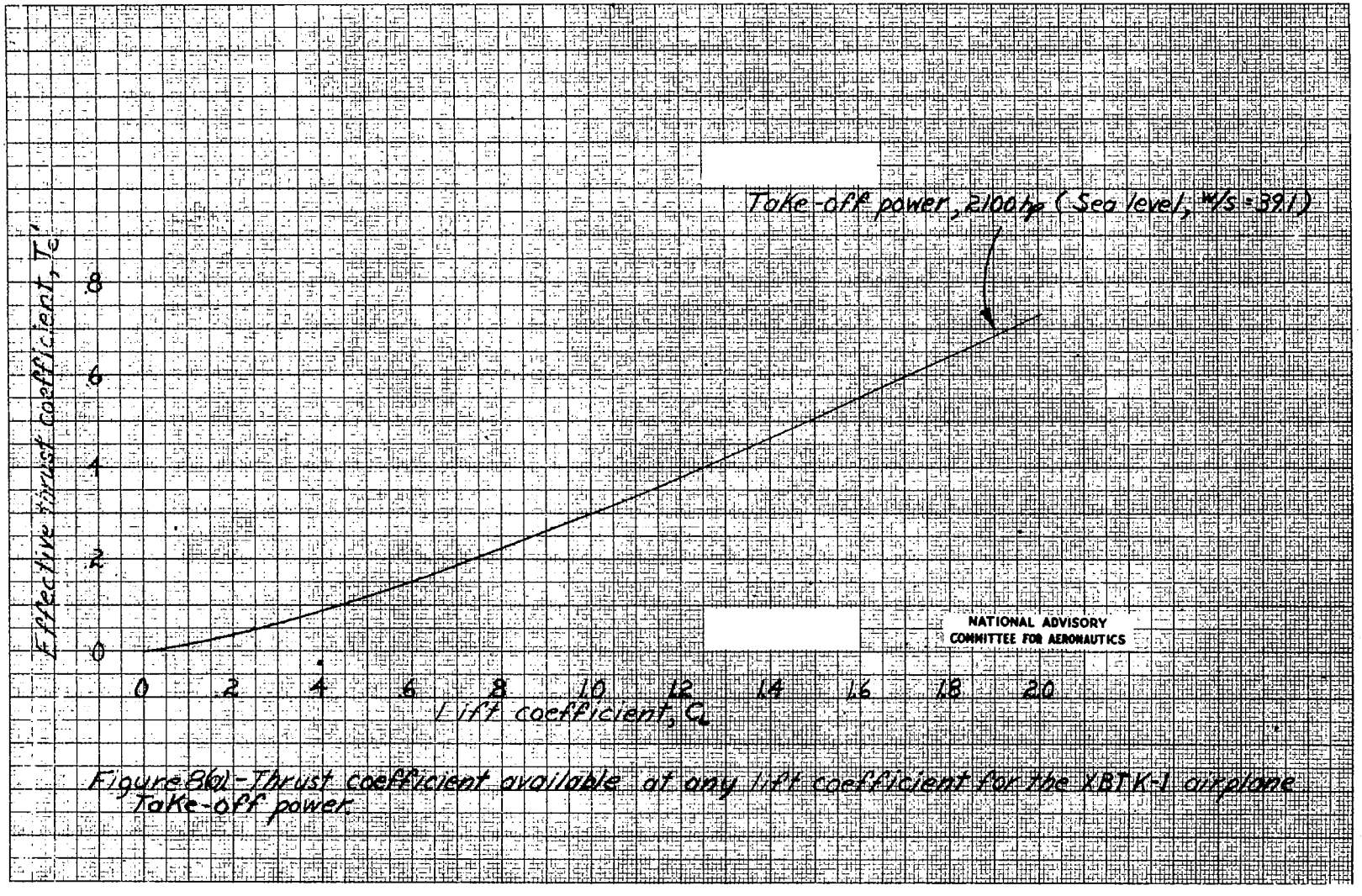

Figure 8(a)-Thrust coefficient available at any lift coefficient for the XBTK-1 airplane. Take-off power.

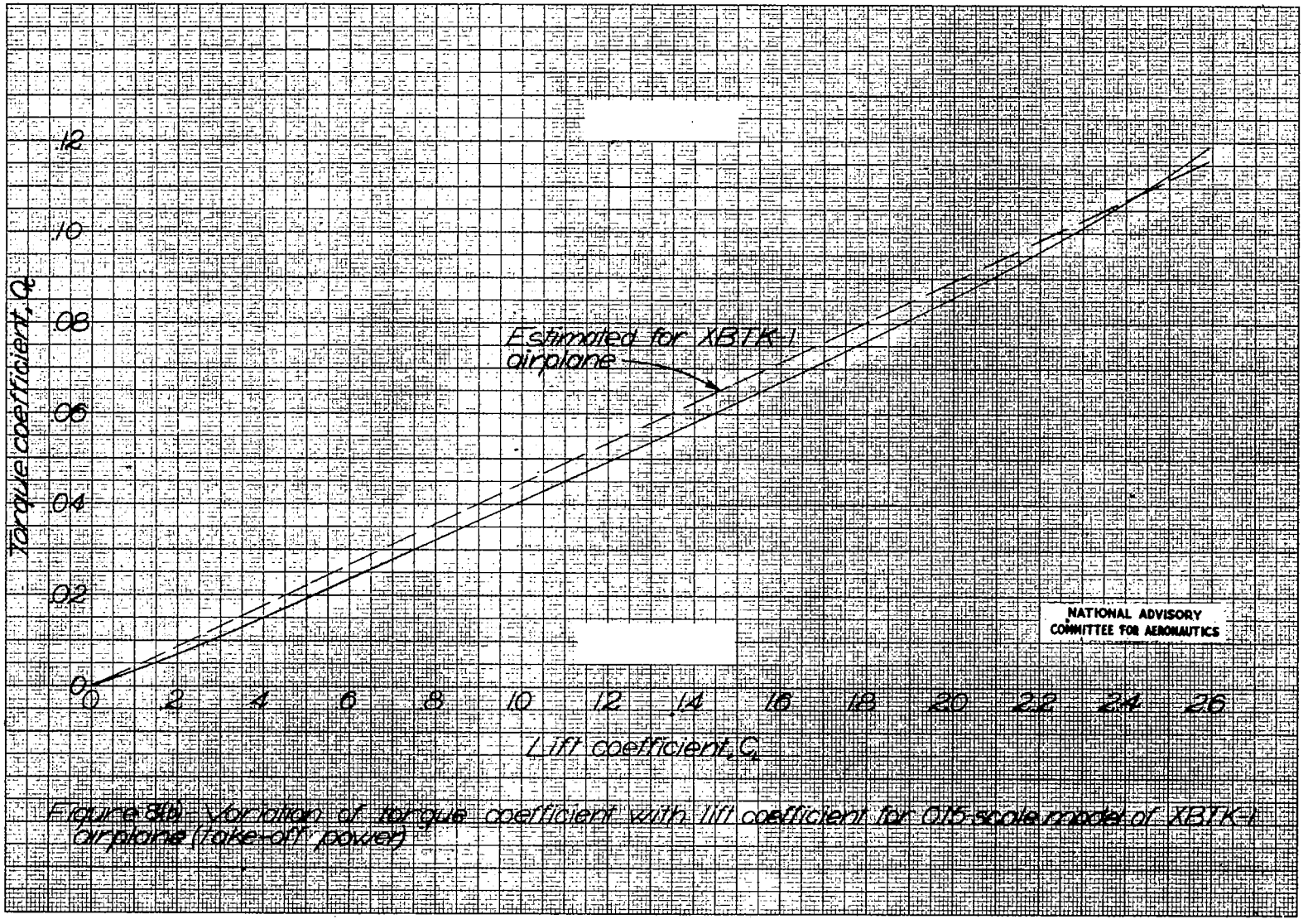

Figure 8(b). Variation of torque coefficient with lift coefficient for 0.15-scale model of XBTK-1 airplane (take-off power).

MR No. L5F20

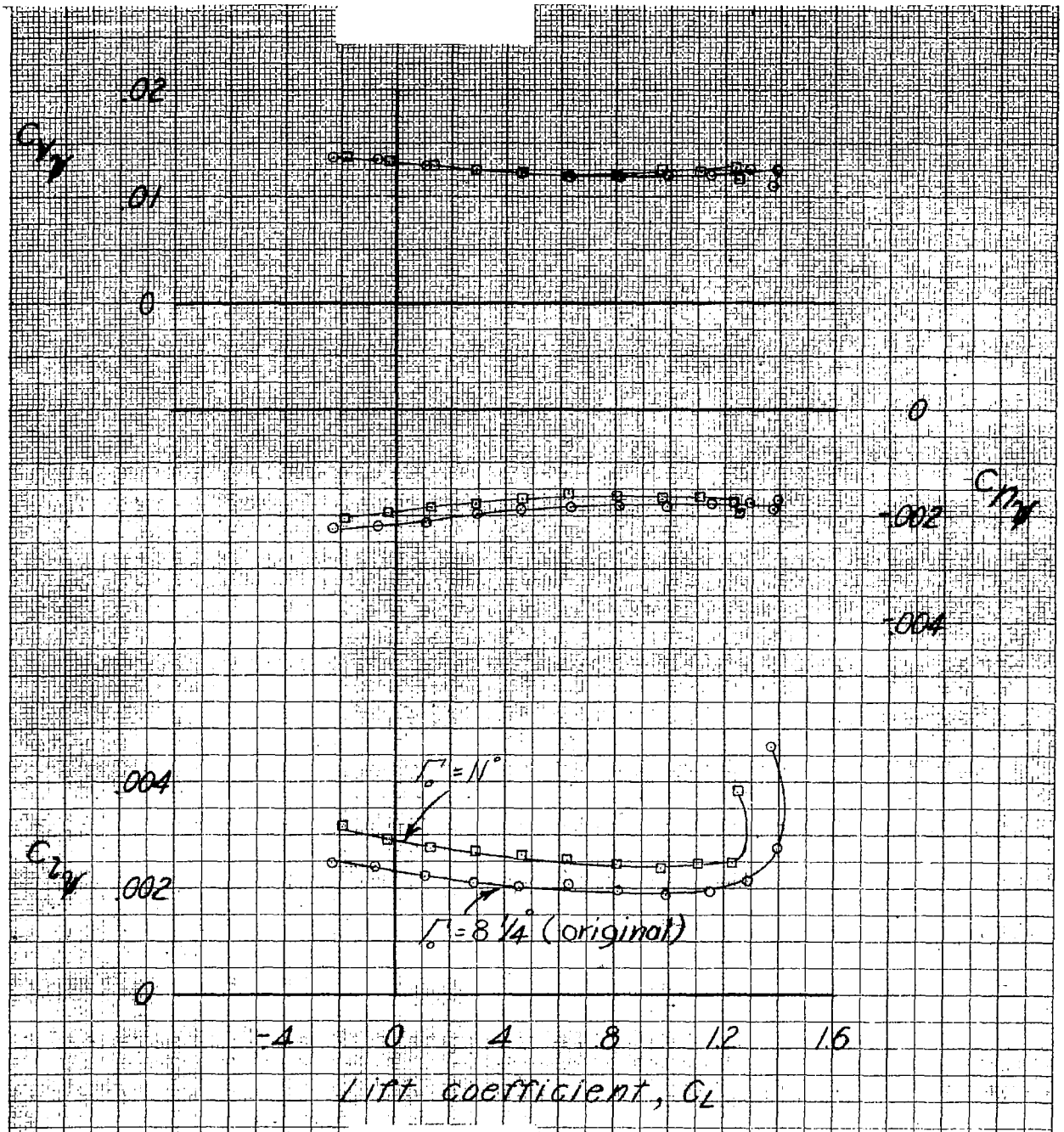

(a) Windmilling, cruising configuration

NATIONAL ADVISORY COMMITTEE FOR AERONAUTICS

Figure 9.- Effect of changing geometric dihedral of outer wing panels on the lateral stability derivatives of the 0.15-scale model of the XBTK-1 airplane. $\delta_r = 0$

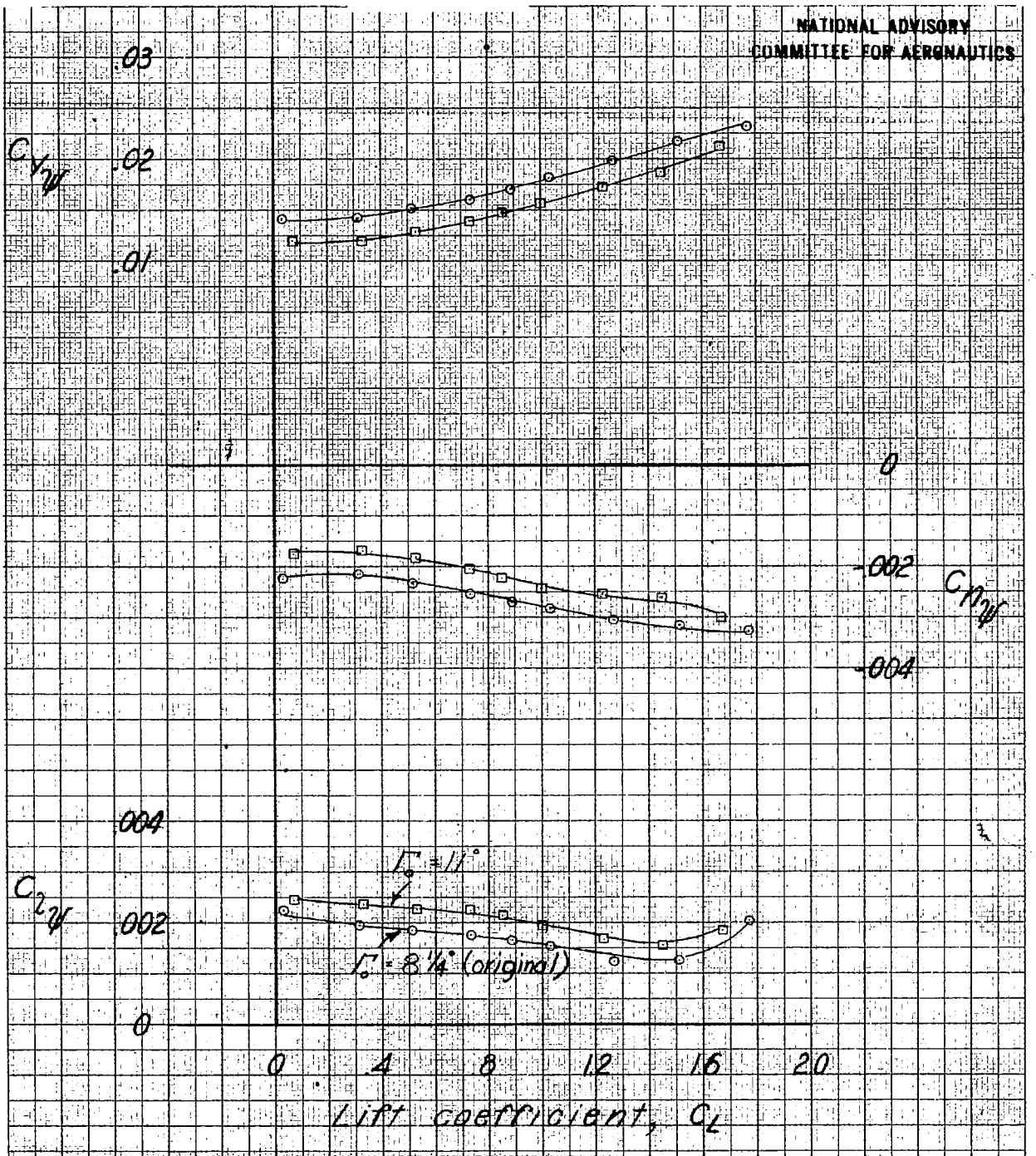

(b) Take-off power, cruising configuration

Figure 9.- continued

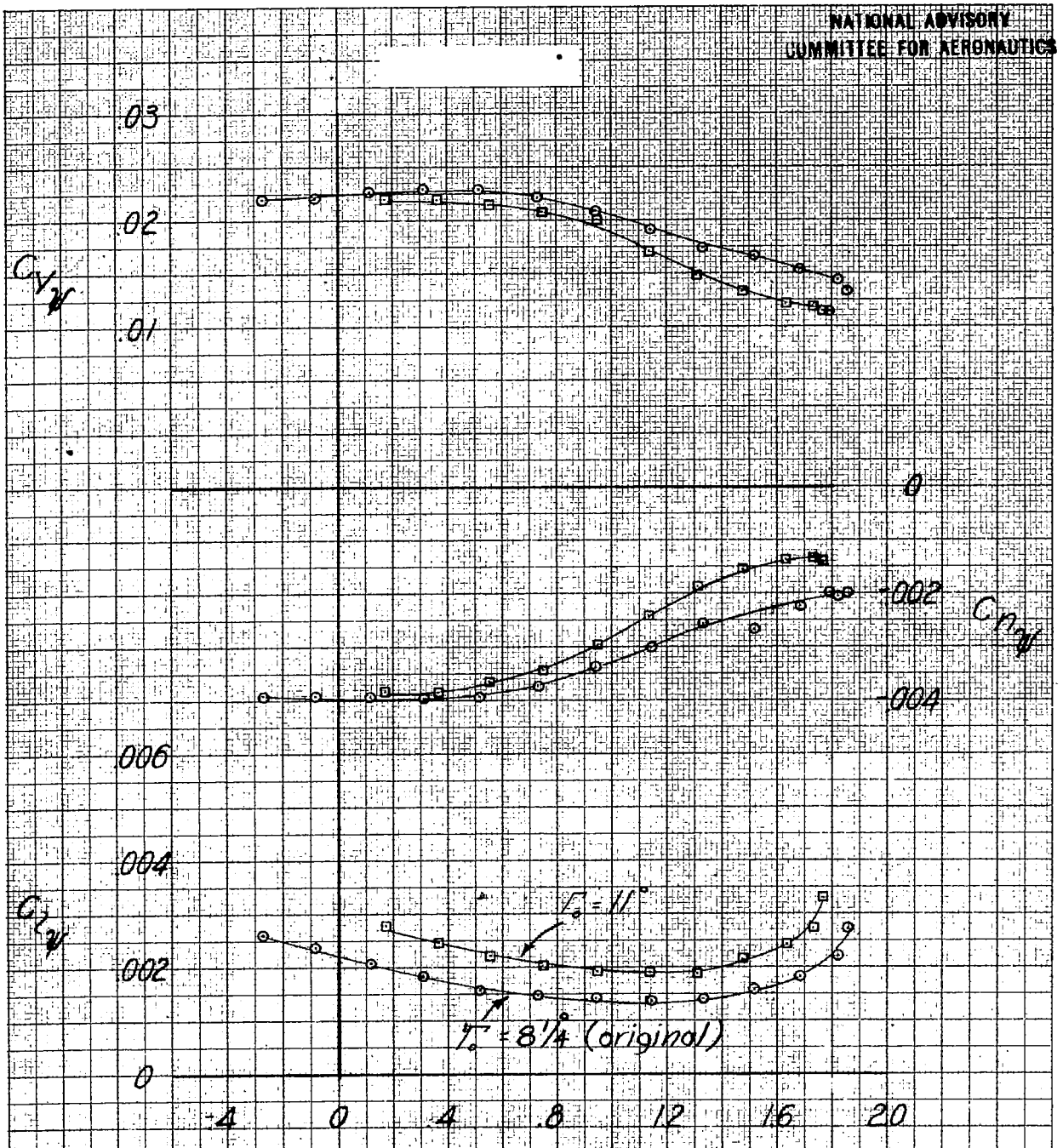

(c) Windmilling, landing configuration

Figure 9.- continued

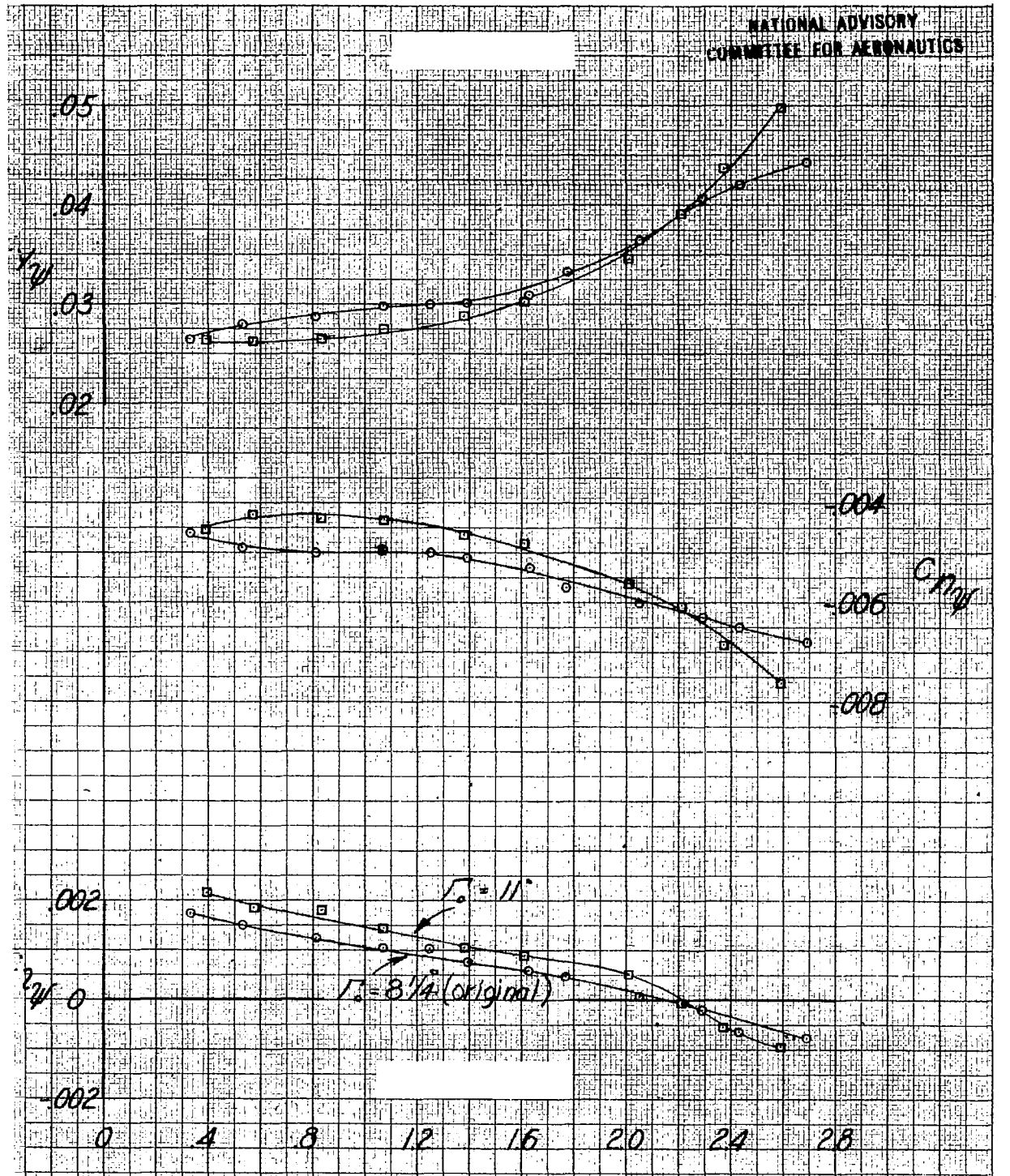

(d) Take-off power, landing configuration

Figure 9.- concluded

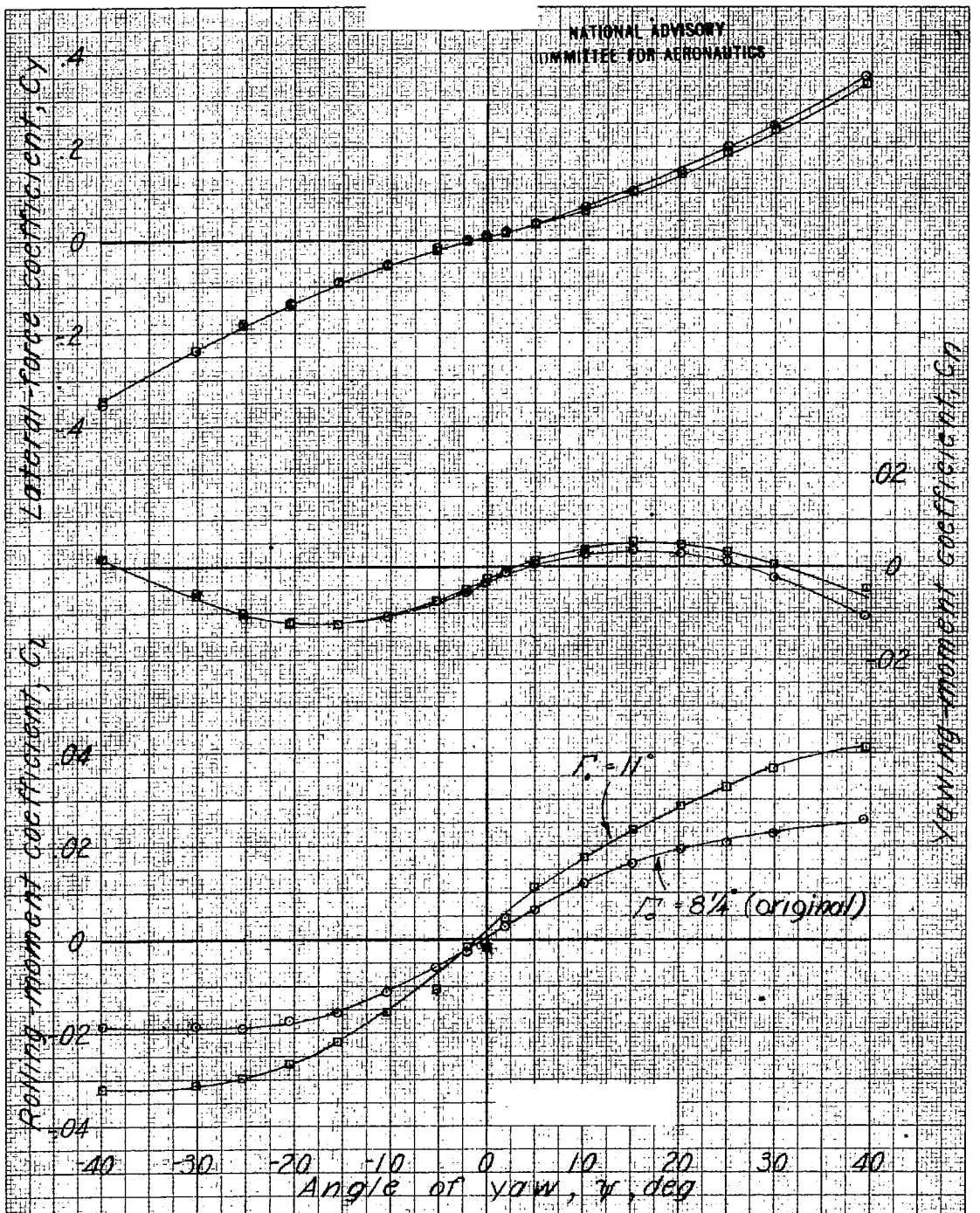

(a) Windmilling, cruising configuration, $\alpha = 11.0°$, $C_L = 1.00$

Figure 10.- Effect of changing geometric dihedral of outer wing panels on the aerodynamic characteristics in yaw of the 0.15-scale model of the XBTK airplane. Tail off.

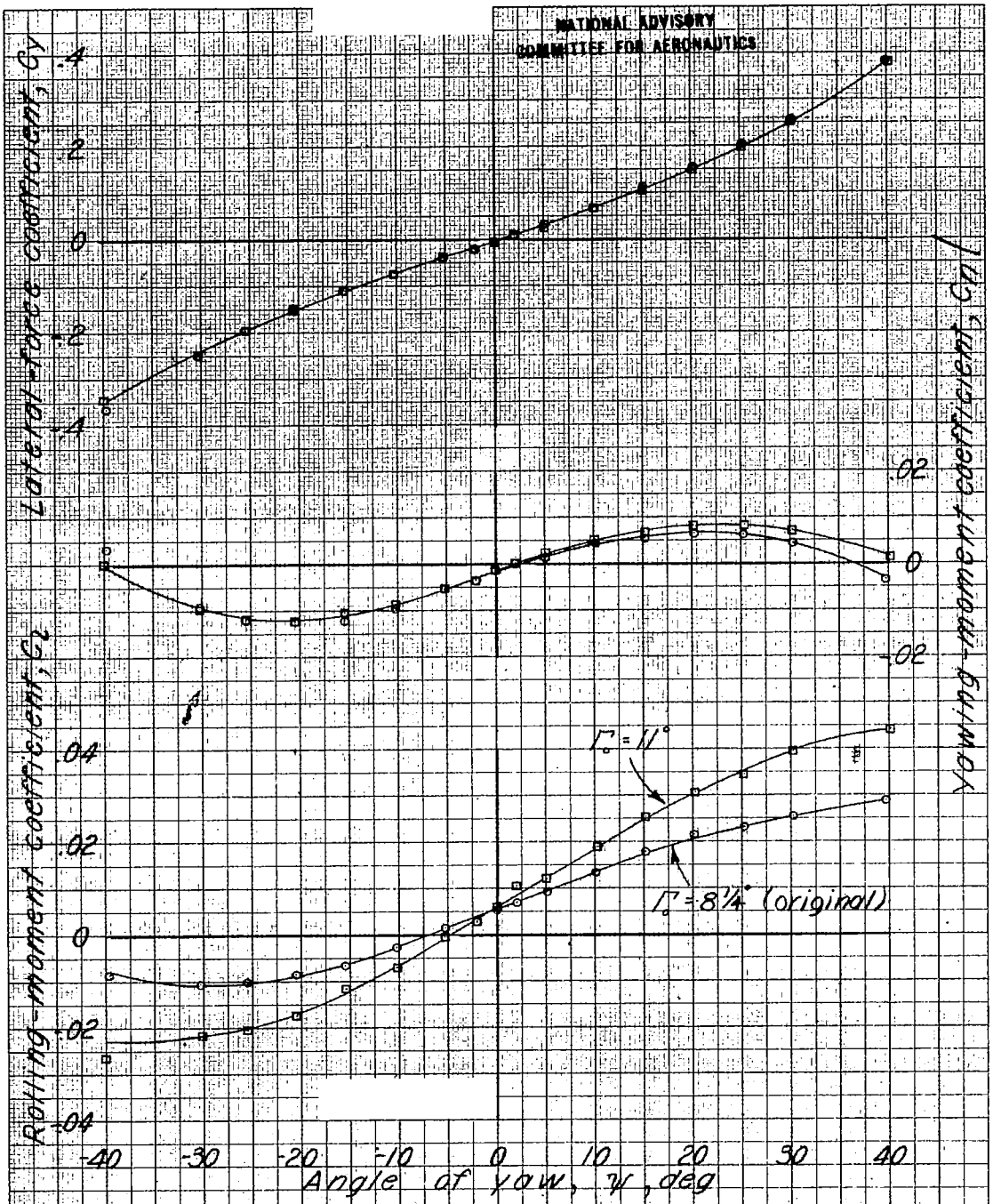

(b) Take-off power, cruising configuration, $\alpha = -0.6°$, $C_L = 0.18$

Figure 10 - continued

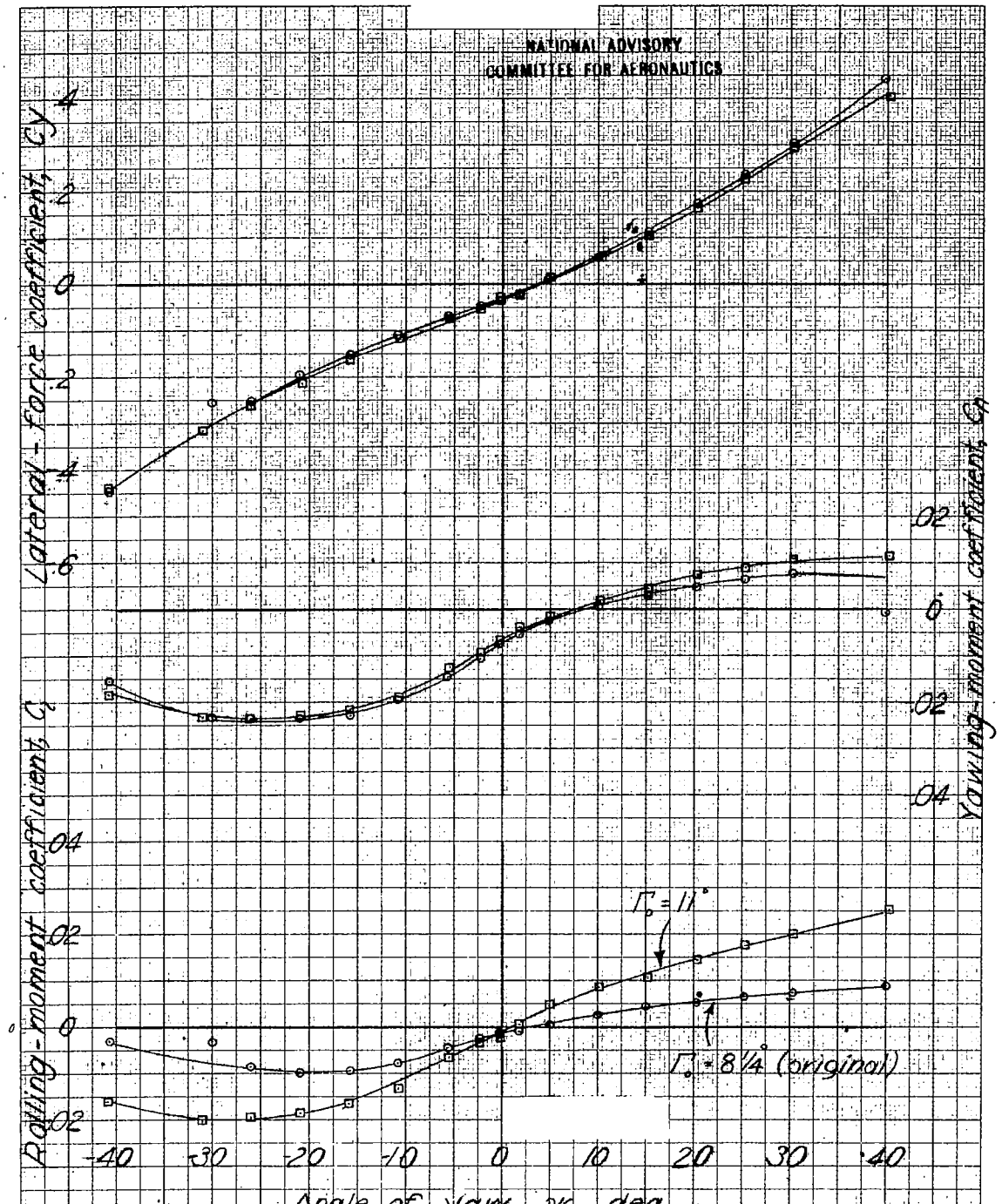

(c) Take-off power, cruising configuration, $\alpha = 7.7°$, $C_L = 0.92$.

Figure 10 .- continued

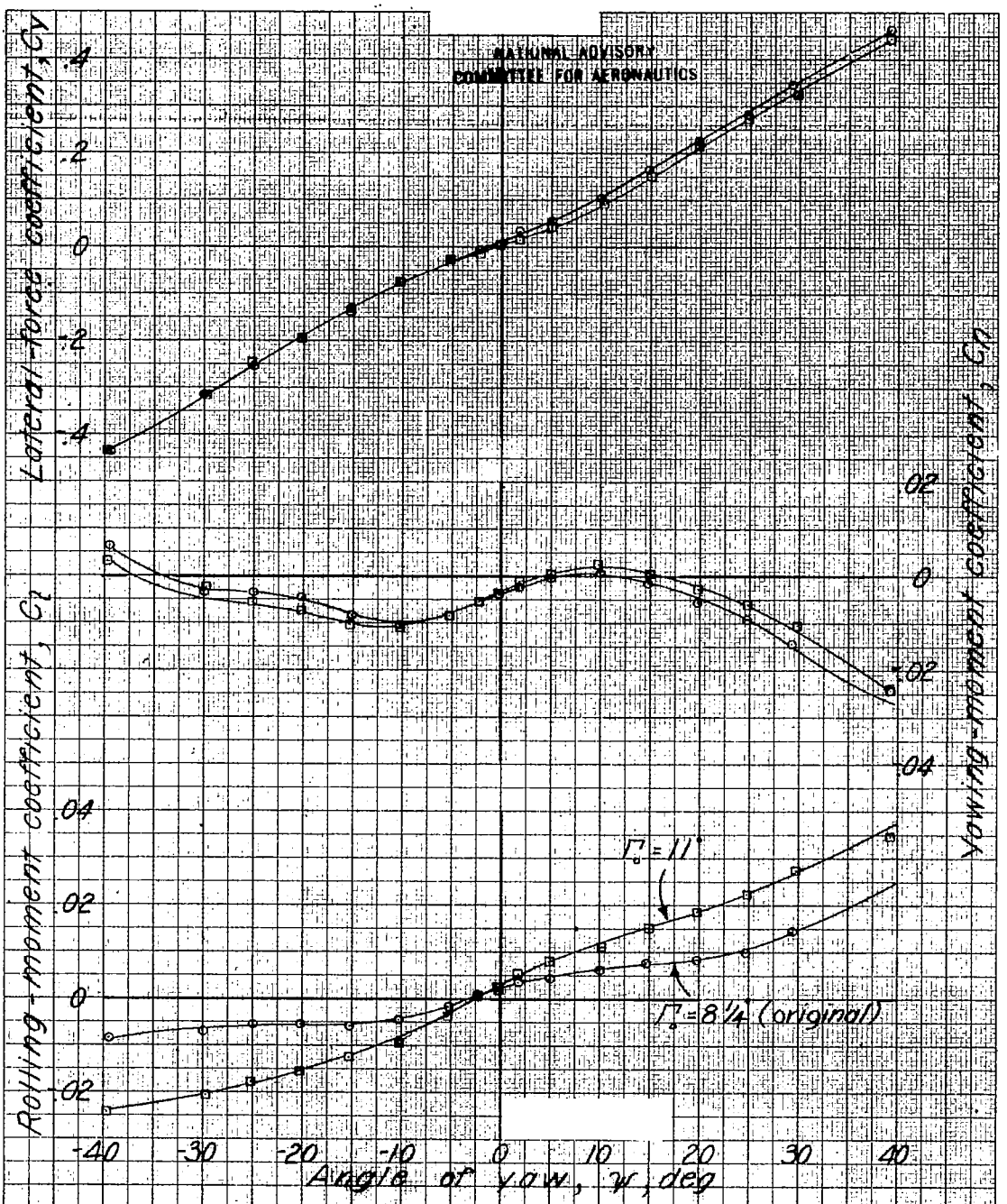

(d) Windmilling, landing configuration, $\alpha = 10.4$, $C_L = 1.55$

Figure 10.- continued.

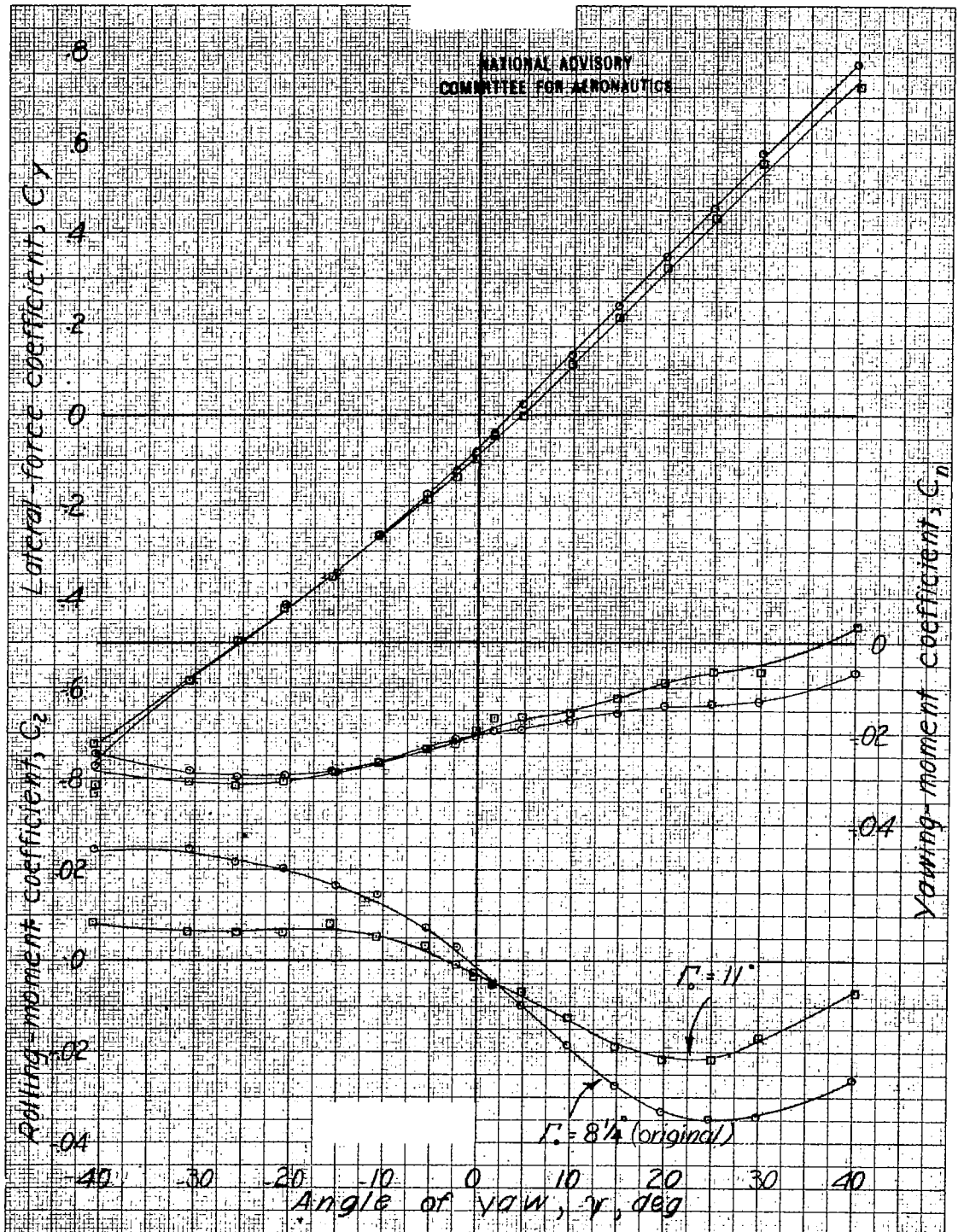

(e) Take-off power, landing configuration, $\alpha = 9.8°$, $C_L = 2.03$

Figure 10 - concluded

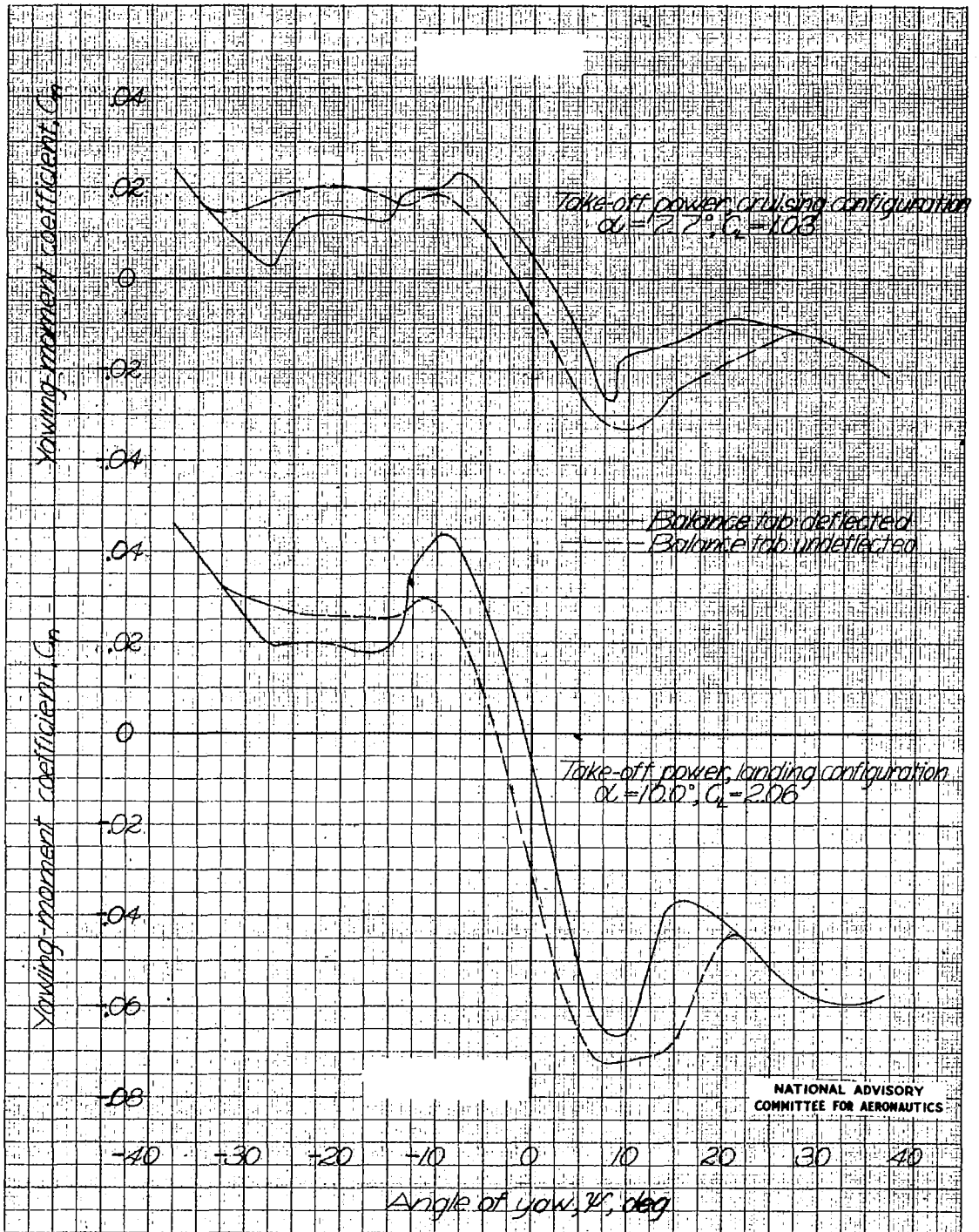

Figure 11.- Rudder-free yawing moment characteristics of the 0.15-scale model of XB7K-1 airplane, trim tab deflection 5°.

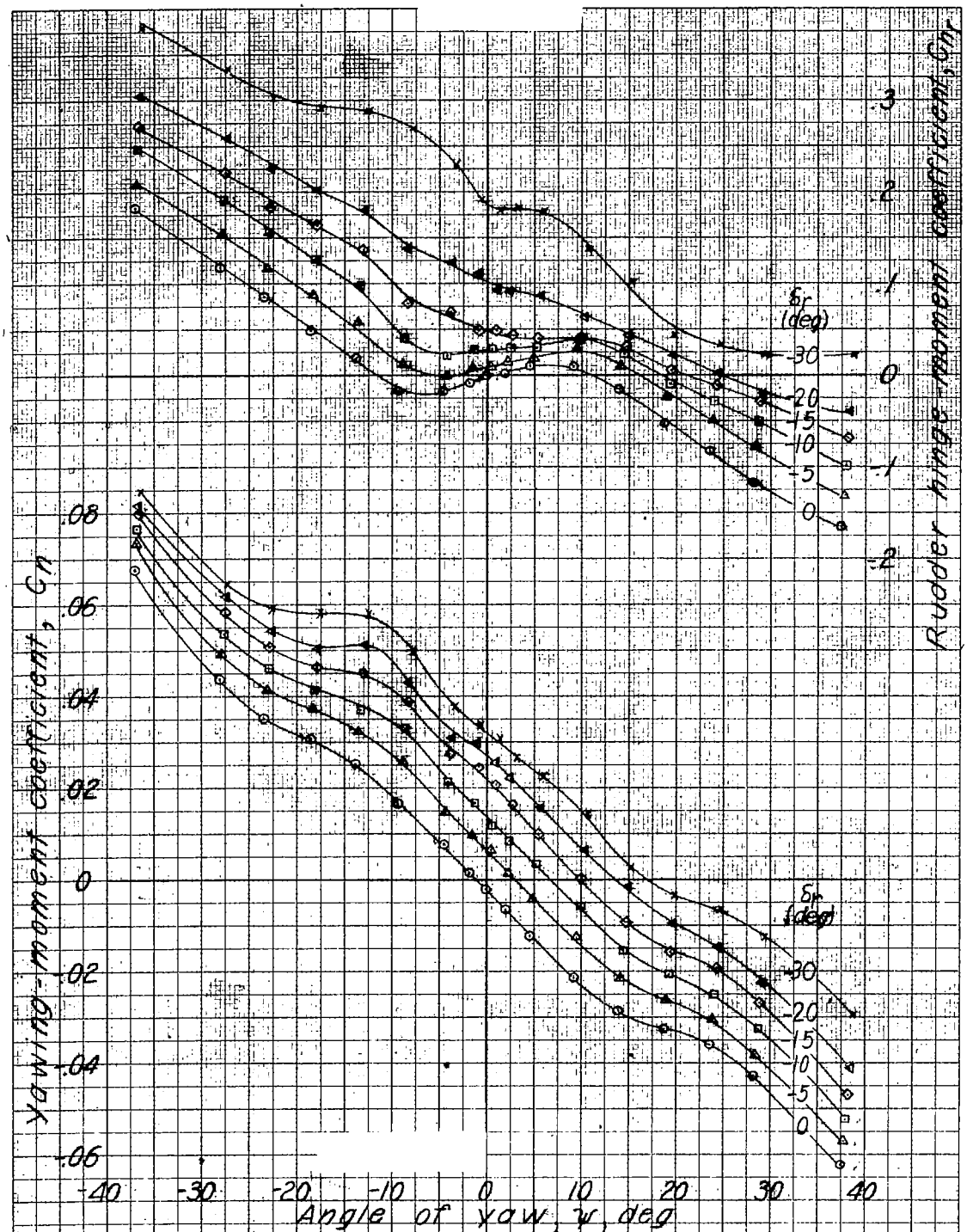

(a) Original sealed rudder

NATIONAL ADVISORY COMMITTEE FOR AERONAUTICS

Figure 12.- Effect of rudder deflection on the aerodynamic characteristics in yaw of a 0.15 scale model of the XBTK-1 airplane. Take-off power, cruising configuration $\alpha = -0.5$, $C_L = 0.23$.

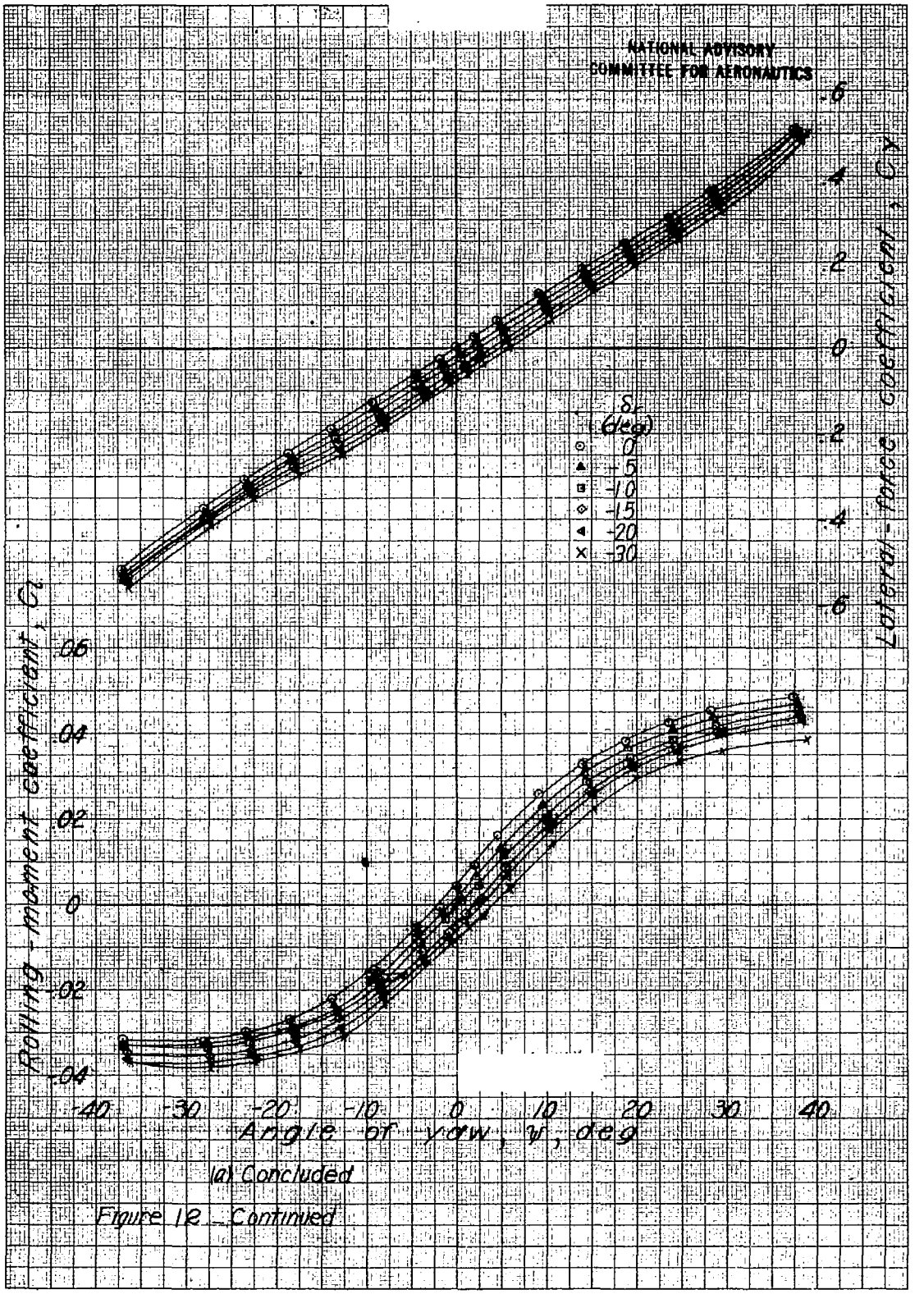

(a) Concluded

Figure 12.- Continued

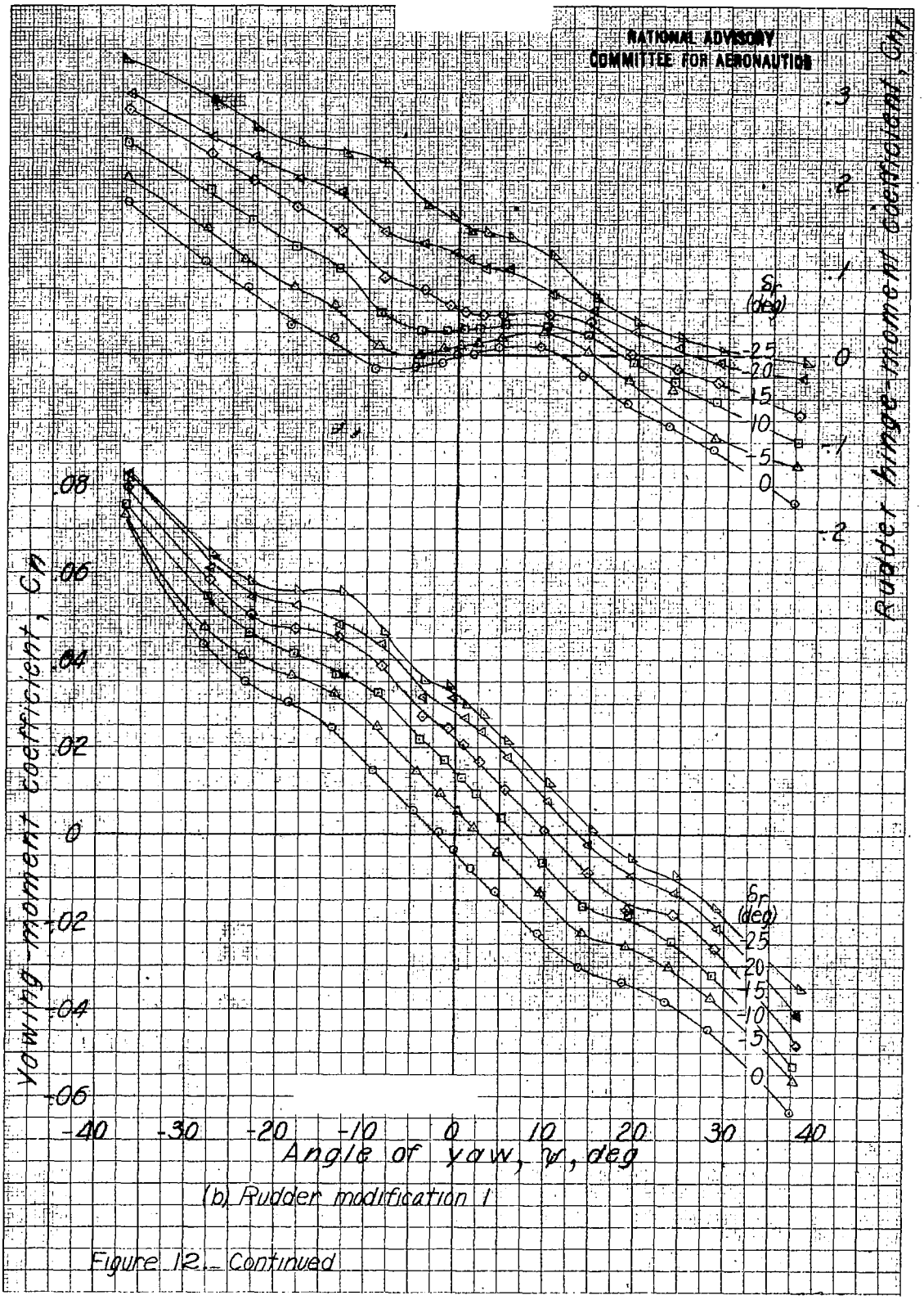

(b) Rudder modification 1

Figure 12.- Continued

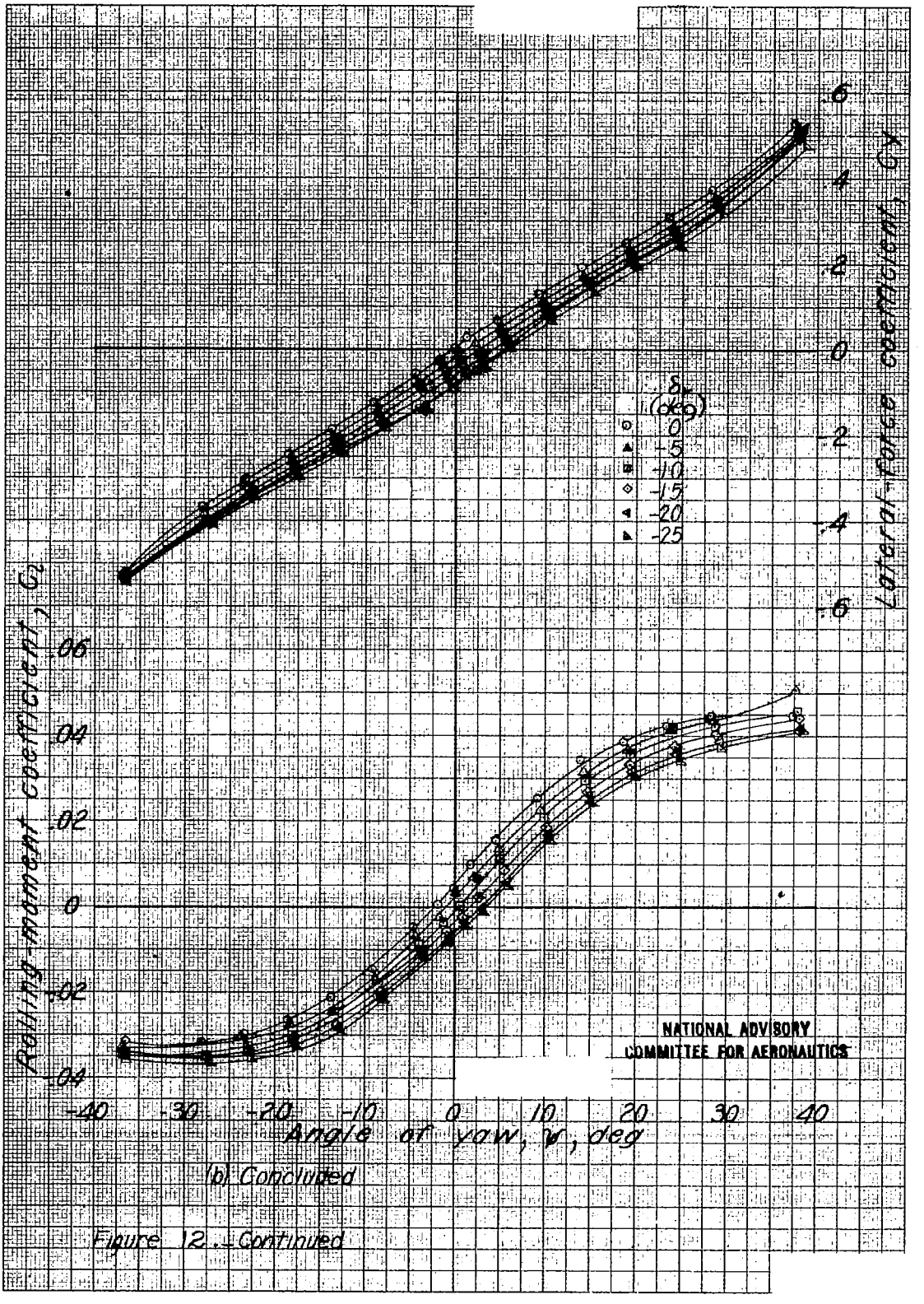

(b) Concluded

Figure 12.- Continued

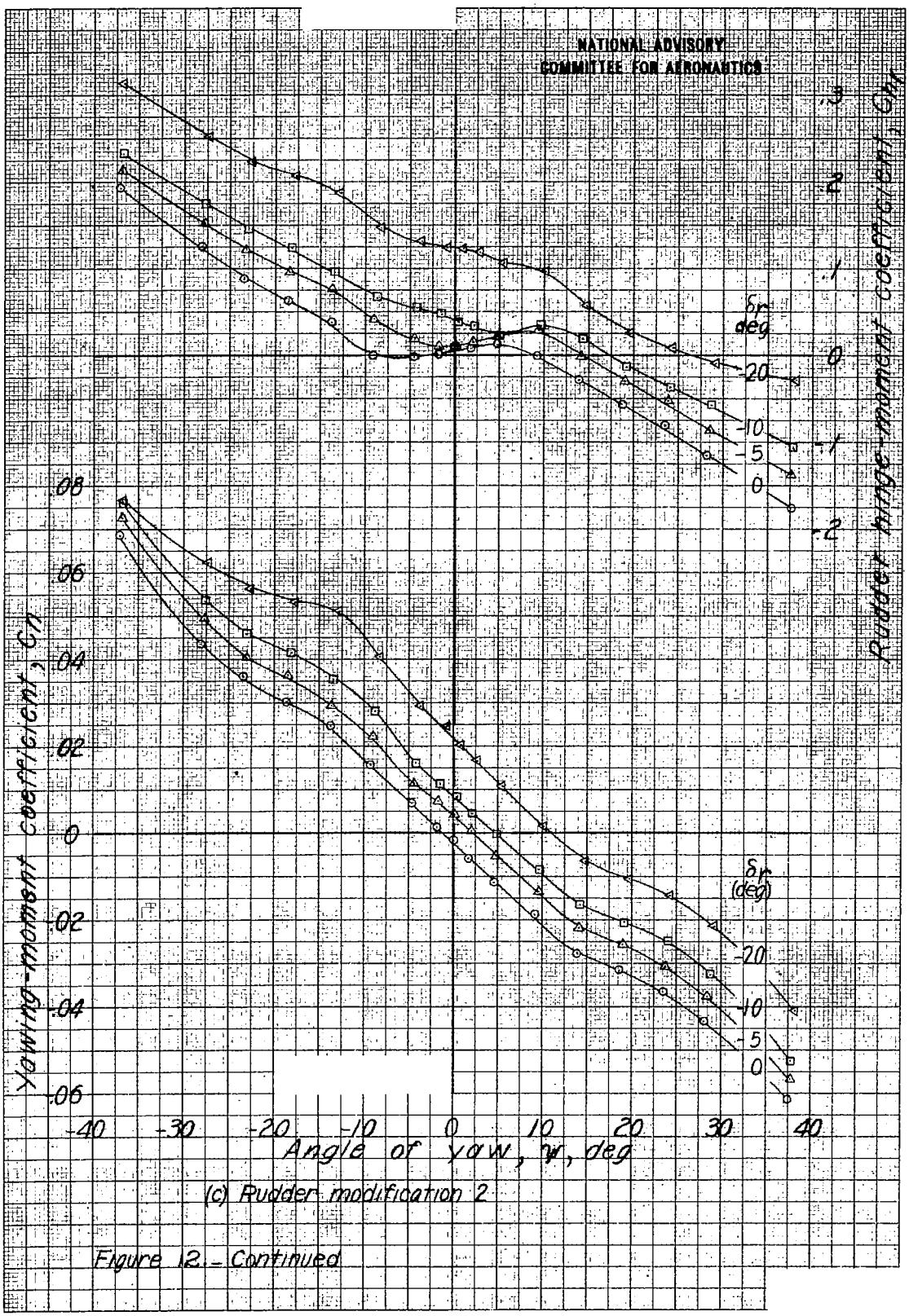

(c) Rudder modification 2

Figure 12.- Continued

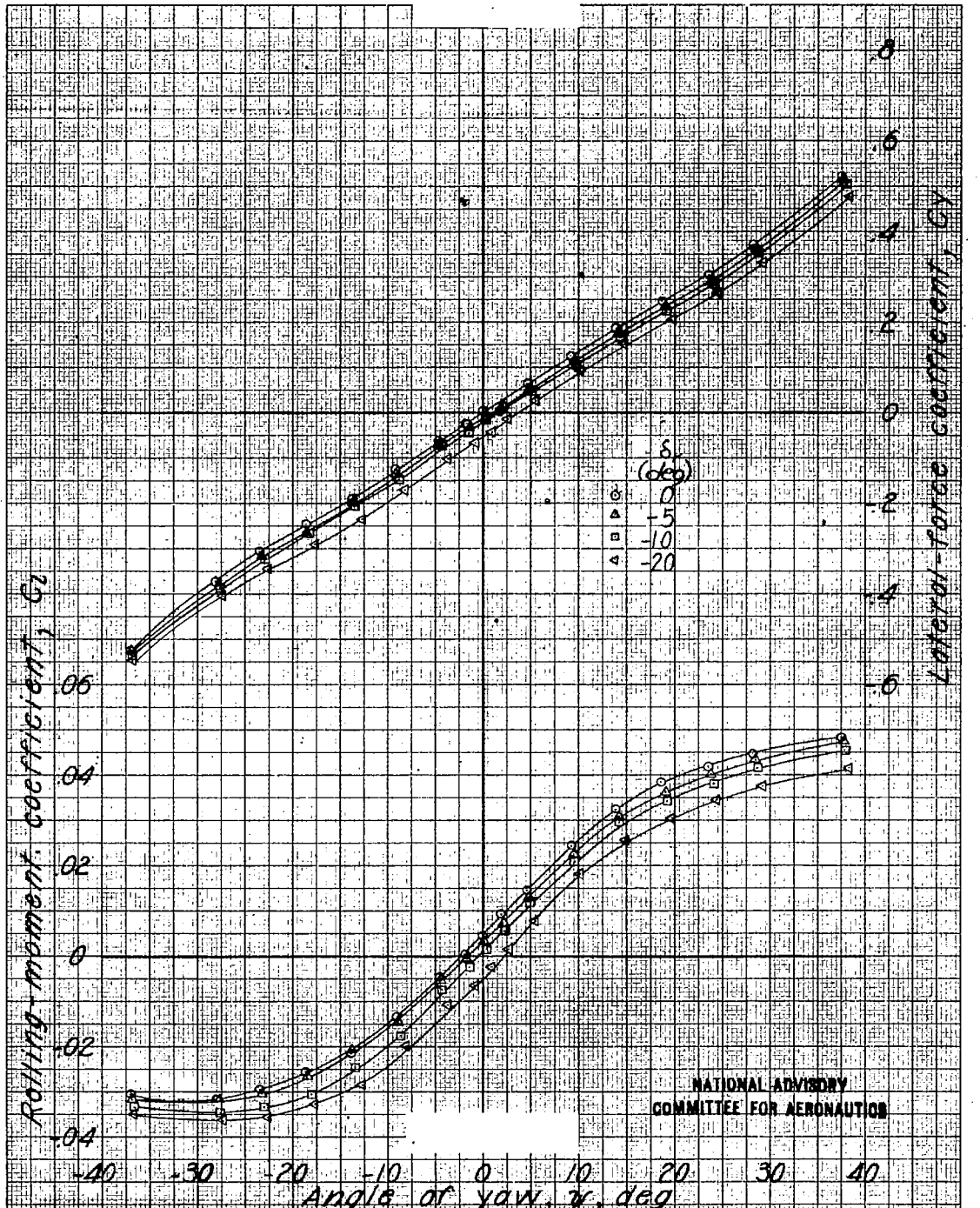

(c) Concluded

Figure 12.- Continued

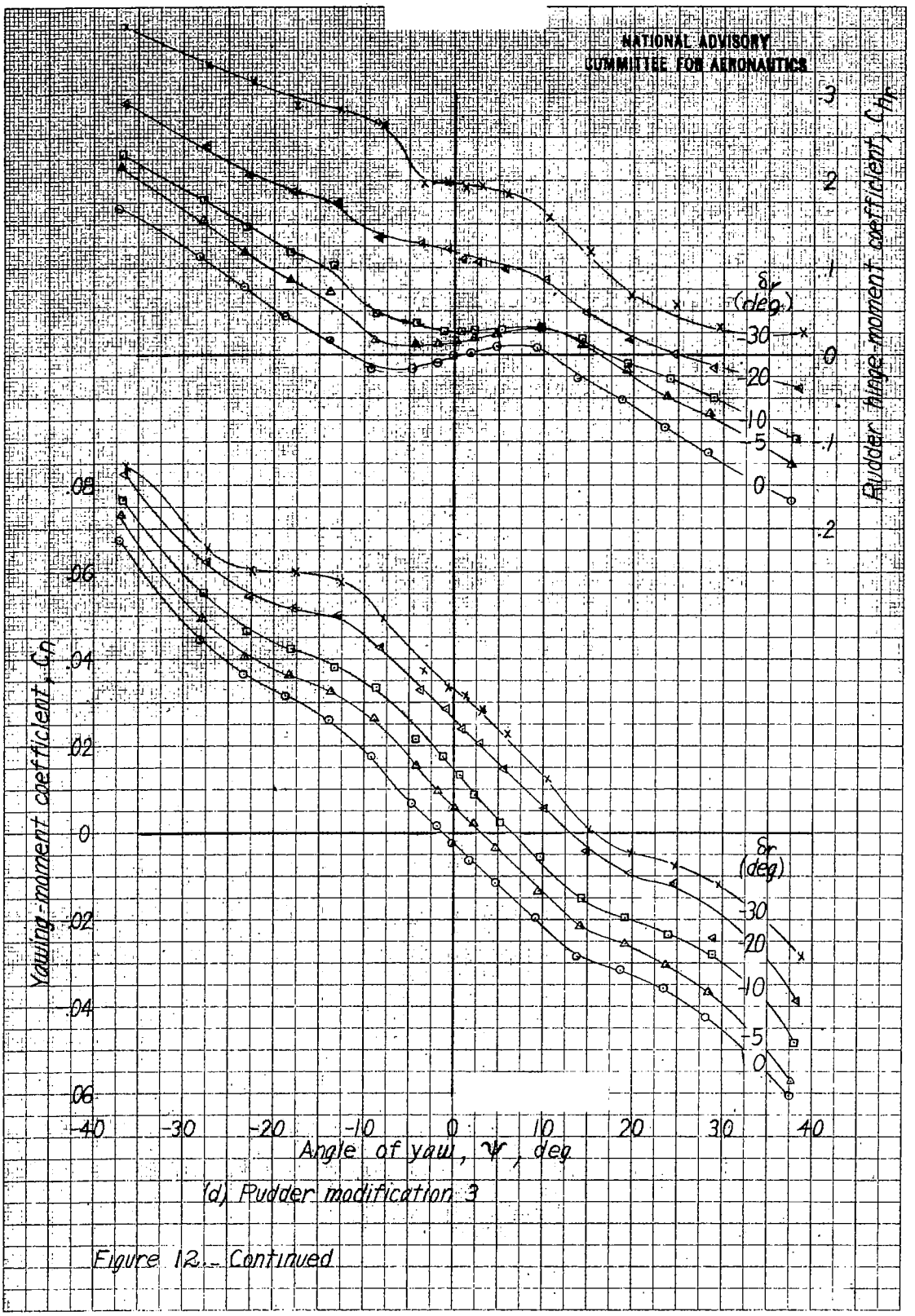

(d) Rudder modification 3

Figure 12.- Continued

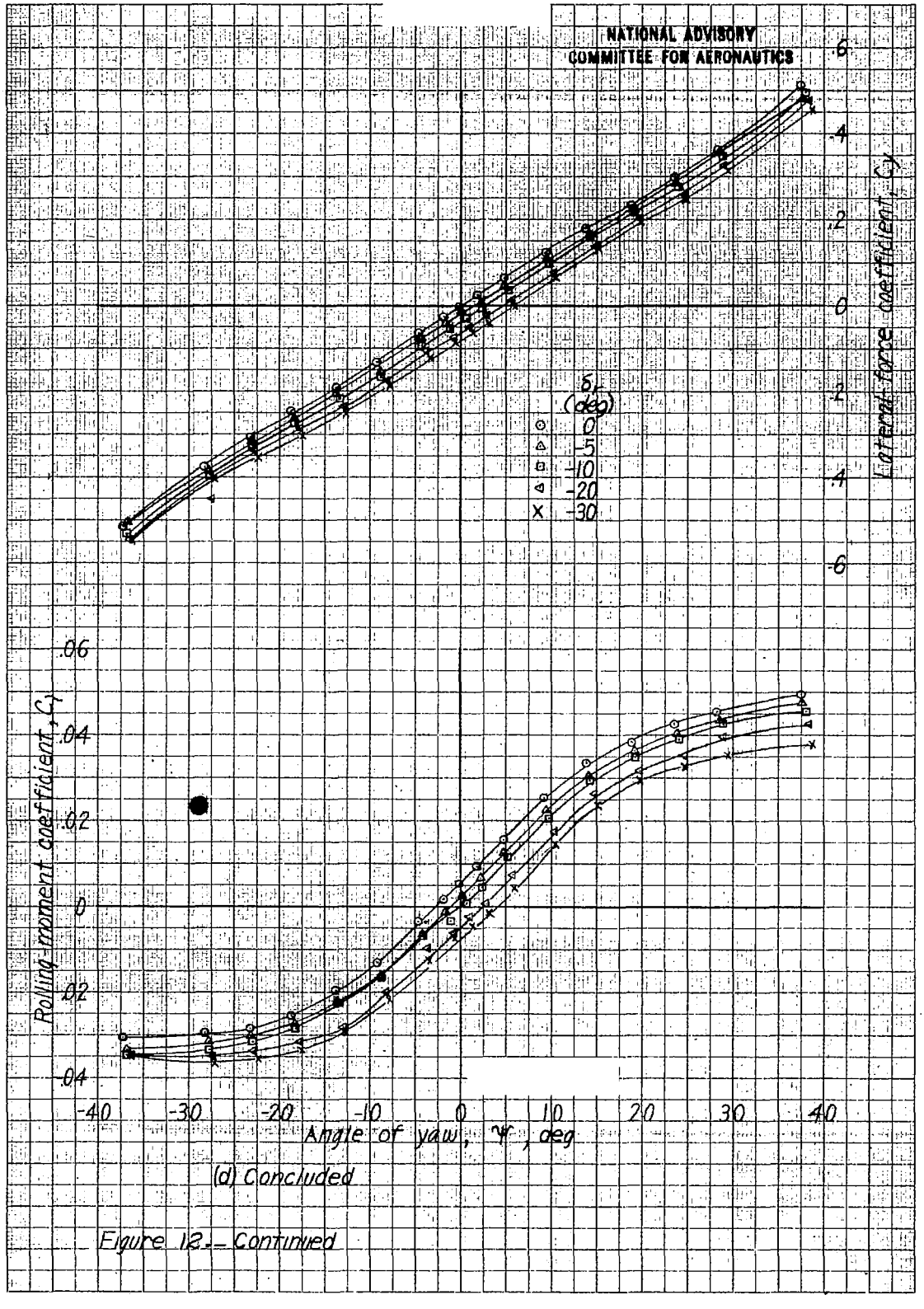

(d) Concluded

Figure 12.-- Continued

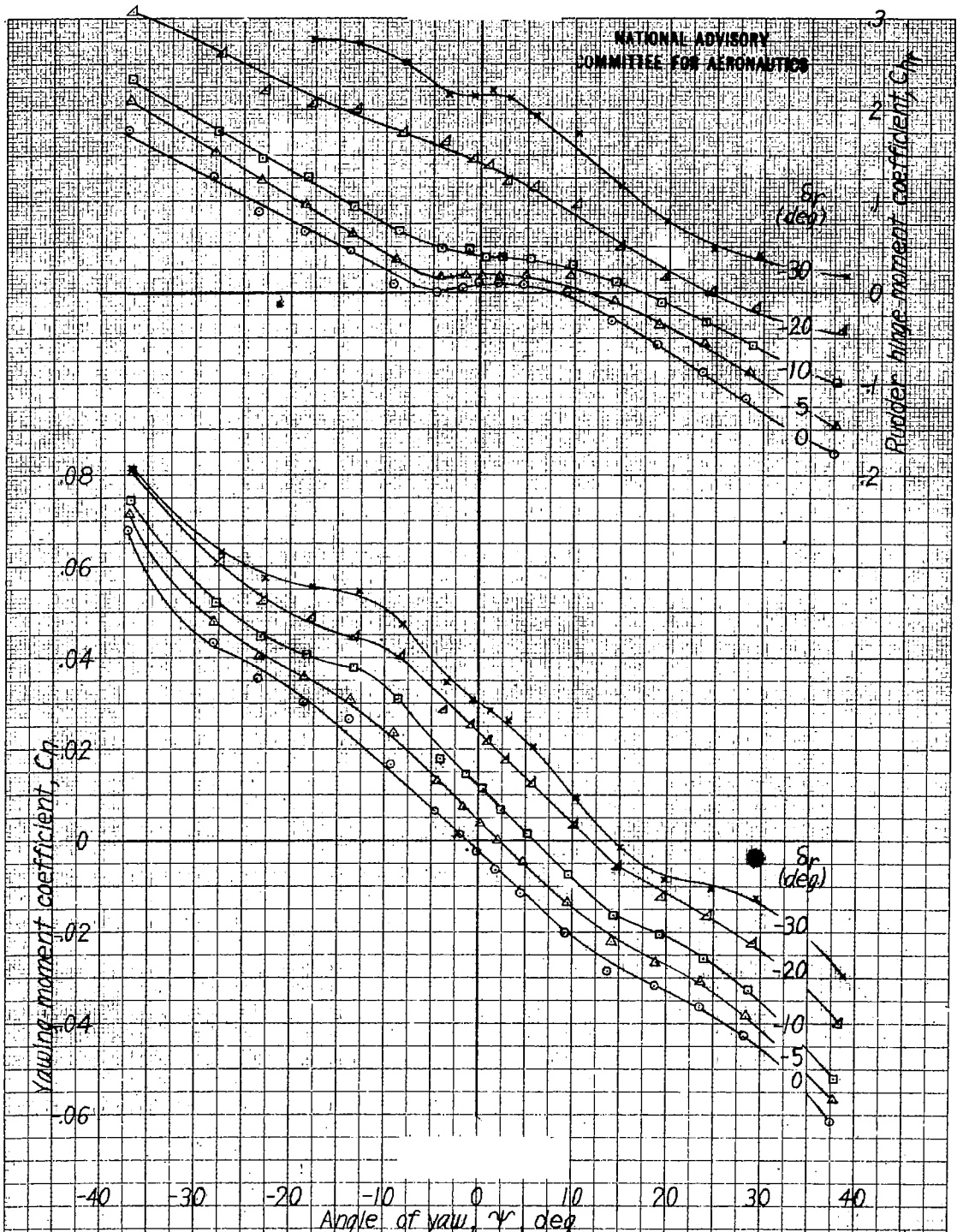

(e) Rudder modification 4

Figure 12.- Continued

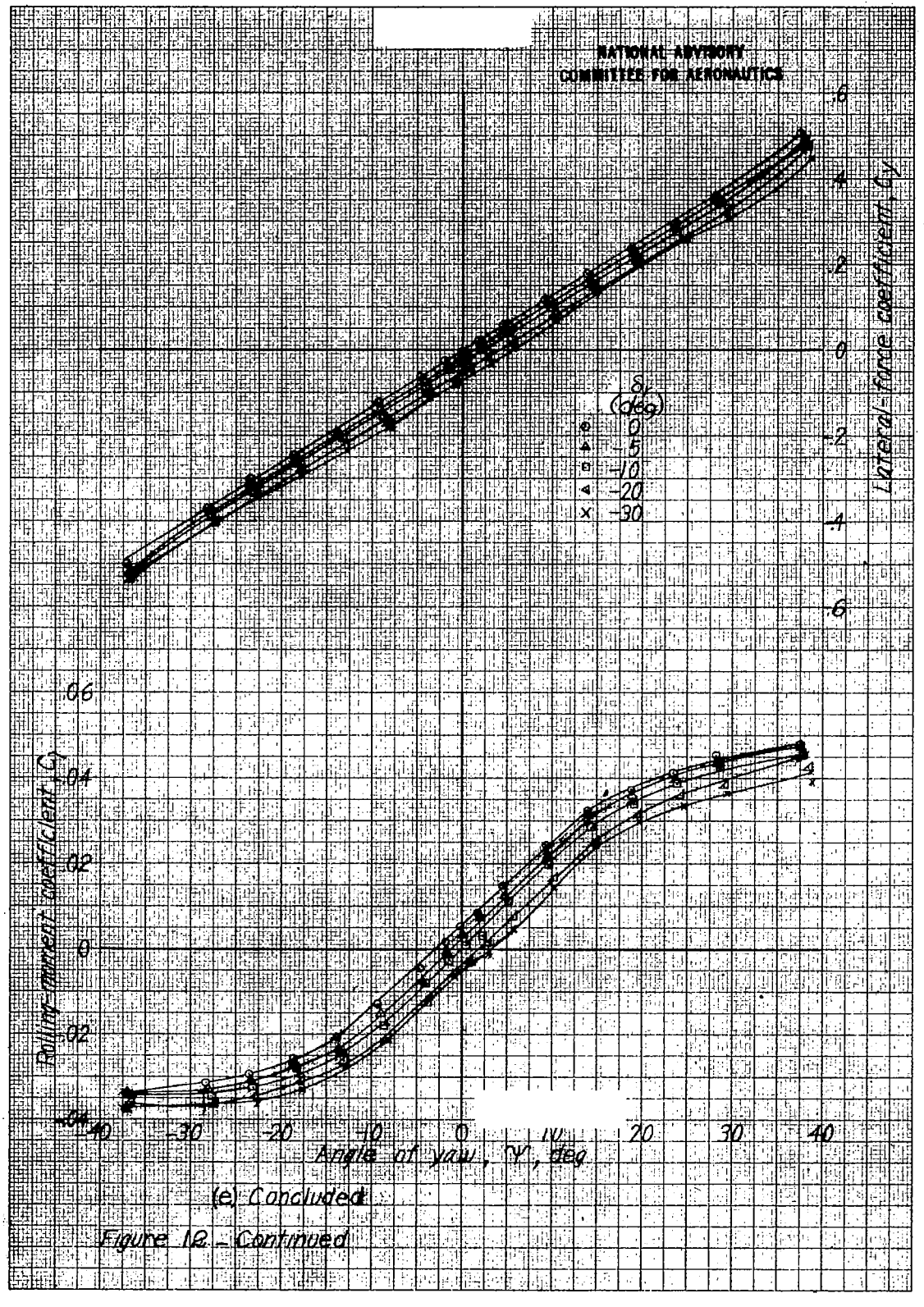

(e) Concluded.

Figure 12.- Continued.

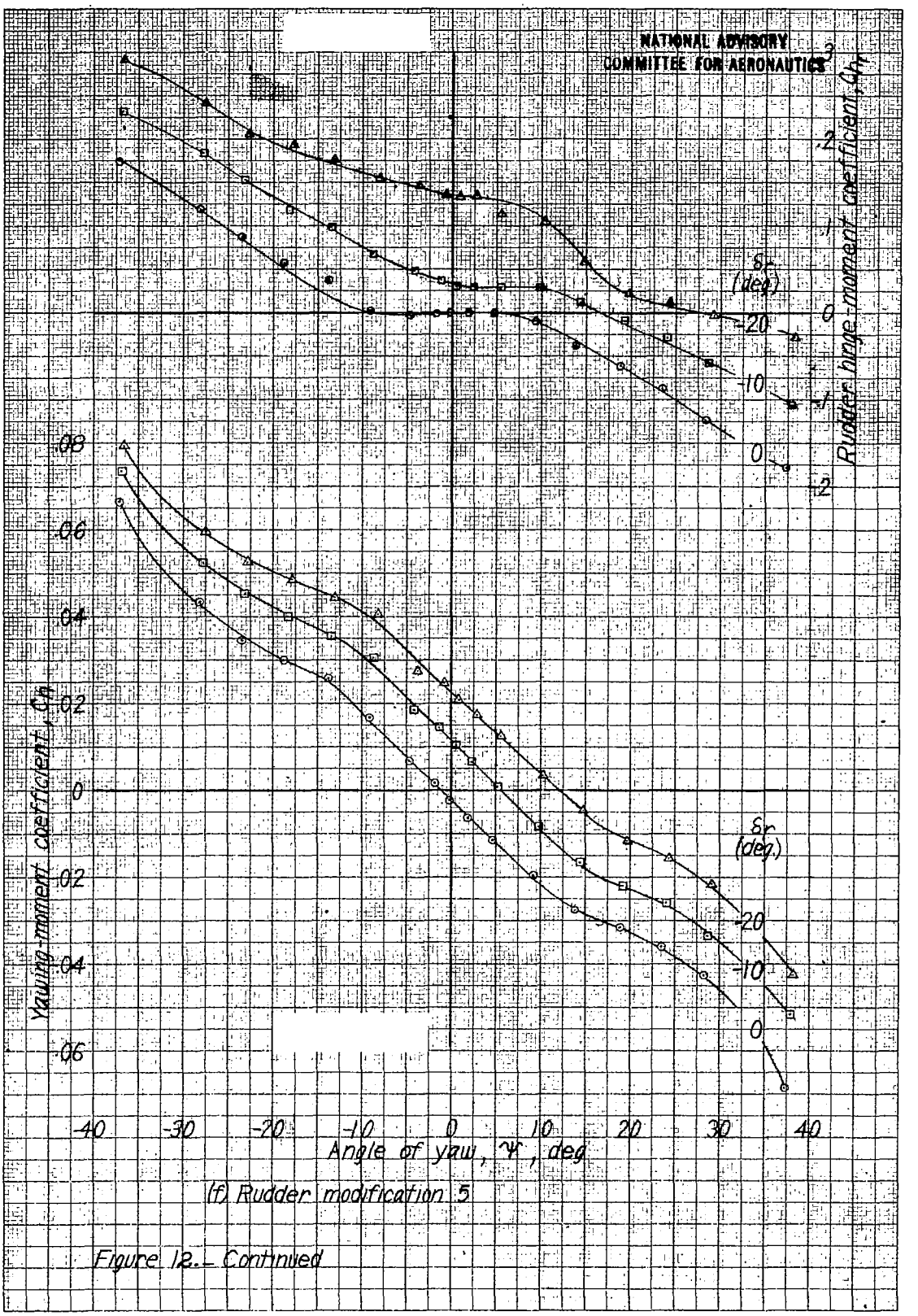

(f) Rudder modification 5

Figure 12.- Continued

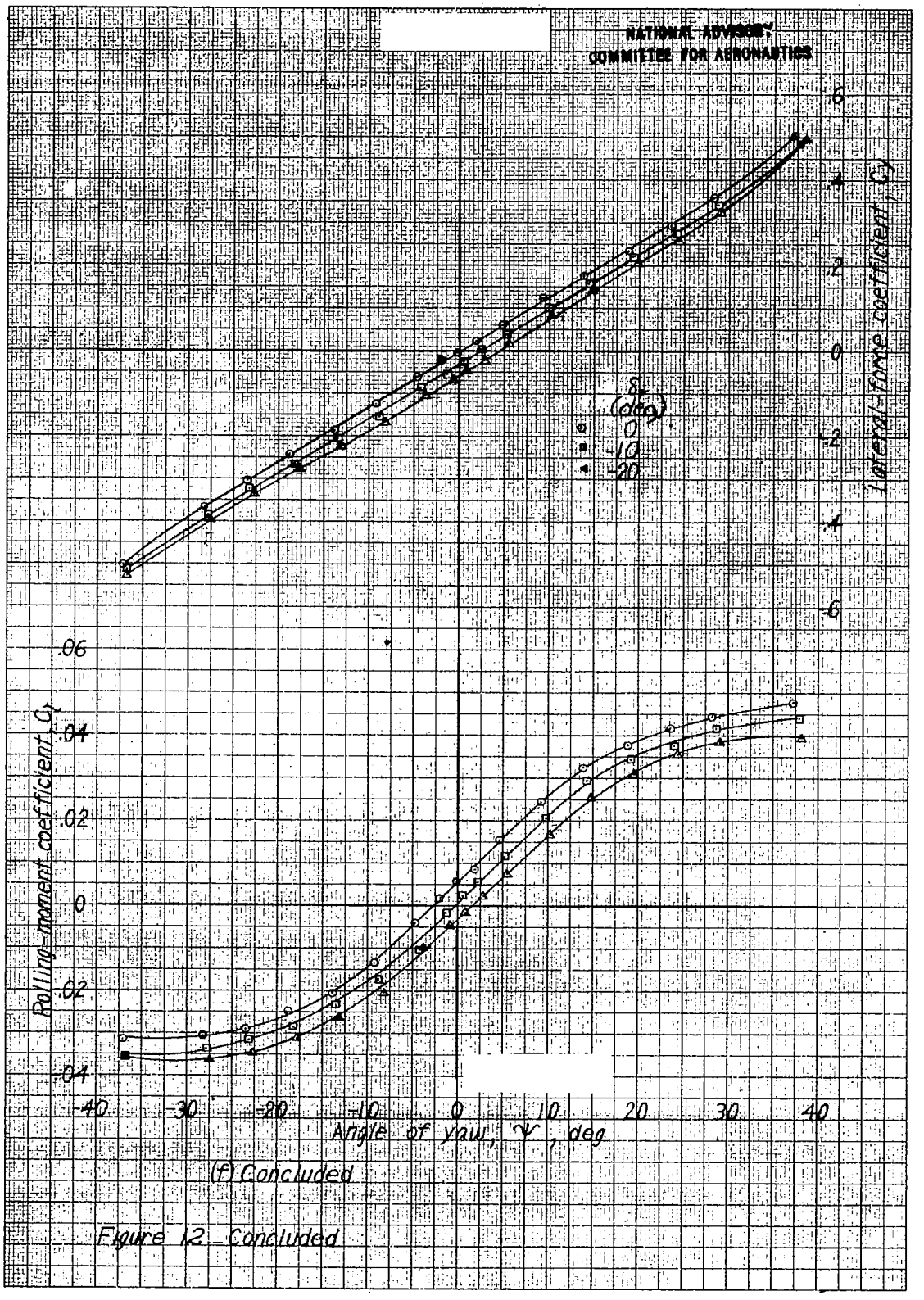

(f) Concluded

Figure 12.- Concluded

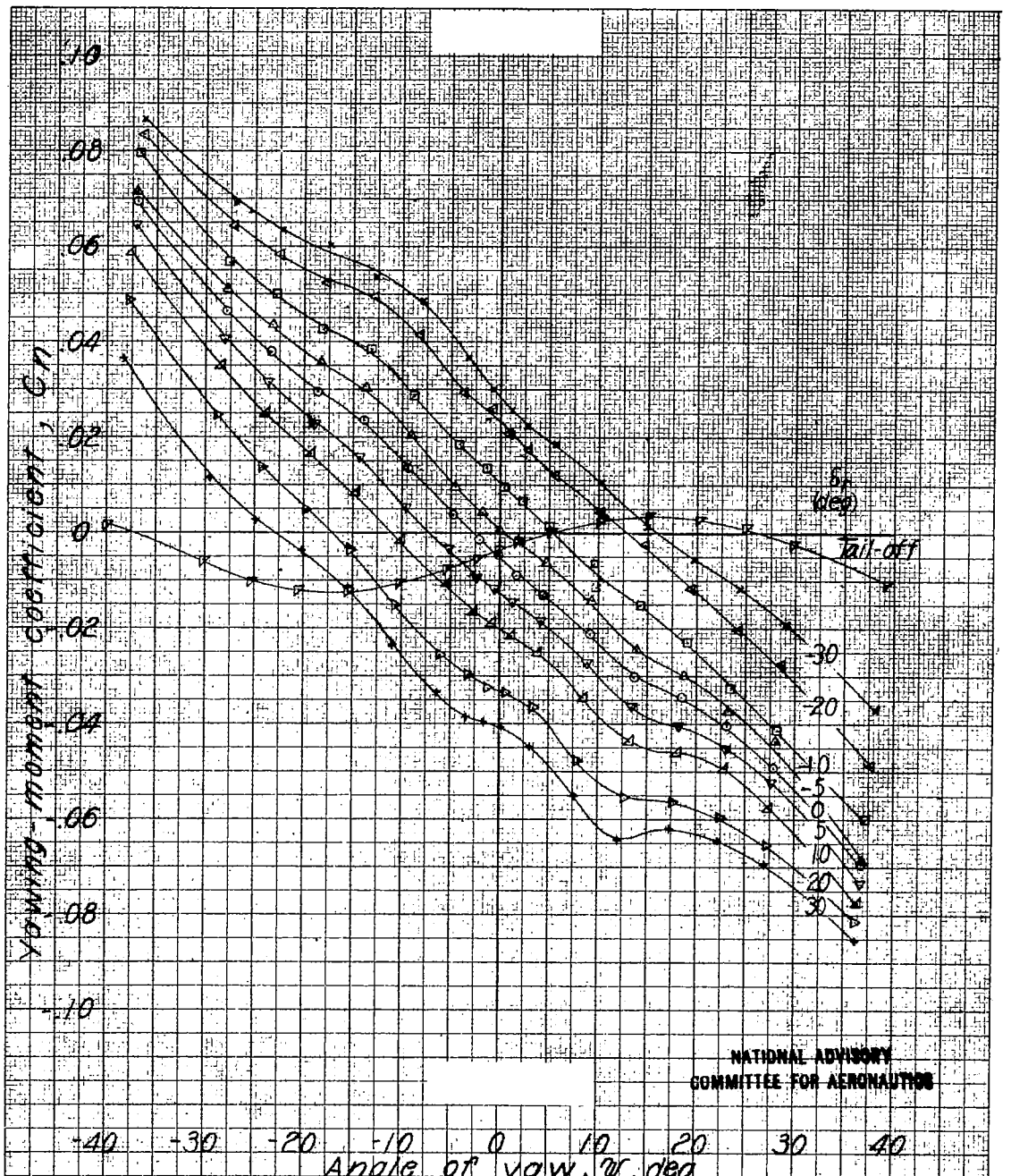

(a) Windmilling, cruising configuration, $\alpha = 11.0$, $C_L = 1.14$

Figure 13.- Effect of rudder deflection on the aerodynamic characteristics in yaw of a 0.15 scale model of the XBTK-1 prototype airplane.

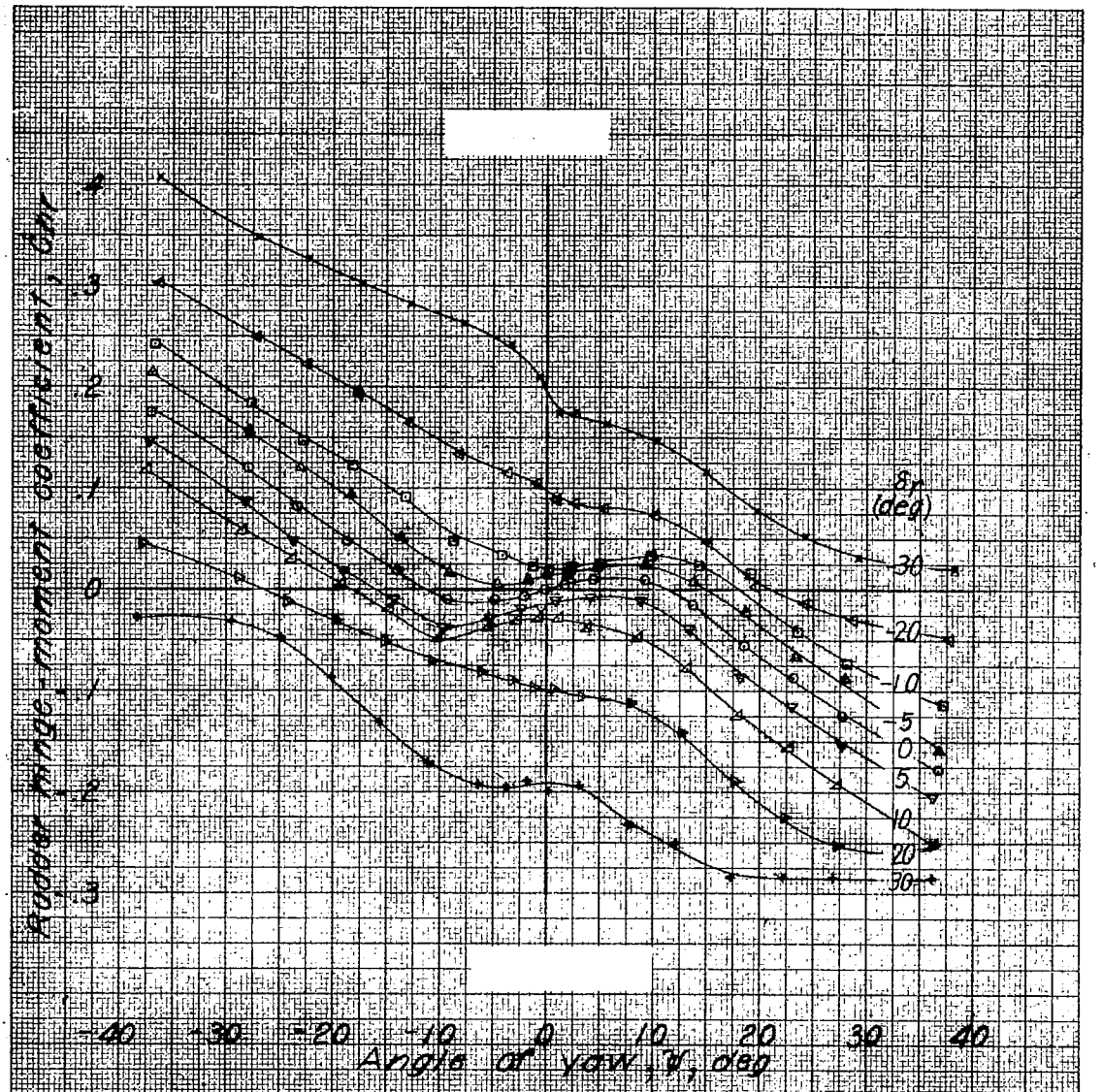

(a) Continued

Figure 13.- Continued

NATIONAL ADVISORY COMMITTEE FOR AERONAUTICS

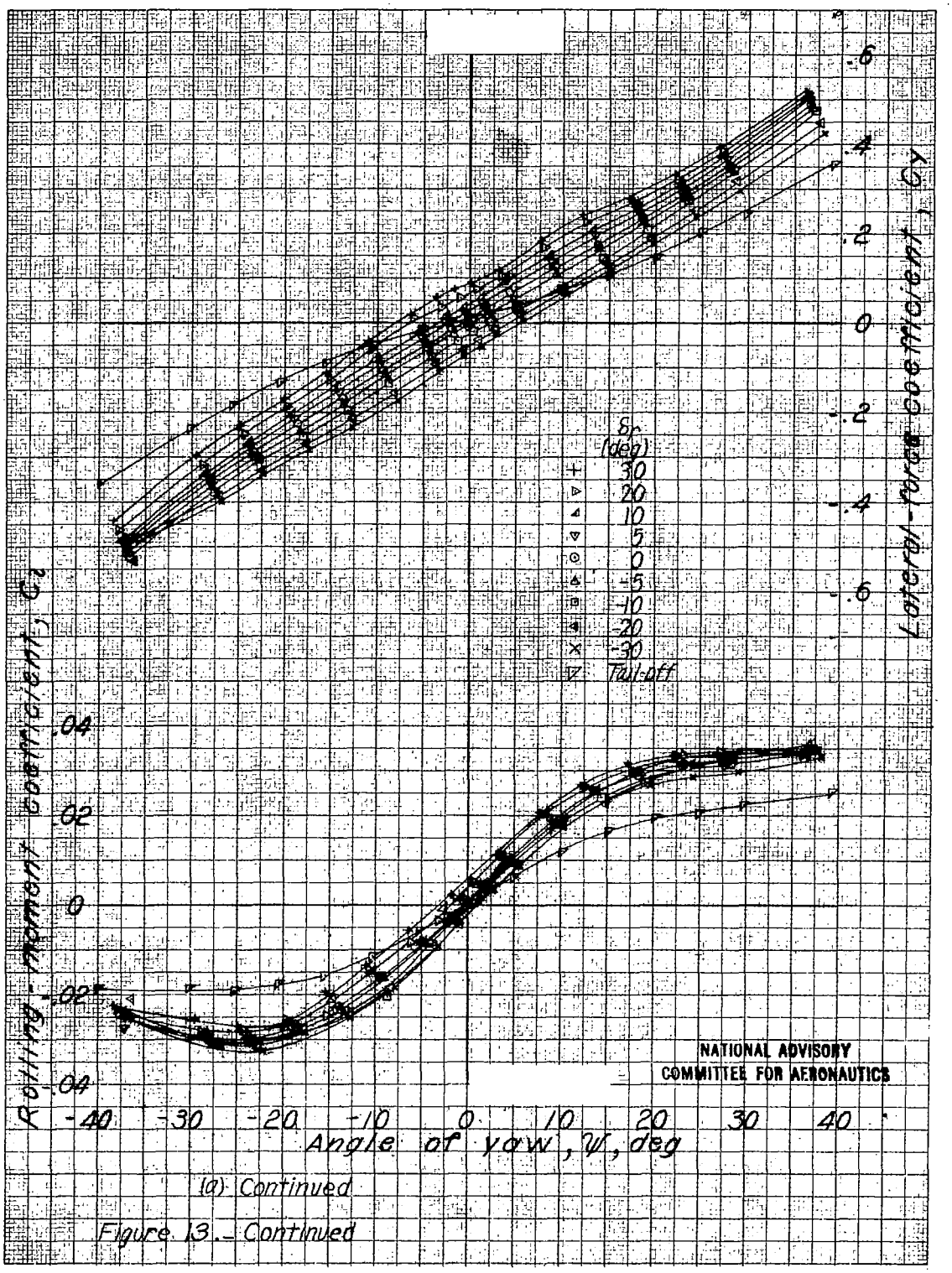

(a) Continued

Figure 13.- Continued

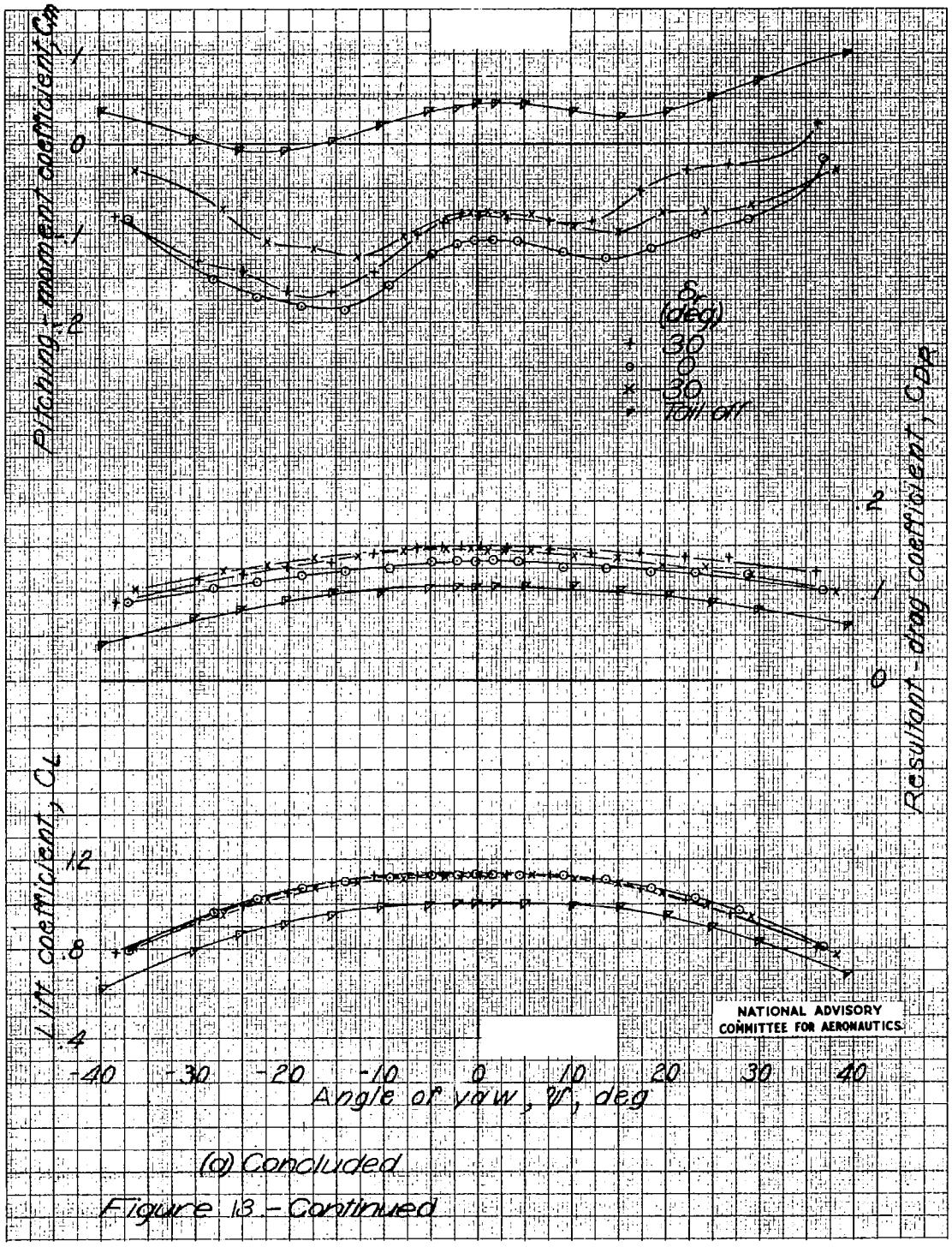

(a) Concluded

Figure 13.- Continued

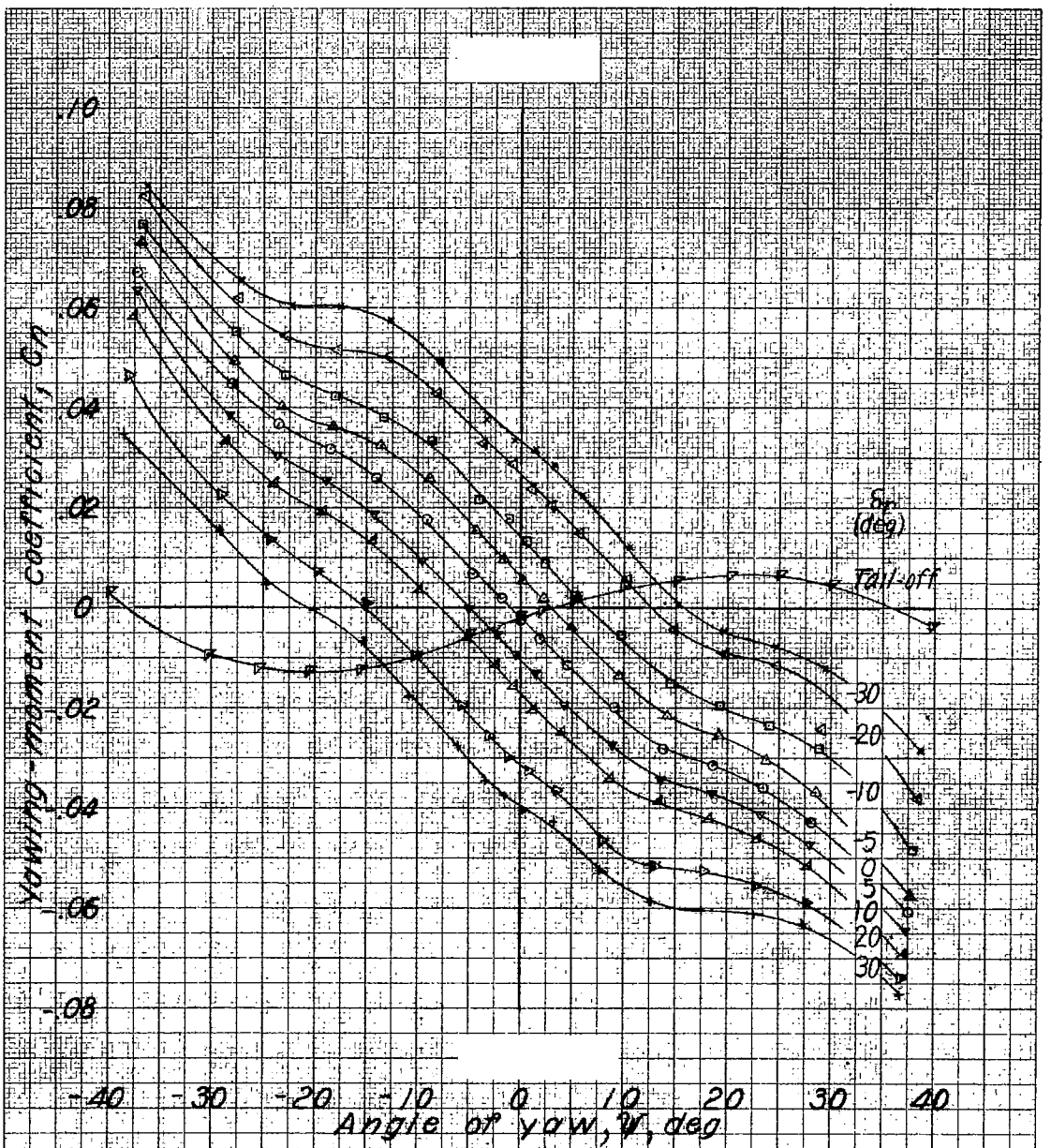

(b) Take-off power, cruising configuration, $\alpha = -0.5$, $C_L = 0.23$

Figure 13.- Continued

NATIONAL ADVISORY
COMMITTEE FOR AERONAUTICS

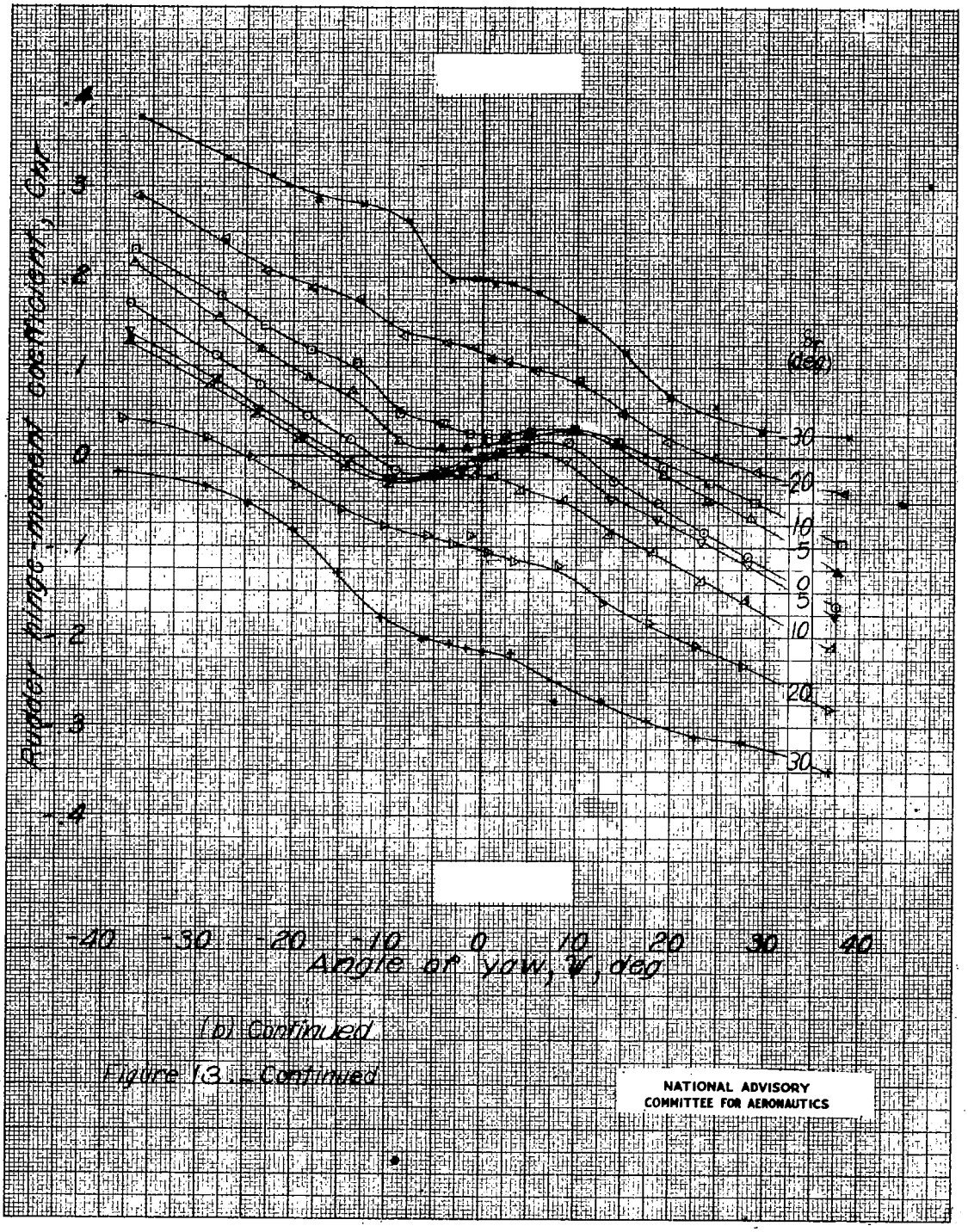

(b) Continued.

Figure 13.- Continued.

NATIONAL ADVISORY
COMMITTEE FOR AERONAUTICS

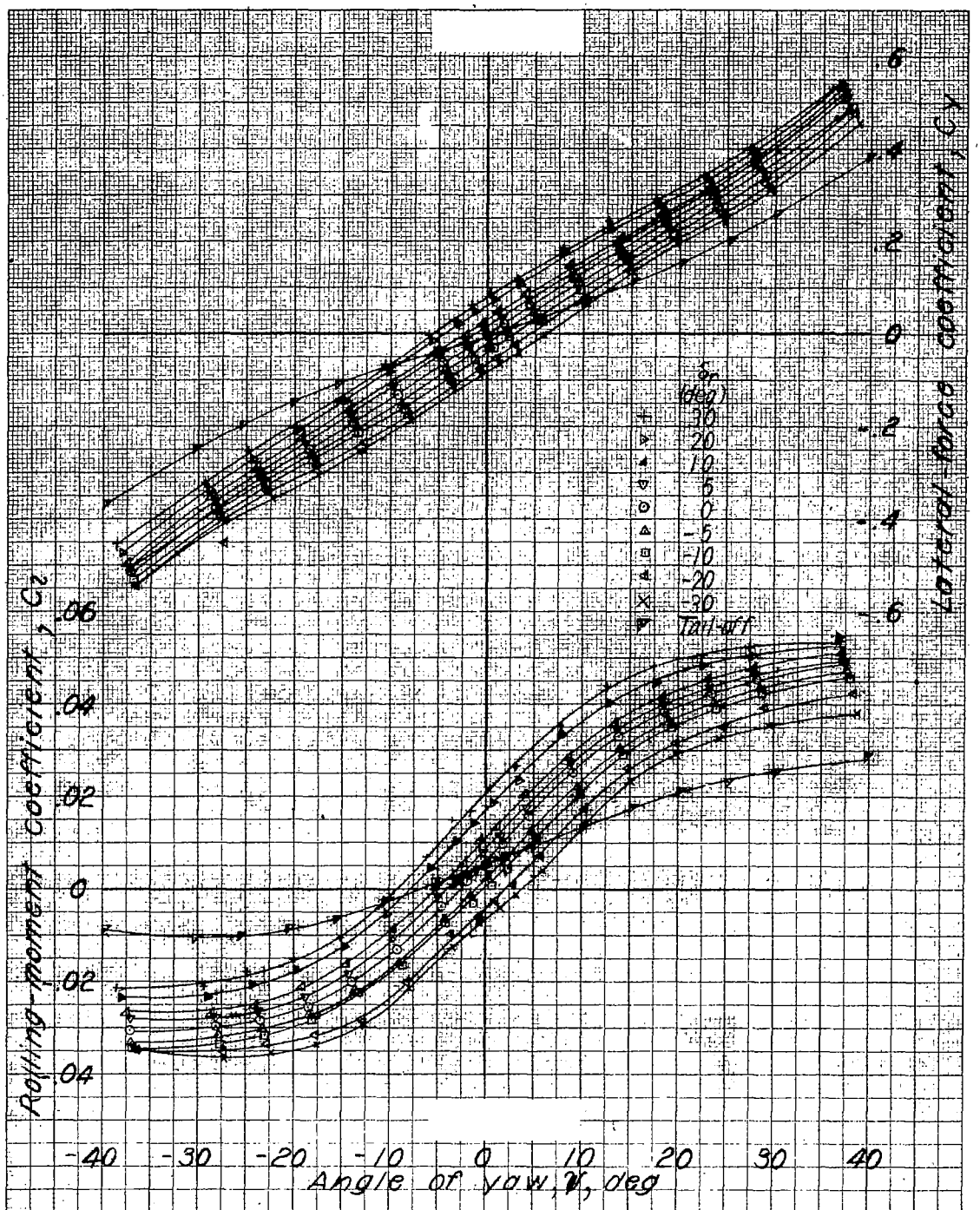

(b) Continued

Figure 13.- Continued

NATIONAL ADVISORY
COMMITTEE FOR AERONAUTICS

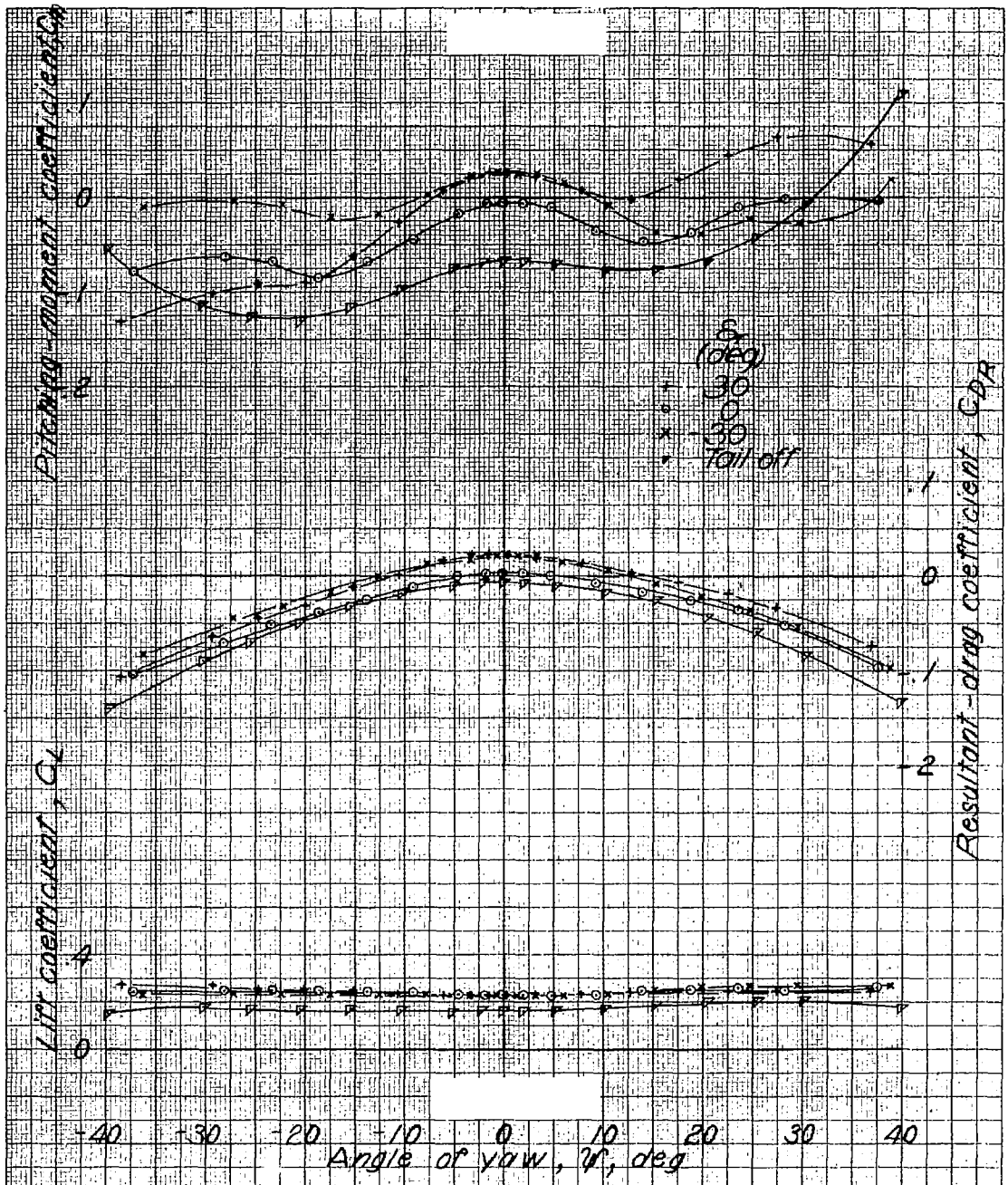

NATIONAL ADVISORY COMMITTEE FOR AERONAUTICS

(b) Concluded

Figure 13.- Continued

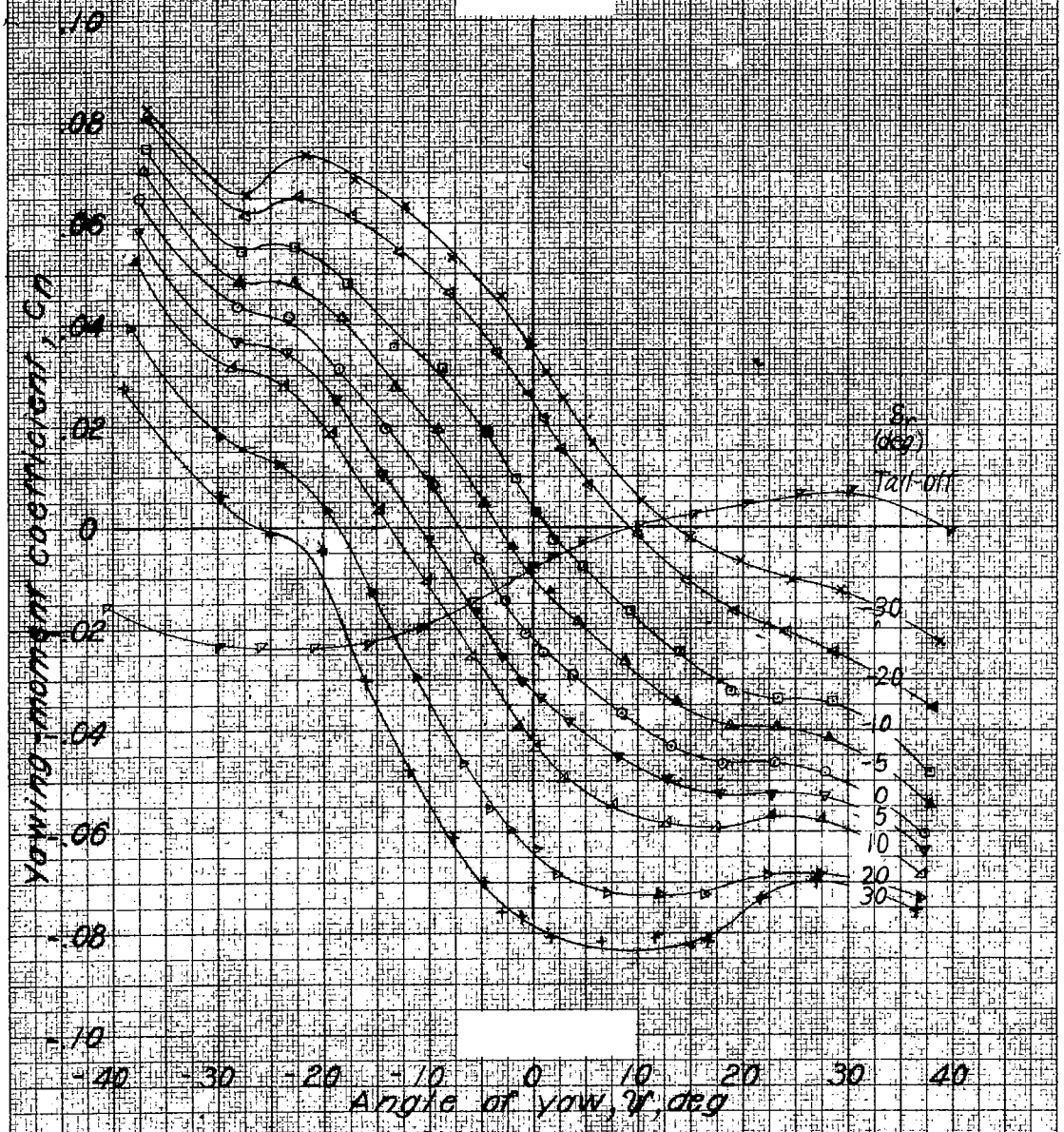

(c) Take-off power, cruising configuration, $\alpha = 7.7$, $C_L = 1.03$

Figure 13.- Continued

NATIONAL ADVISORY COMMITTEE FOR AERONAUTICS

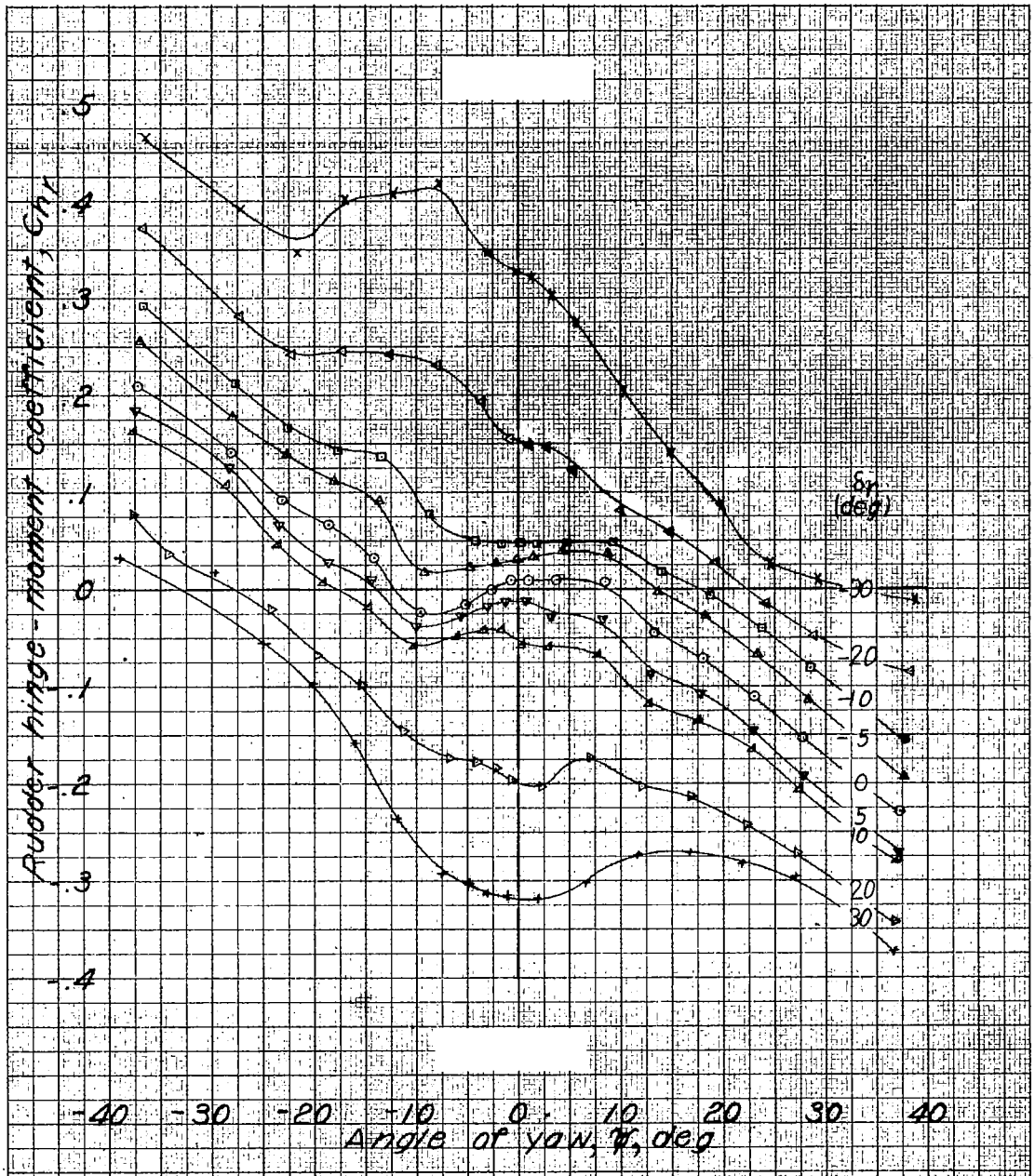

(c) Continued

Figure 13.- Continued

NATIONAL ADVISORY COMMITTEE FOR AERONAUTICS

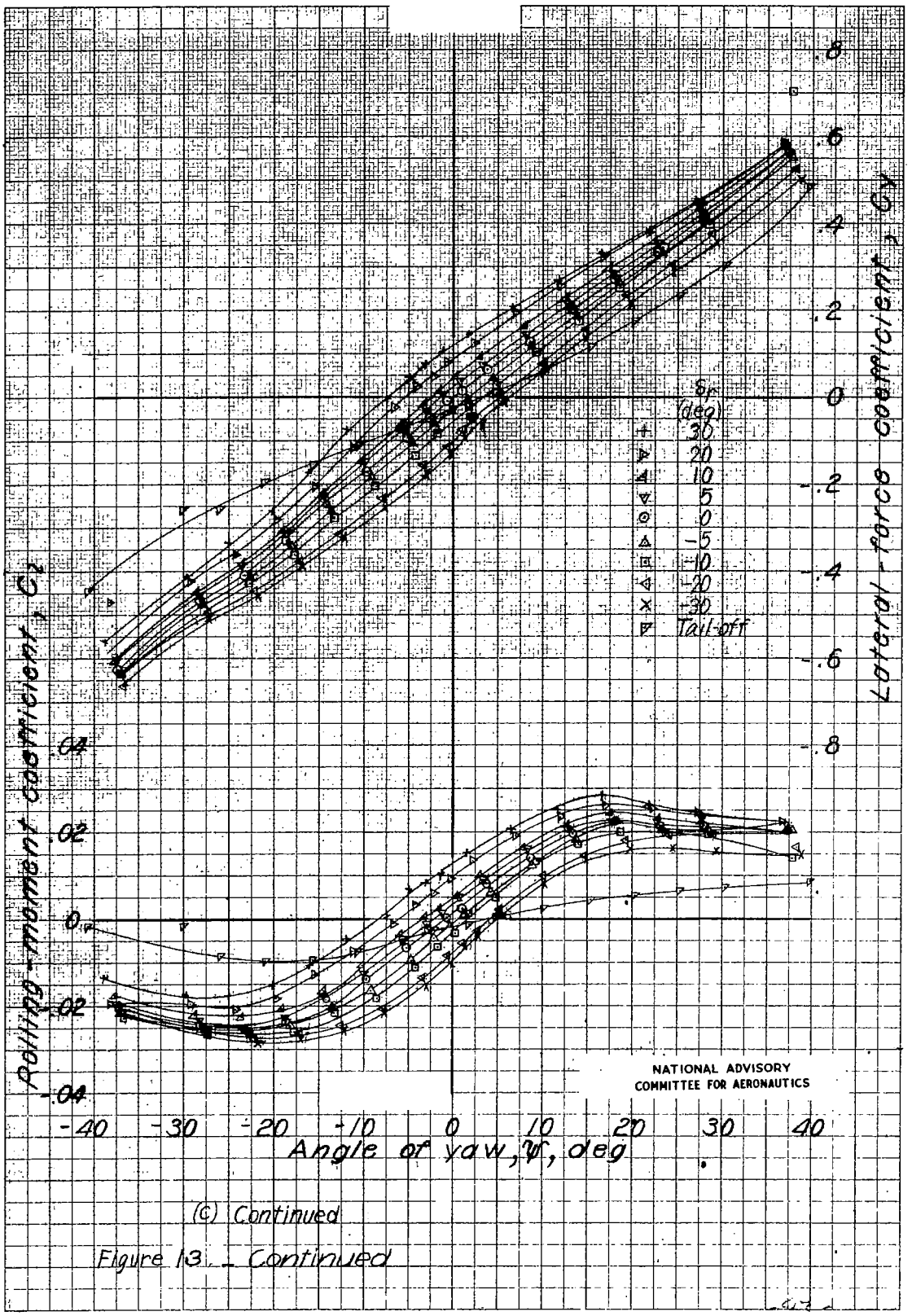

(c) Continued

Figure 13.- Continued

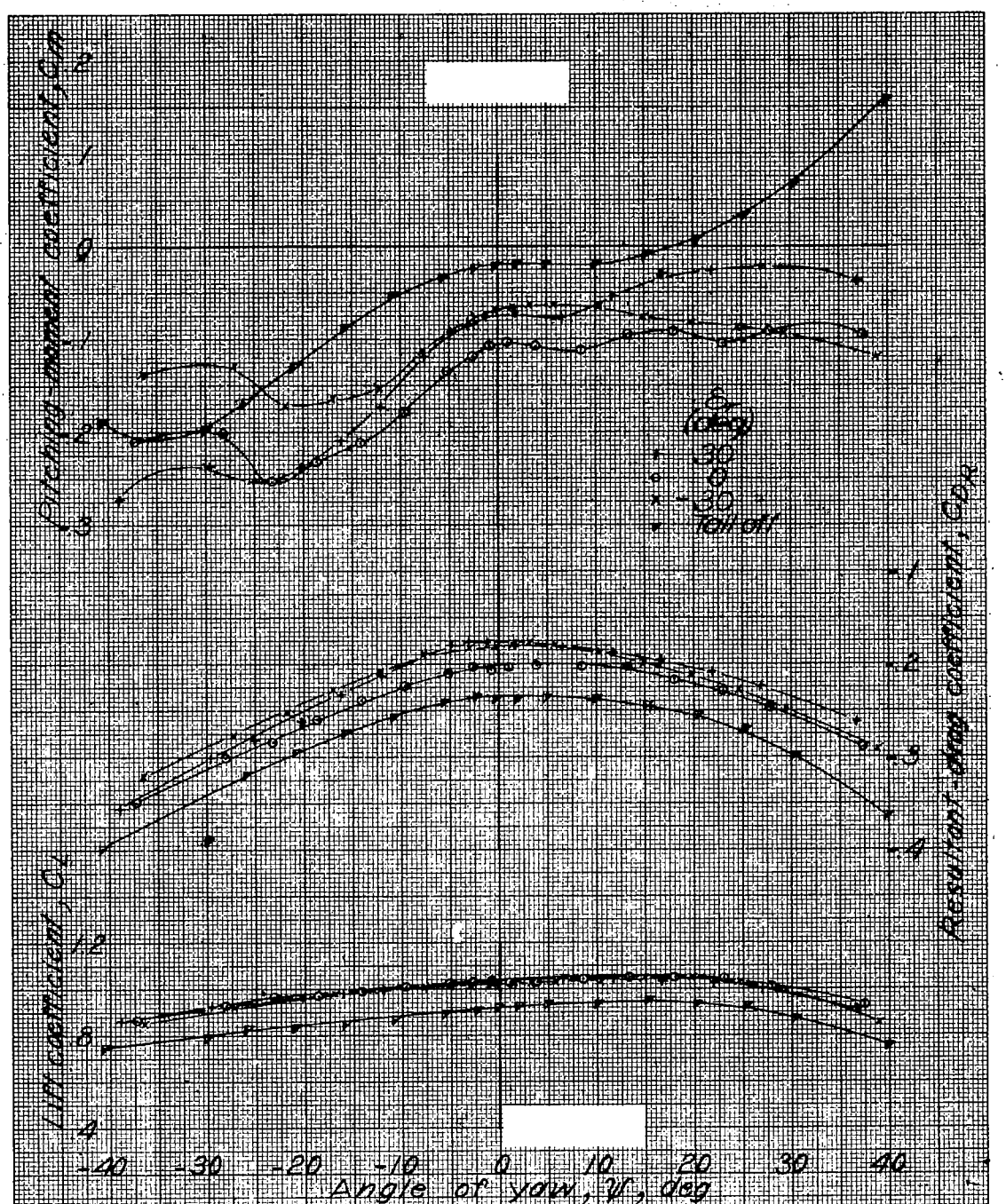

NATIONAL ADVISORY COMMITTEE FOR AERONAUTICS

(c) Concluded

Figure 13 - Continued

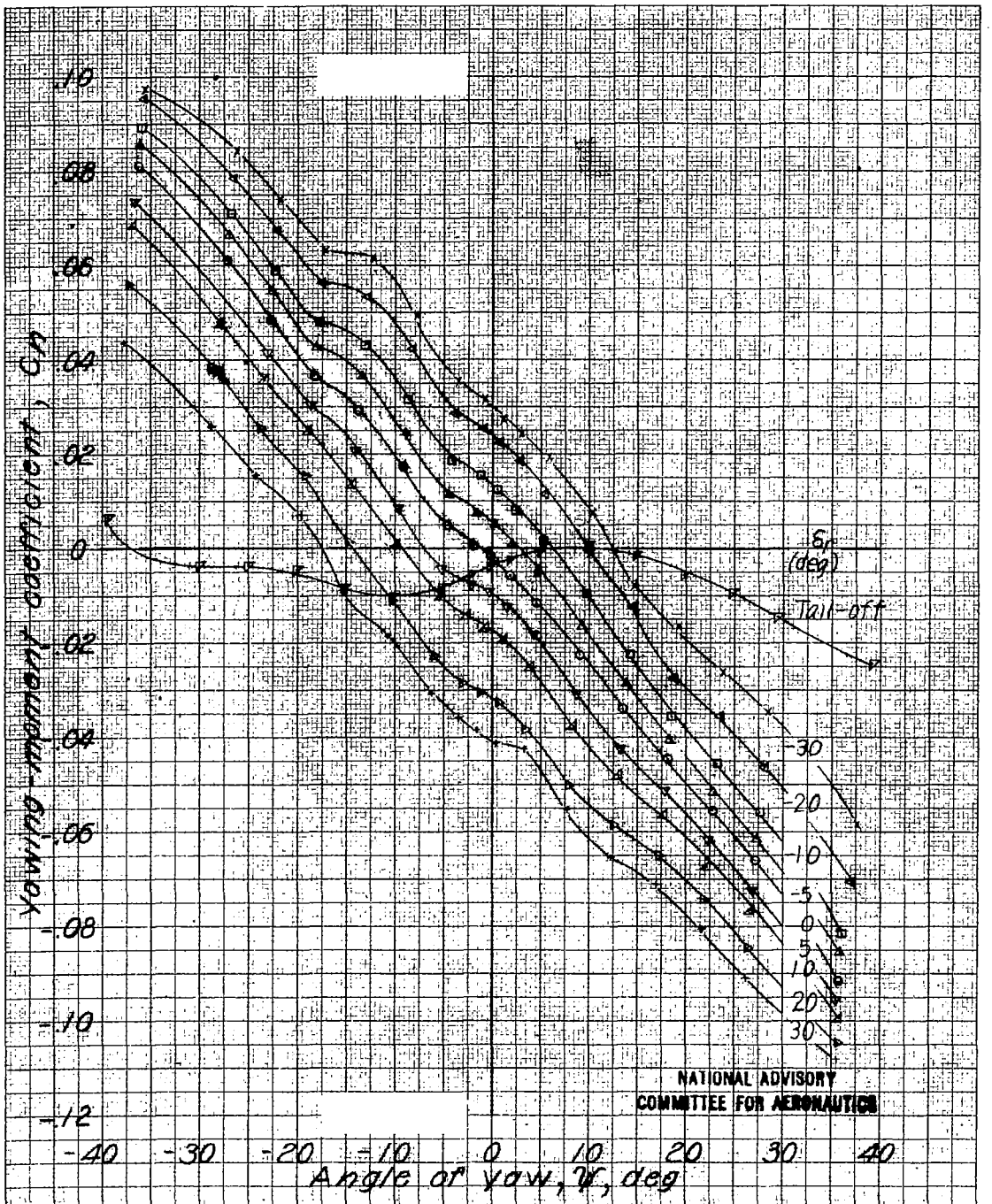

(d) Windmilling, landing configuration, $\alpha = 10.5$, $C_L = 1.63$

Figure 13.- Continued

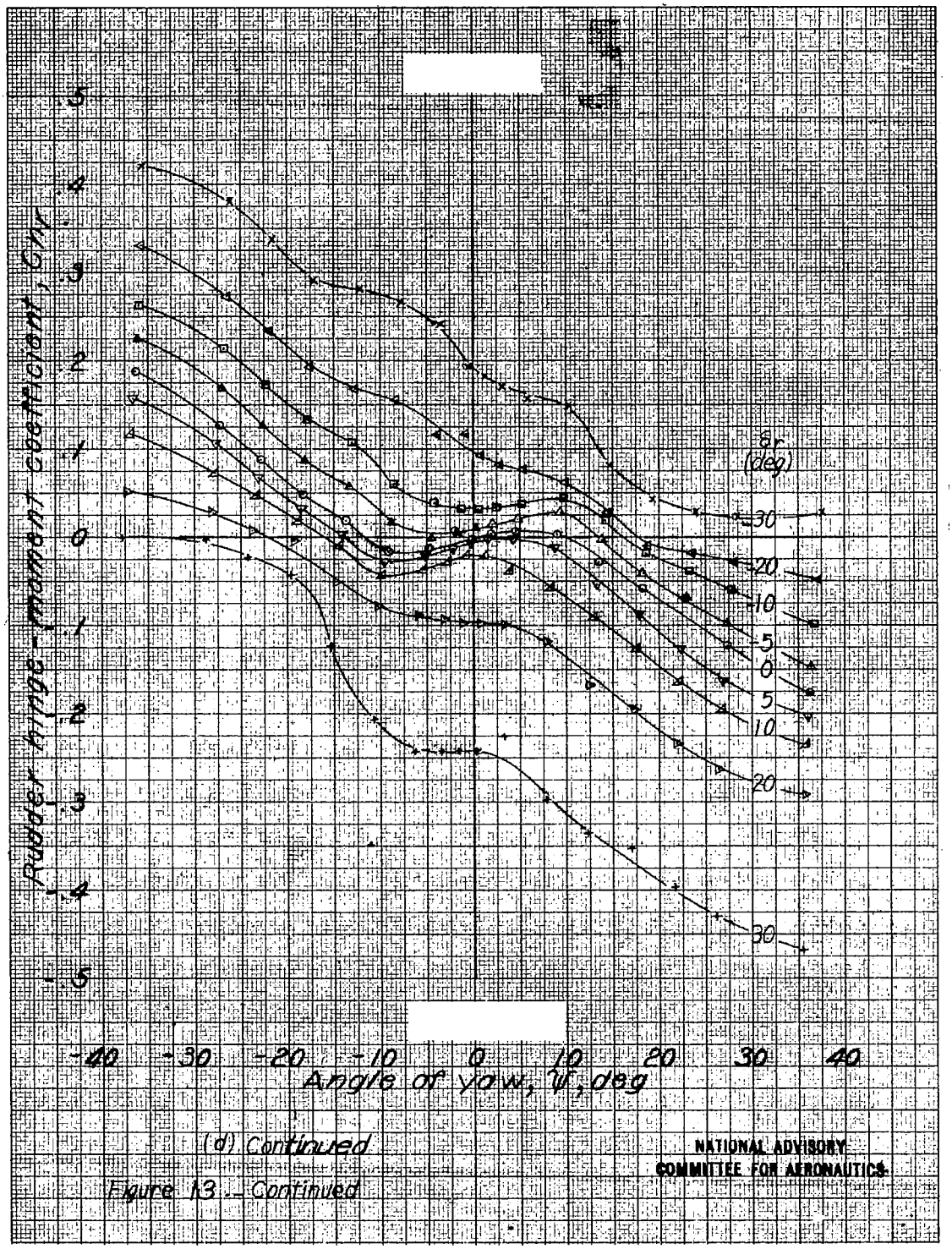

(d) Continued

Figure 13.- Continued

NATIONAL ADVISORY COMMITTEE FOR AERONAUTICS

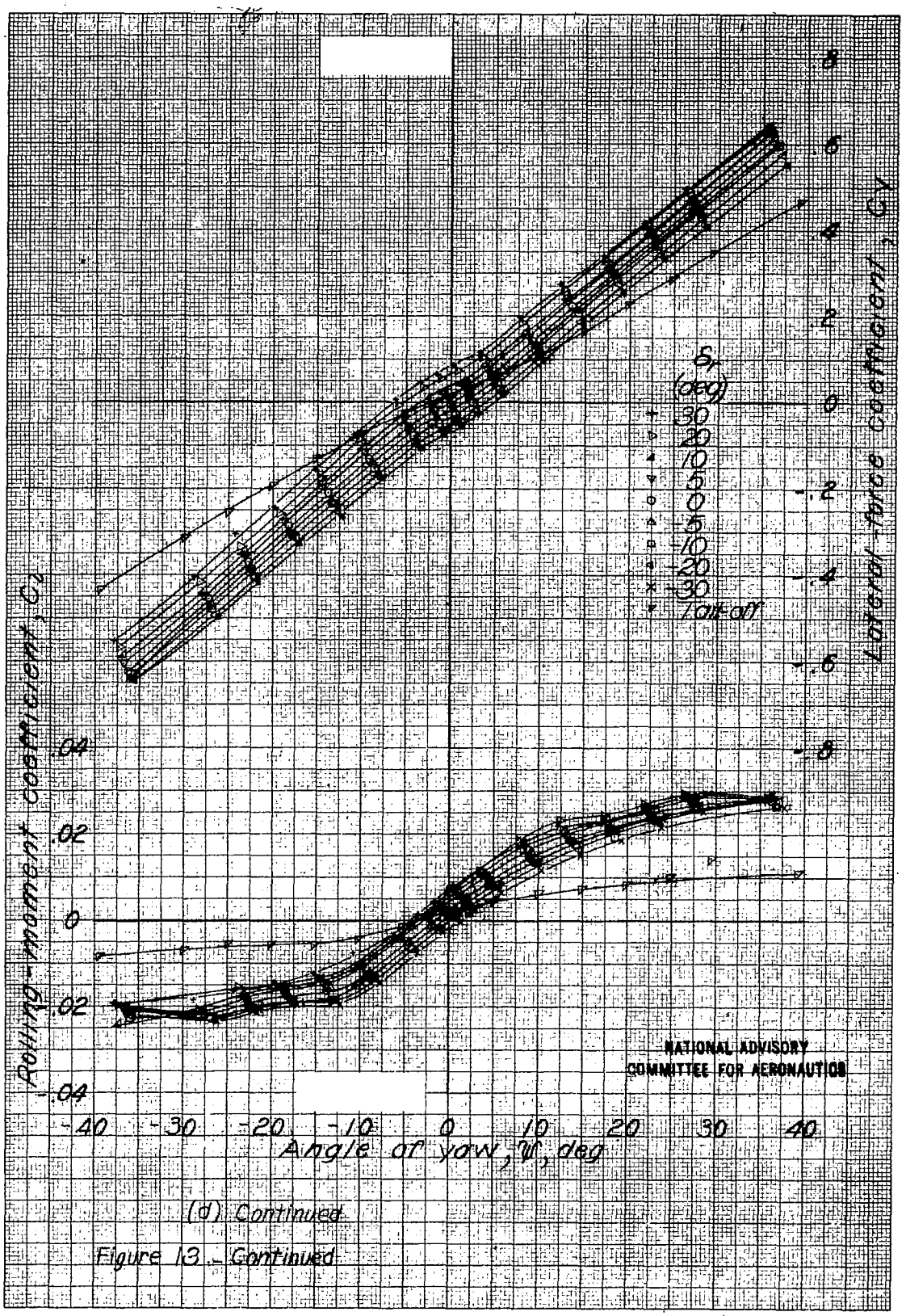

(d) Continued.

Figure 13.- Continued.

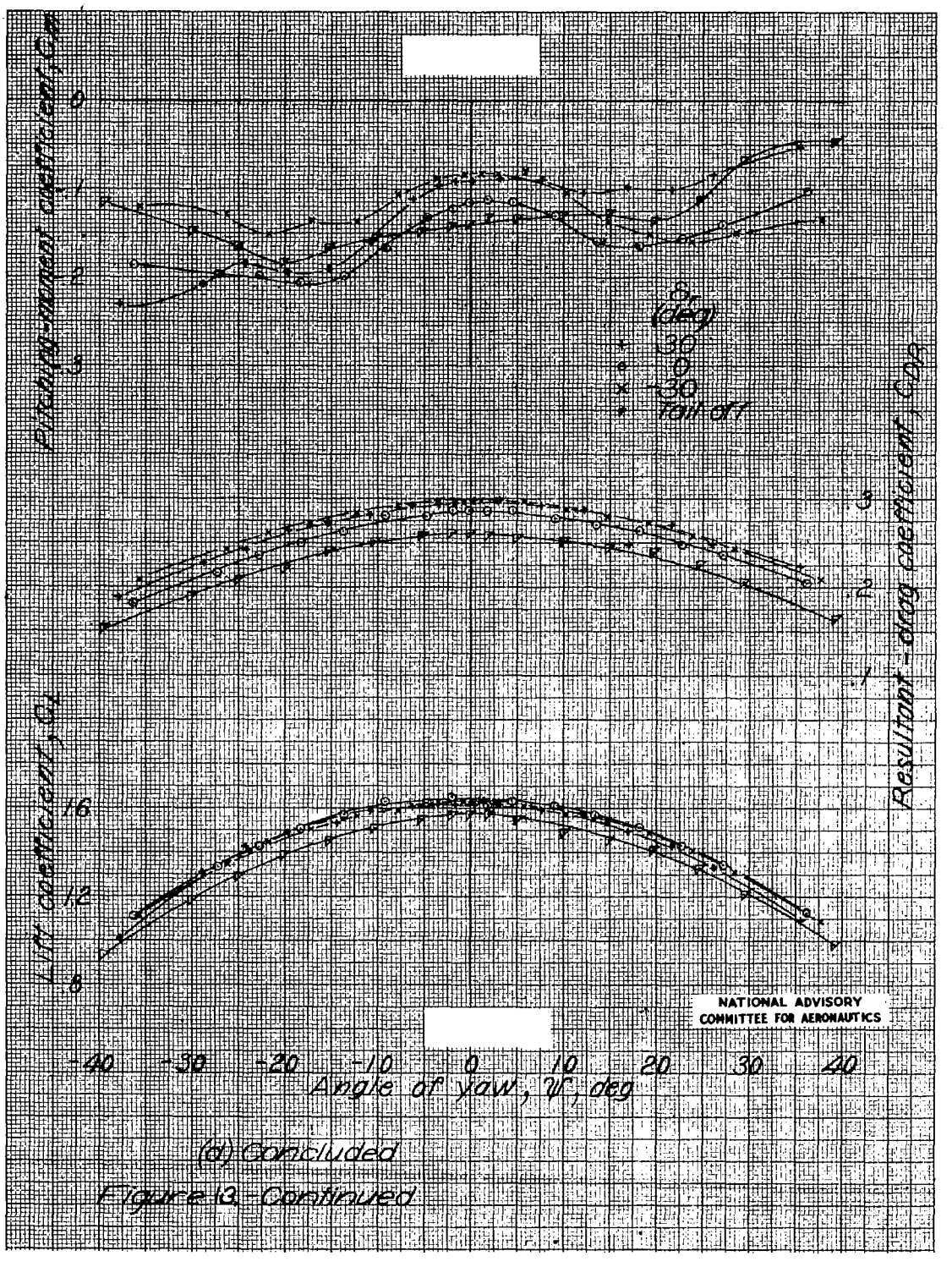

(d) Concluded

Figure 13.- Continued

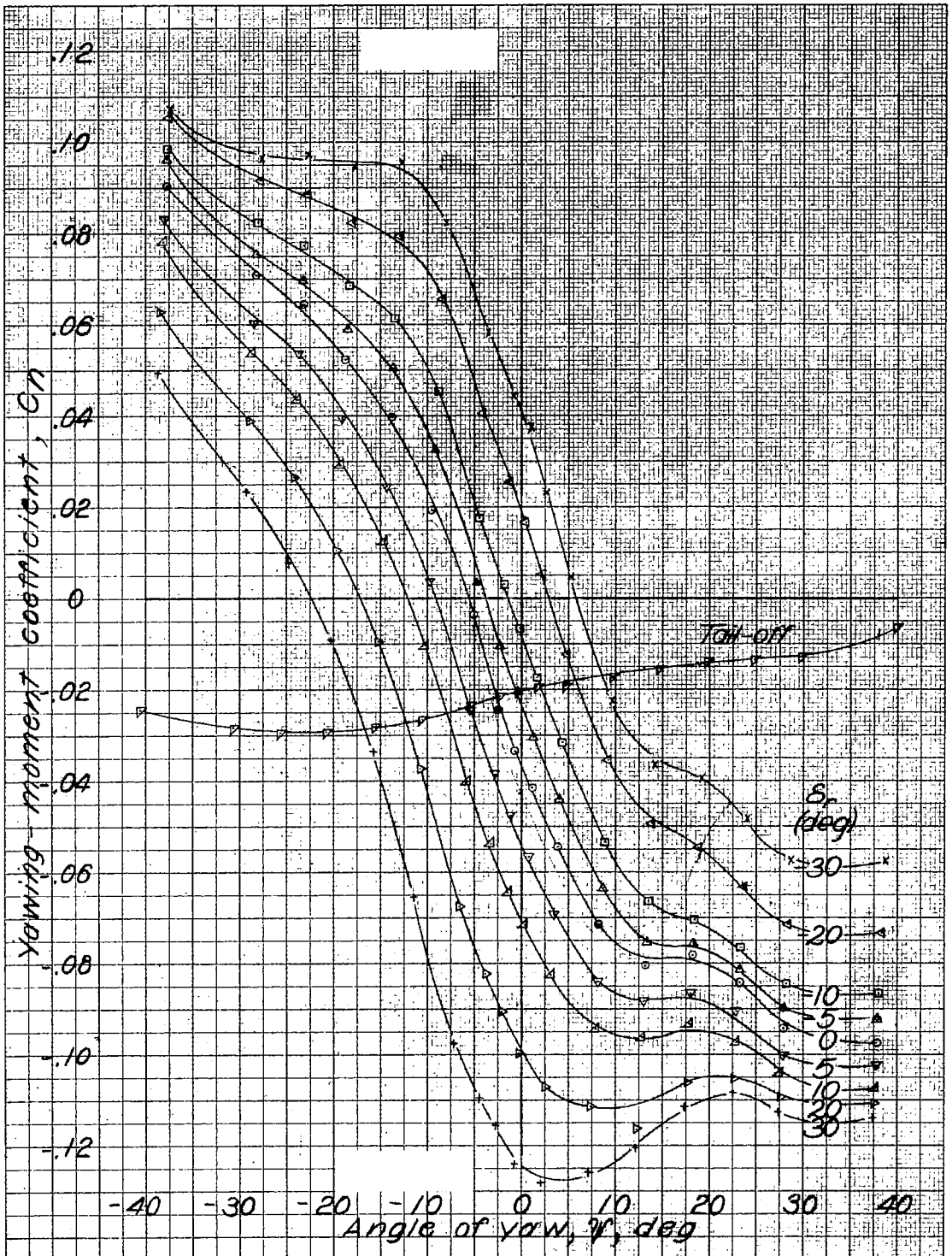

(e) Take-off power, landing configuration, $\alpha = 10.0$, $C_L = 2.06$

Figure 13 - Continued

NATIONAL ADVISORY COMMITTEE FOR AERONAUTICS

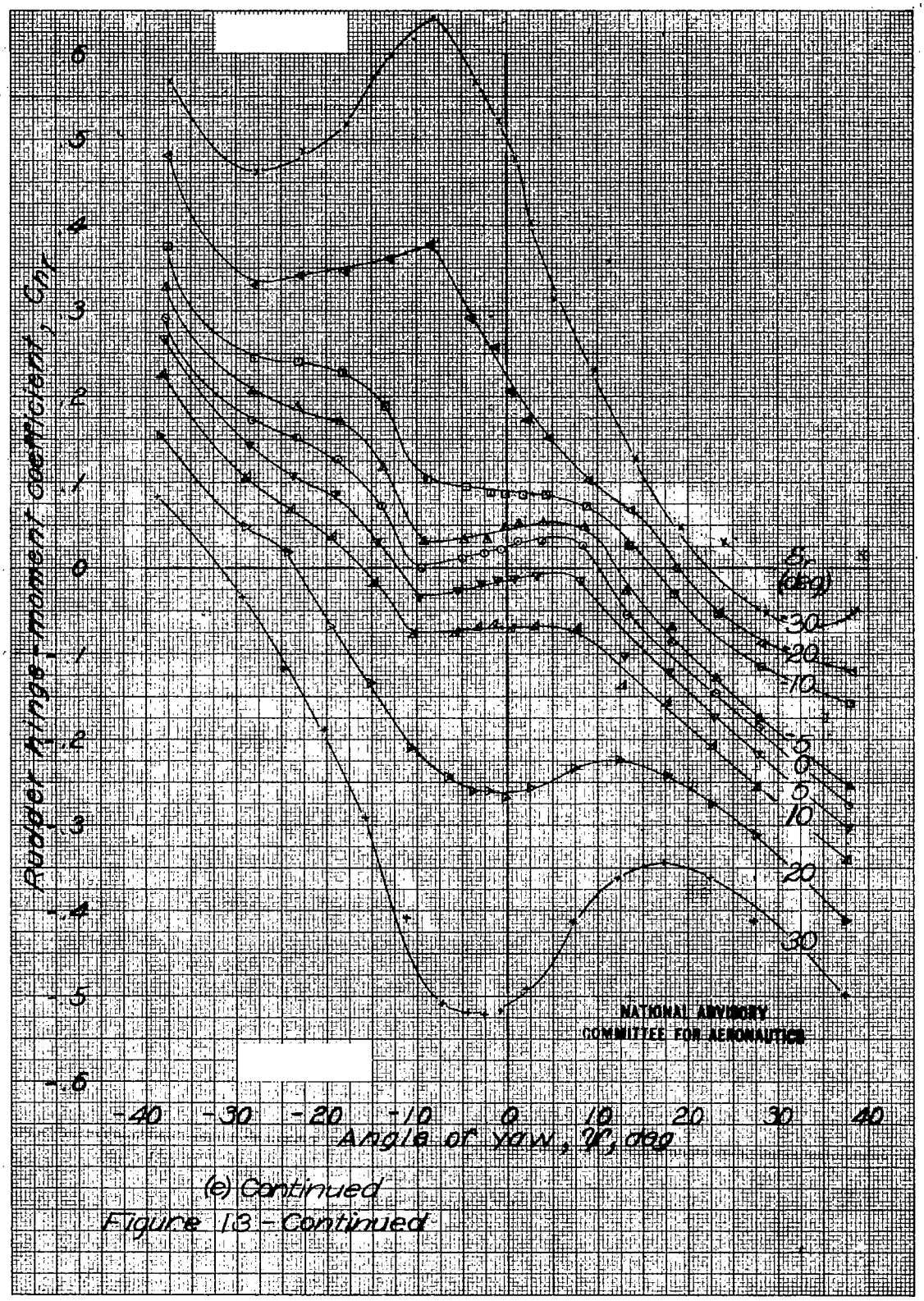

(e) Continued

Figure 13 - Continued

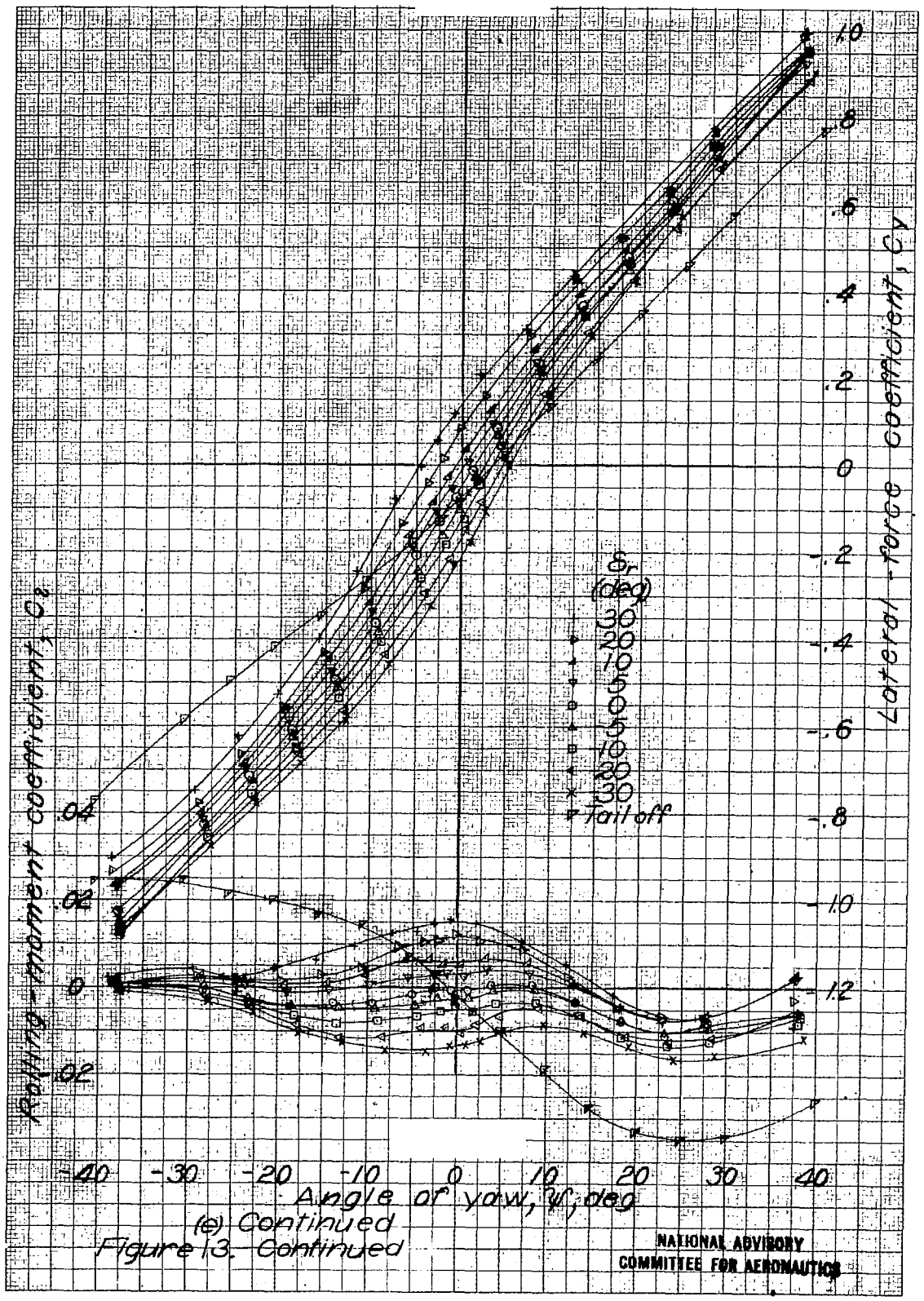

(e) Continued

Figure 13. Continued

NATIONAL ADVISORY
COMMITTEE FOR AERONAUTICS

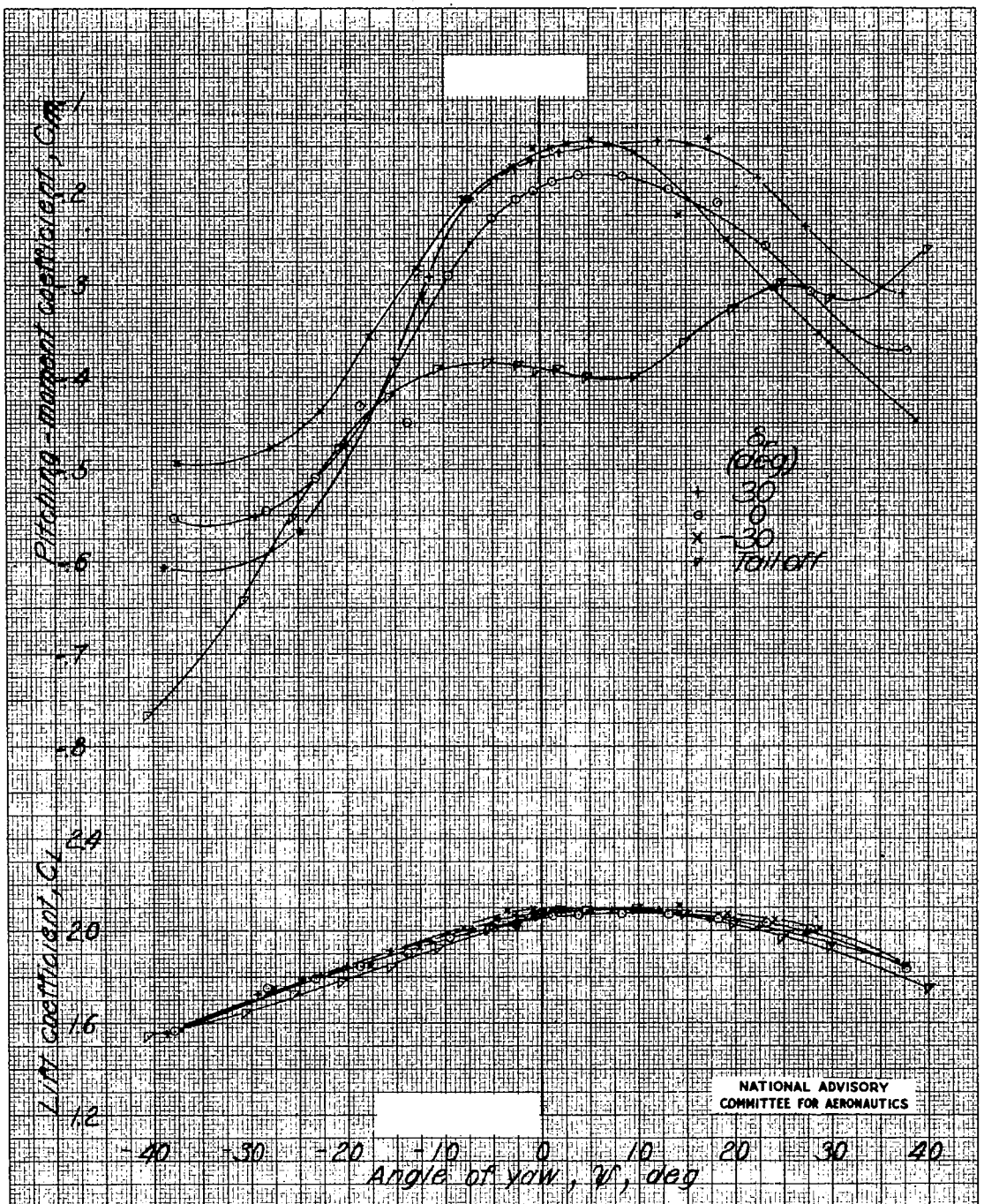

(e) Continued

Figure 13 - Continued

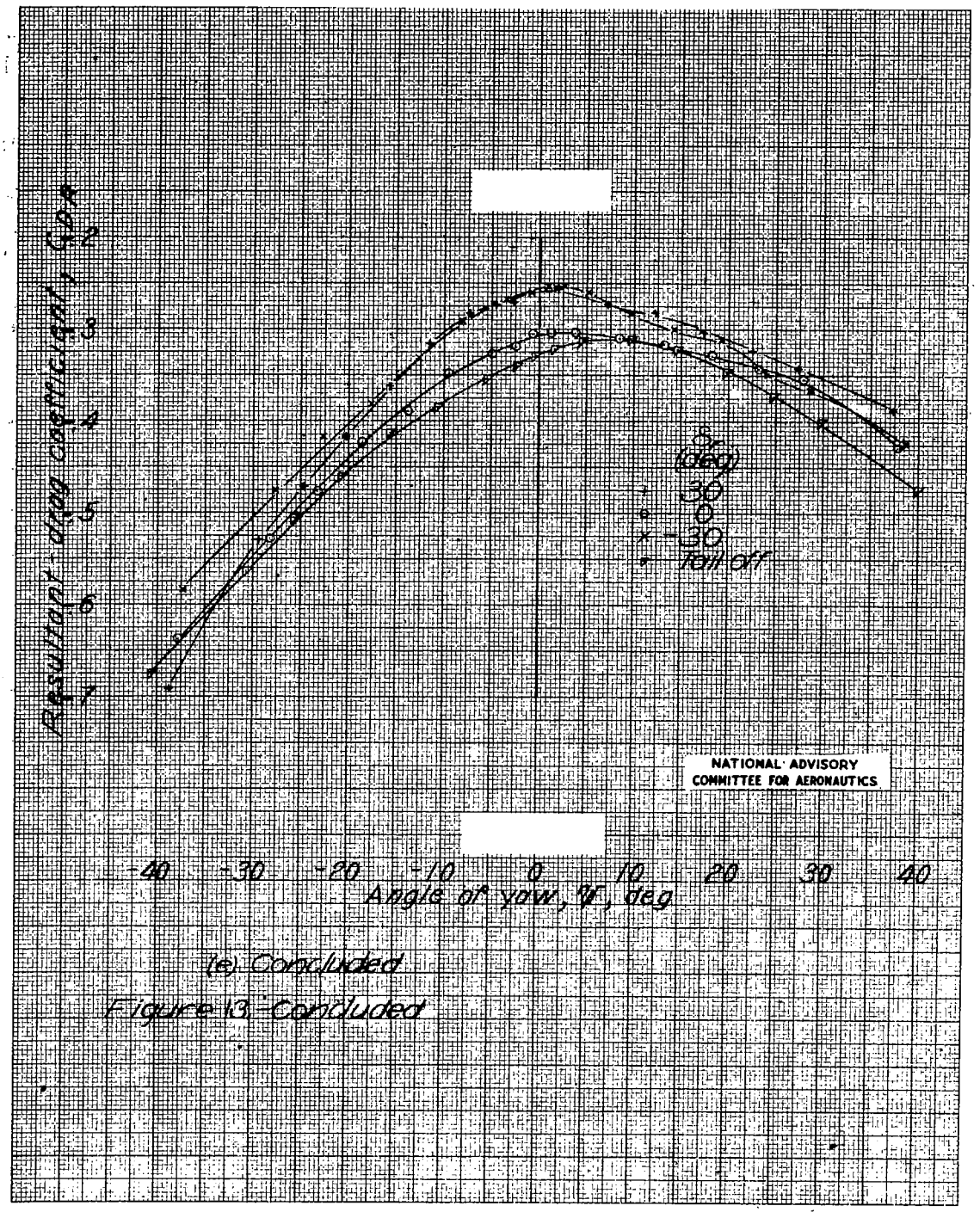

(e) Concluded

Figure 13.- Concluded

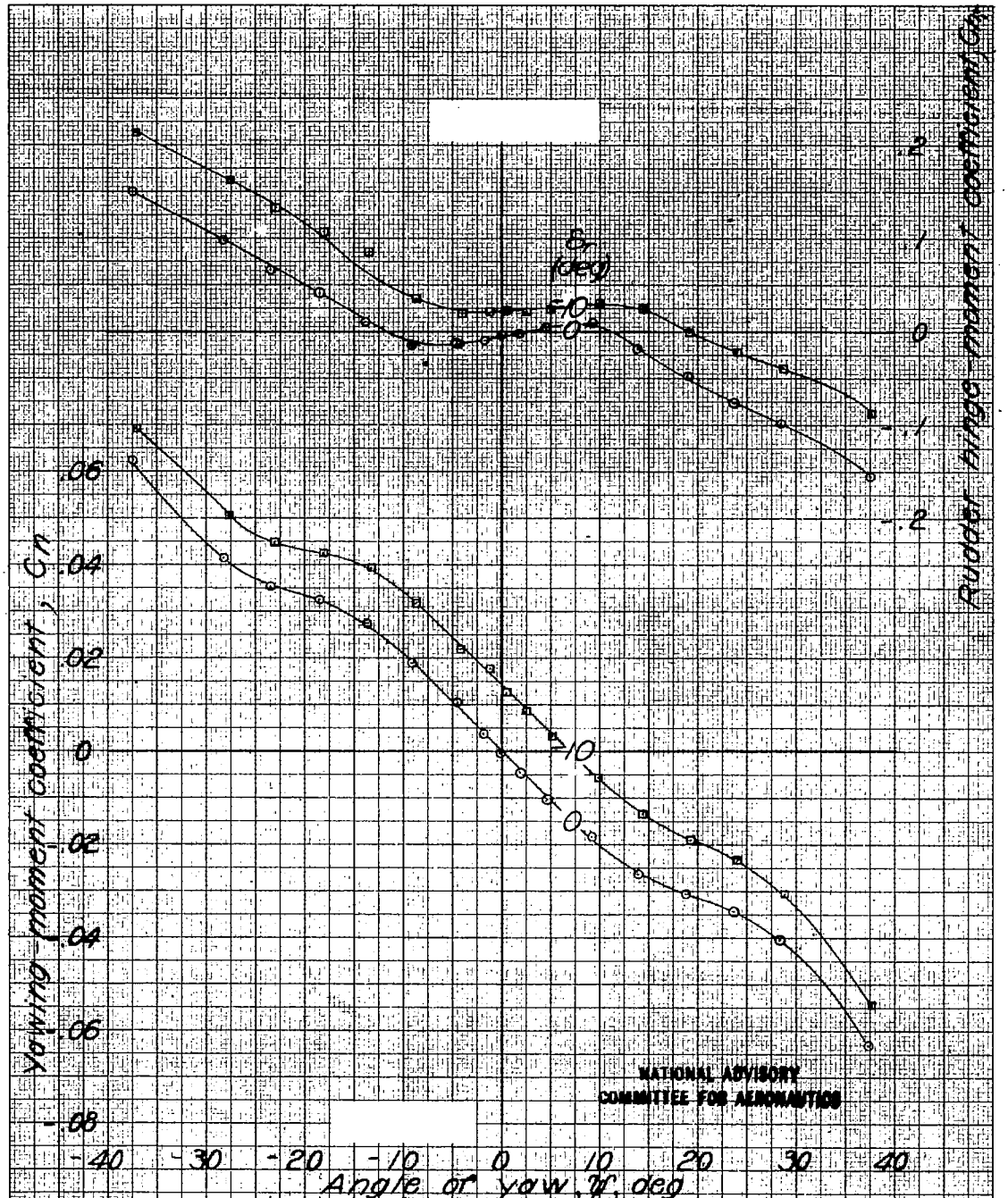

Figure 14.- Effect of rudder deflection on the aerodynamic characteristics in yaw of a 0.05 scale model of the XBTK-1 prototype airplane; windmilling; dive configuration. $\alpha = 1.0$, $C_L = 0.15$

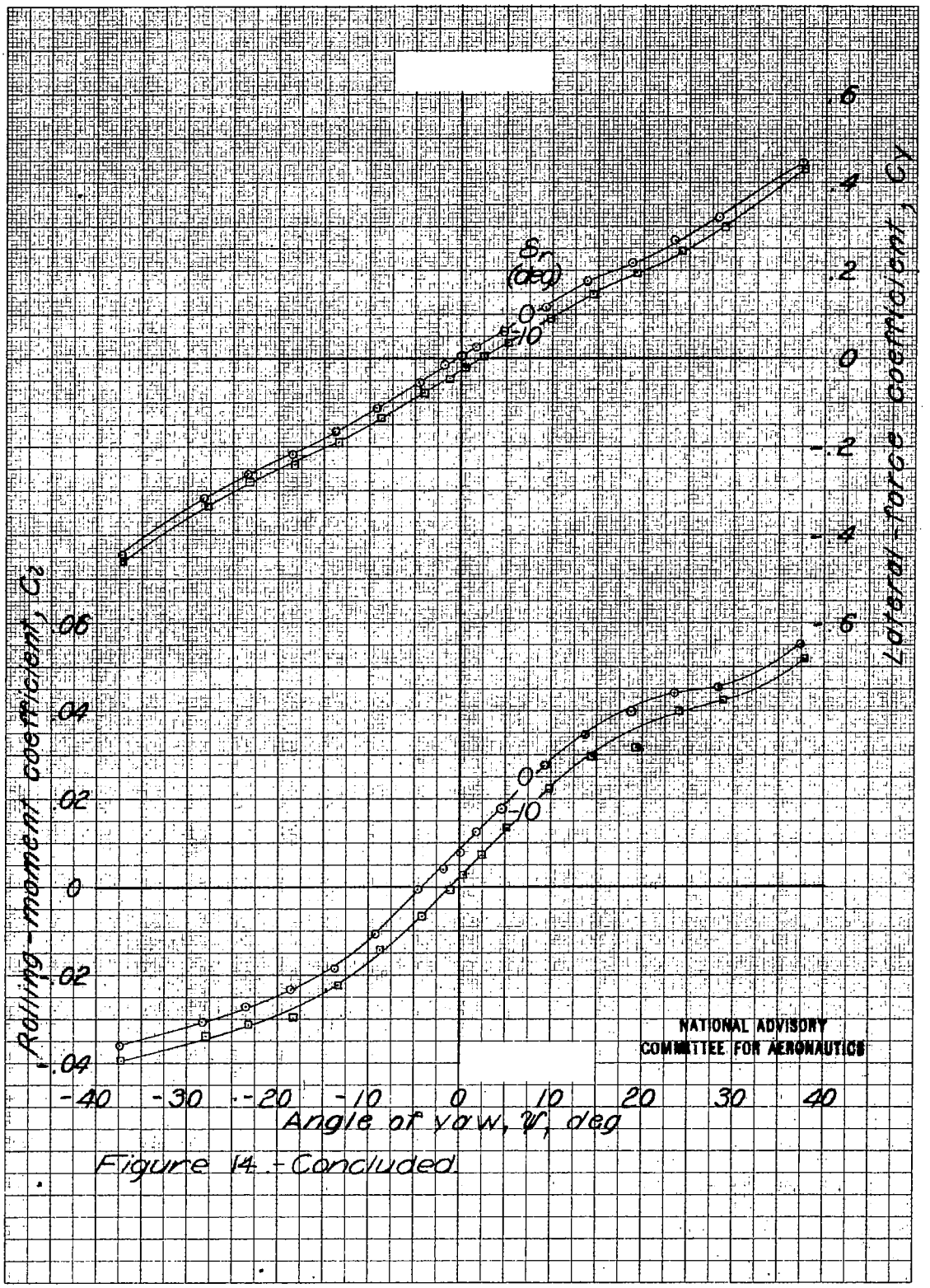

Figure 14.- Concluded.

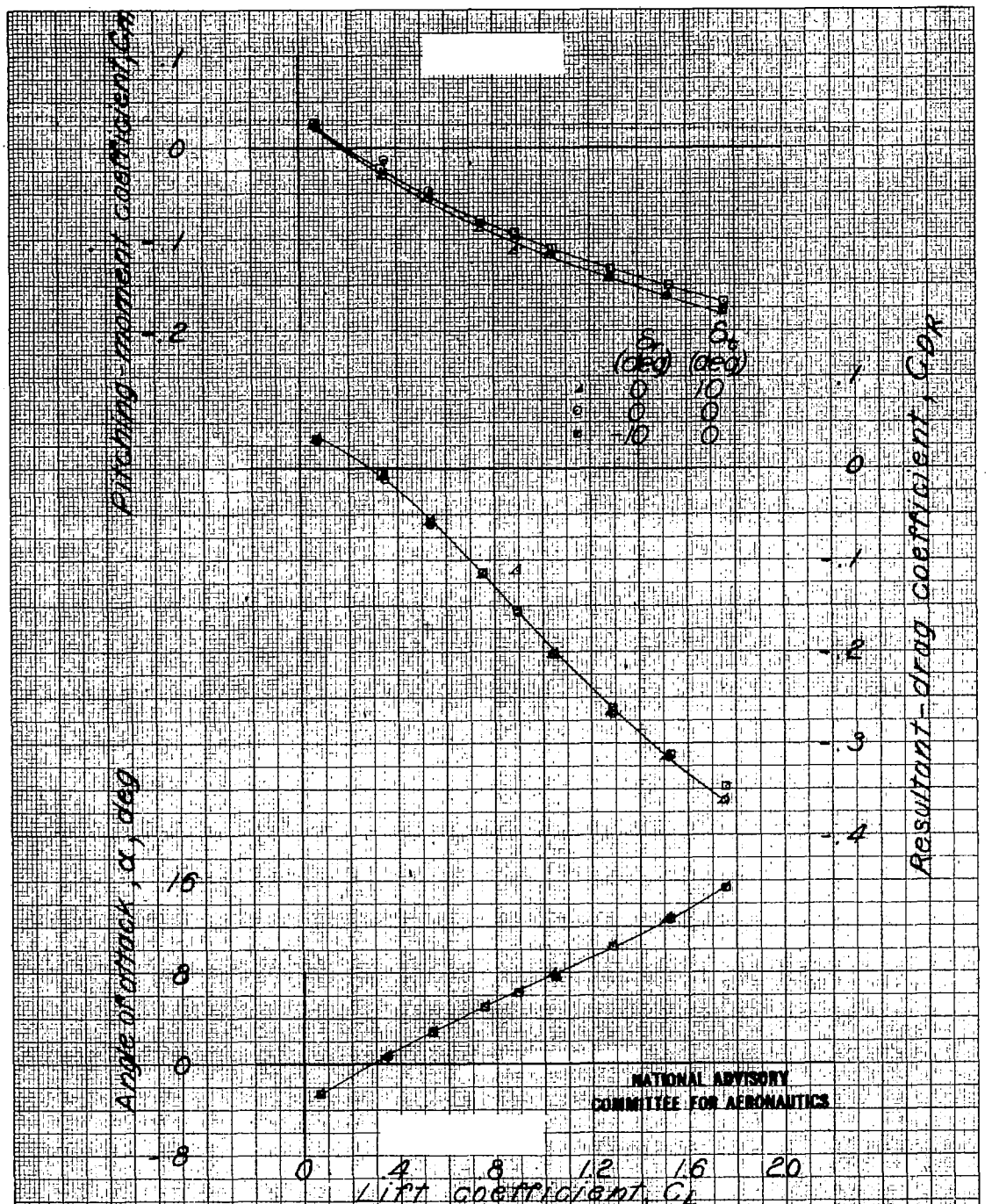

Figure 15.- Effect of rudder deflection on the aerodynamic characteristics in pitch of a 0.15-scale model of the XBTK-1 prototype airplane. Take-off power, cruising configuration. $\psi = 0°$

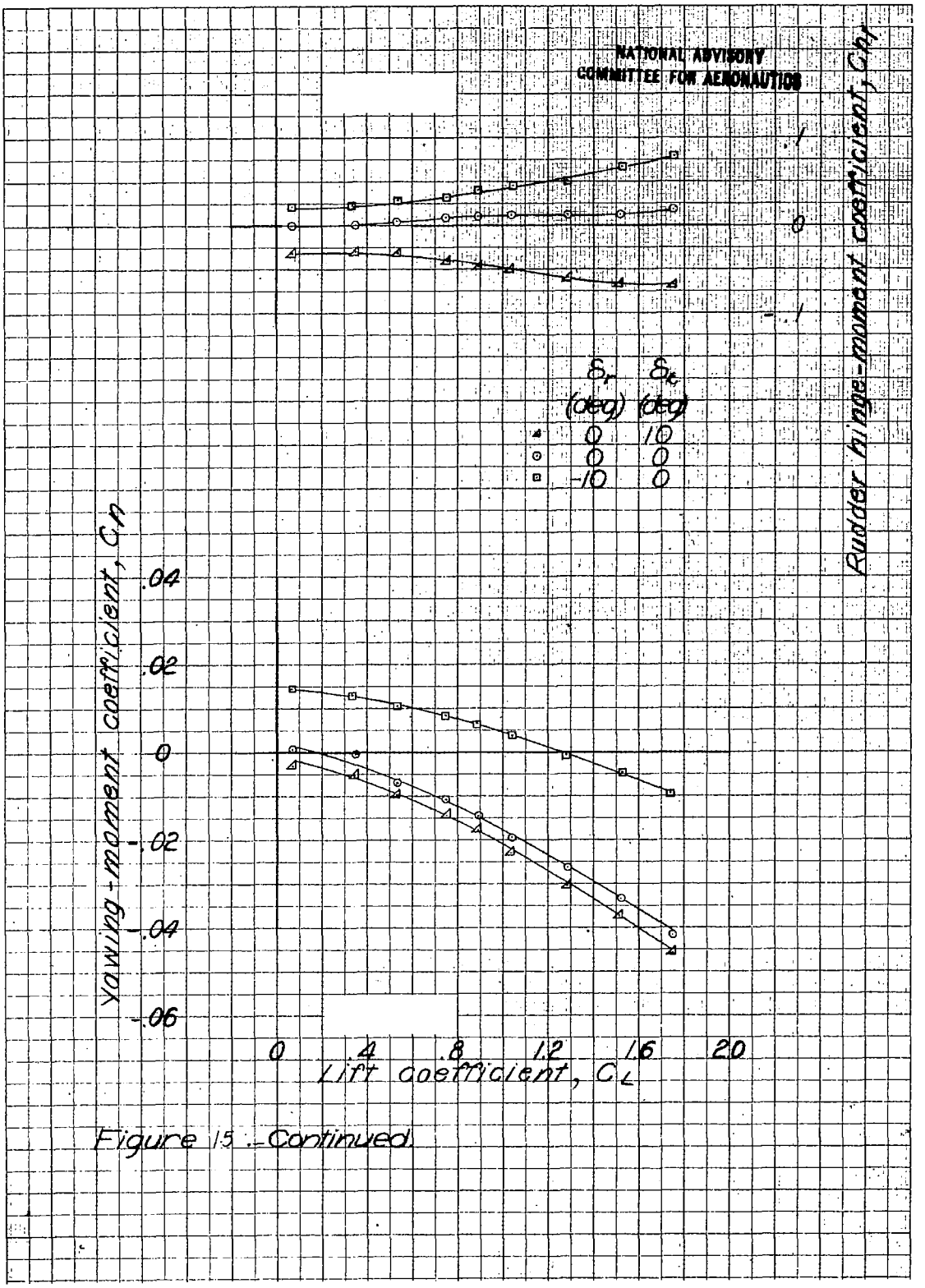

Figure 15.- Continued.

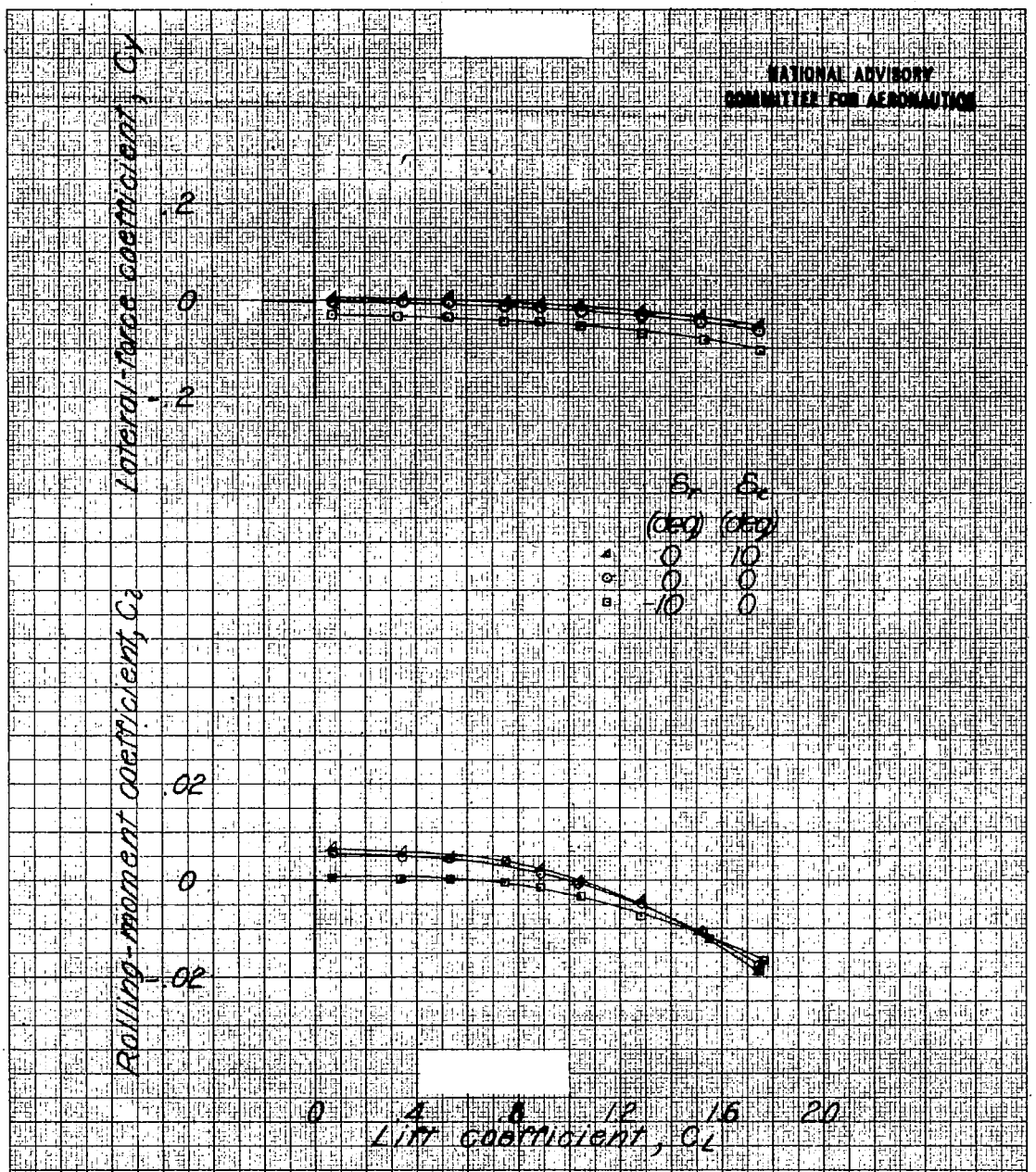

Figure 15 - Concluded.

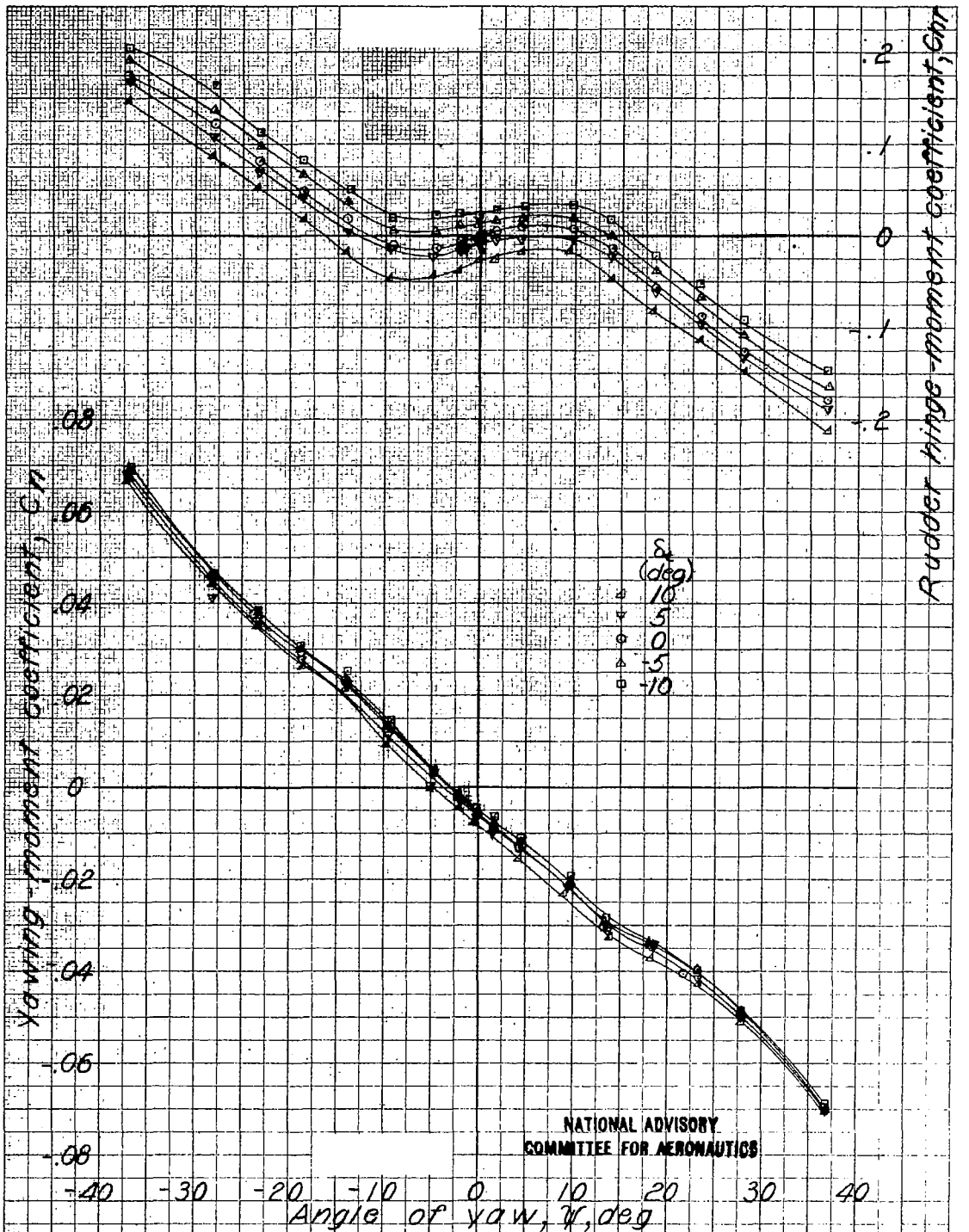

(a) Windmilling, cruising configuration, $\alpha = 11.0°$, $C_L = 1.14$

Figure 16.- Effect of rudder tab deflection on the aerodynamics characteristics in yaw of a 0.15 scale model of the XBTK-1 prototype airplane. $\delta_r = 0°$.

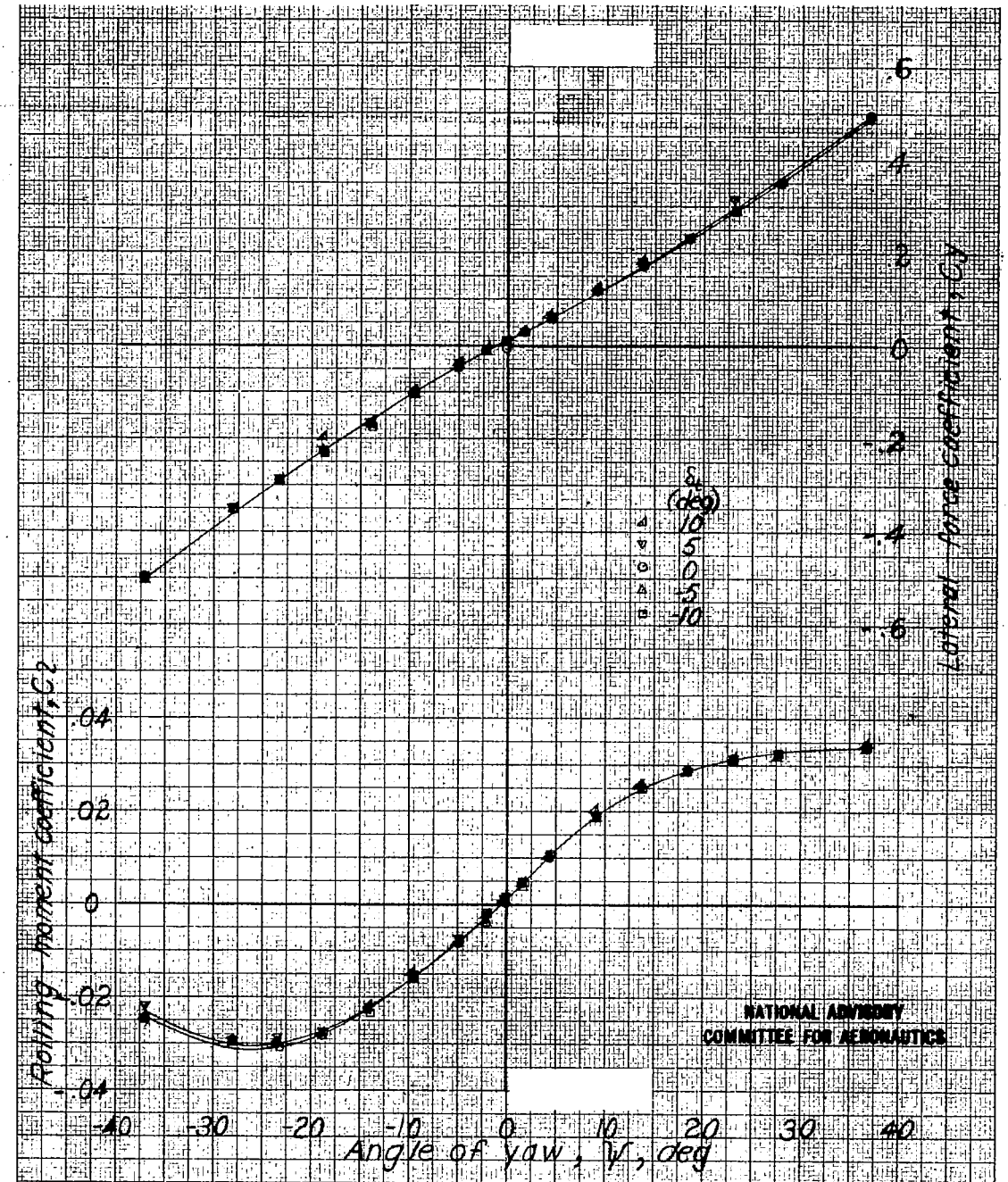

(a) Concluded

Figure 16 .- Continued

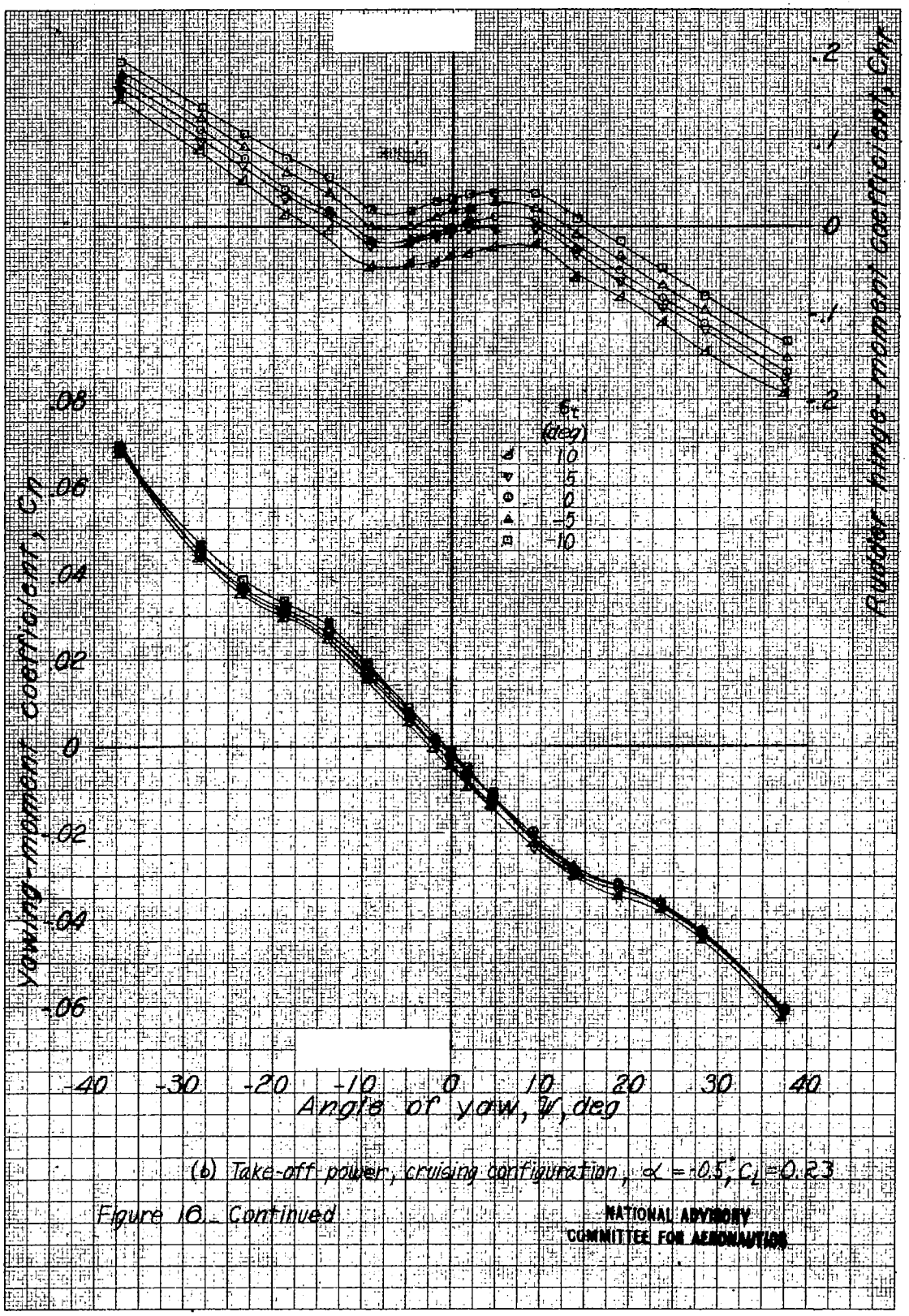

(b) Take-off power, cruising configuration, $\alpha = -0.5°$, $C_L = 0.23$

Figure 16.- Continued

NATIONAL ADVISORY COMMITTEE FOR AERONAUTICS

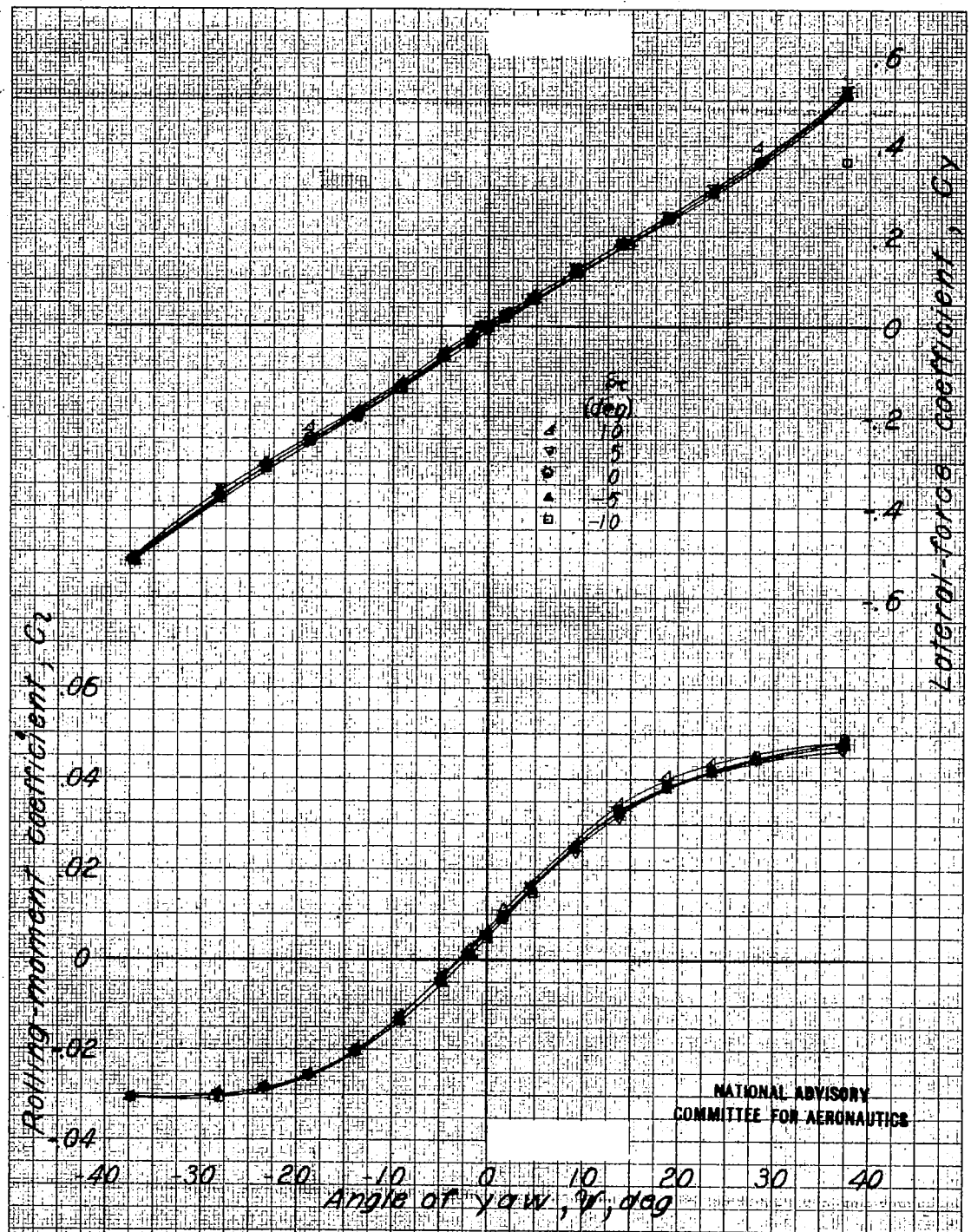

(b) Concluded

Figure 18.- Continued

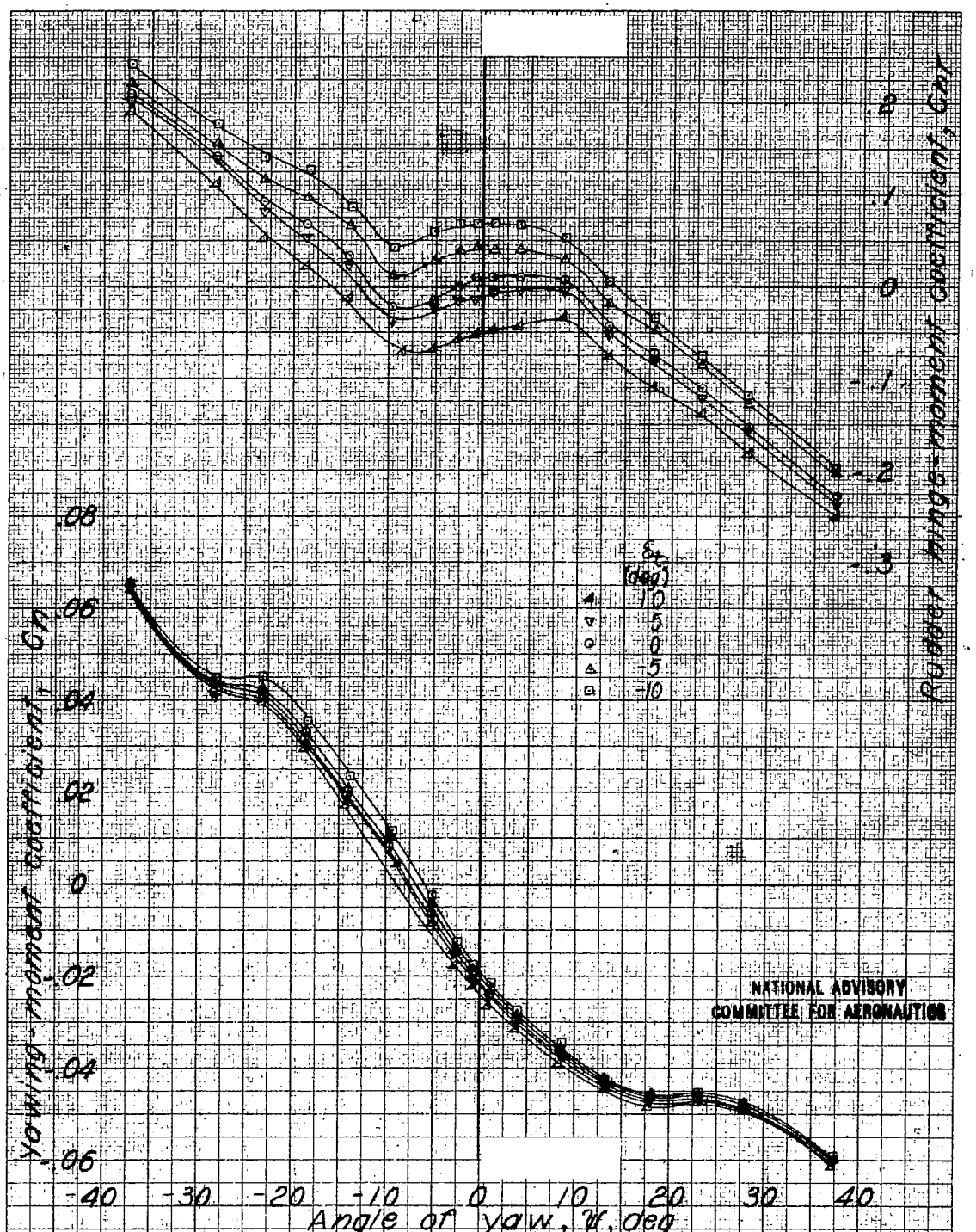

(c) Take-off power, cruising configuration, $\alpha = 7.7°$, $C_L = 2.03$

Figure 16.- Continued.

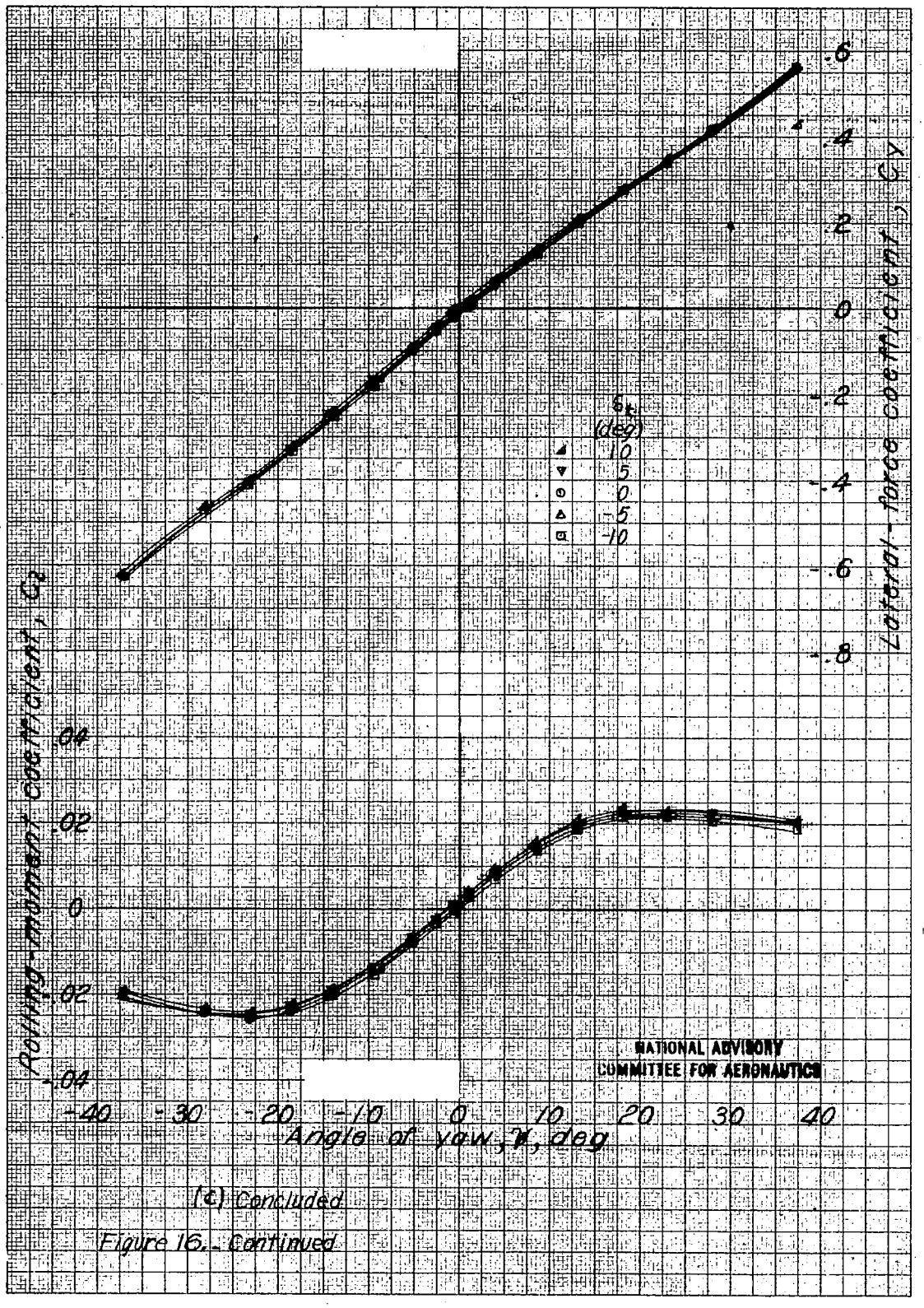

(c) Concluded

Figure 16.- Continued

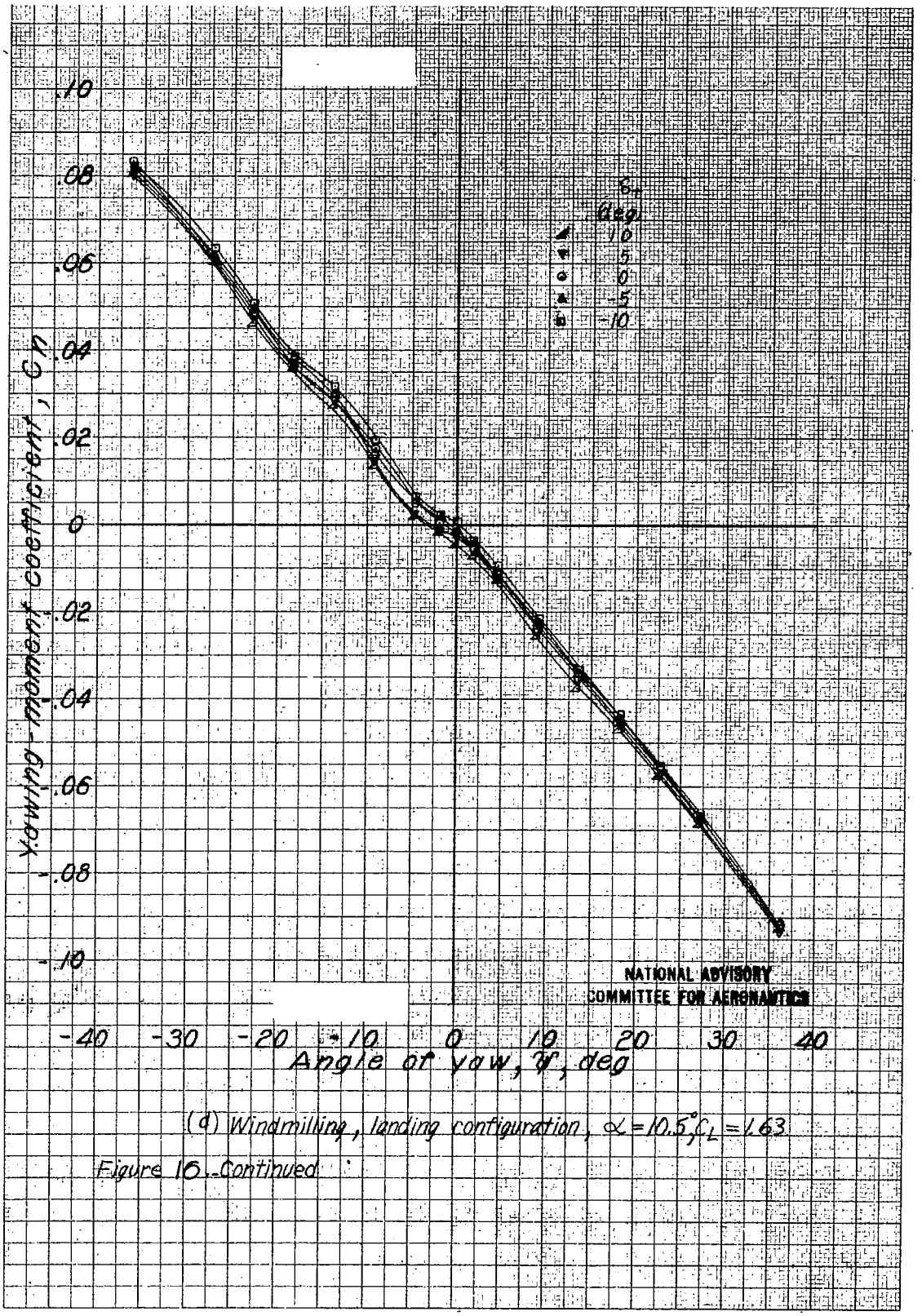

(d) Windmilling, landing configuration, $\alpha = 10.5^\circ$, $C_L = 1.63$

Figure 16.- Continued.

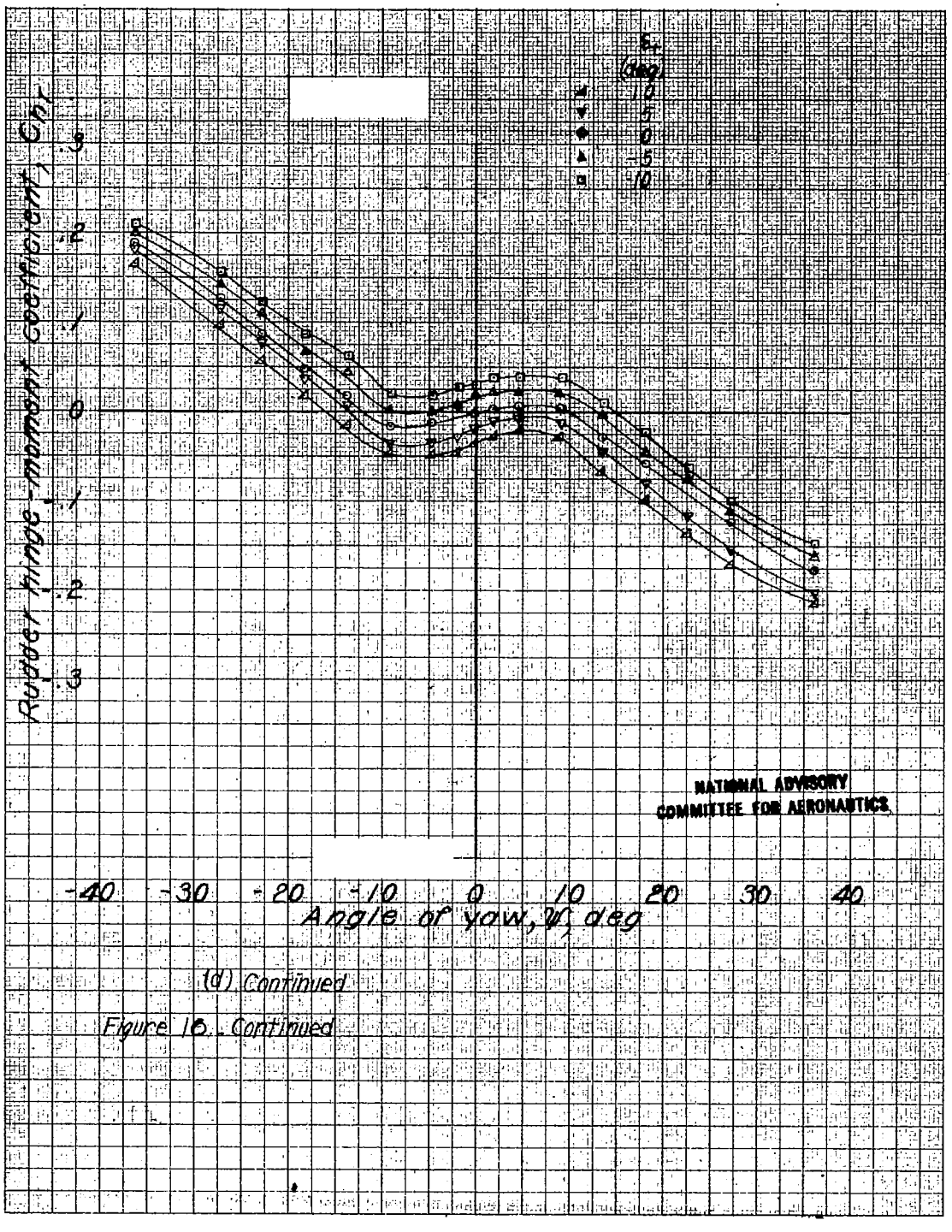

(d) Continued

Figure 16. Continued

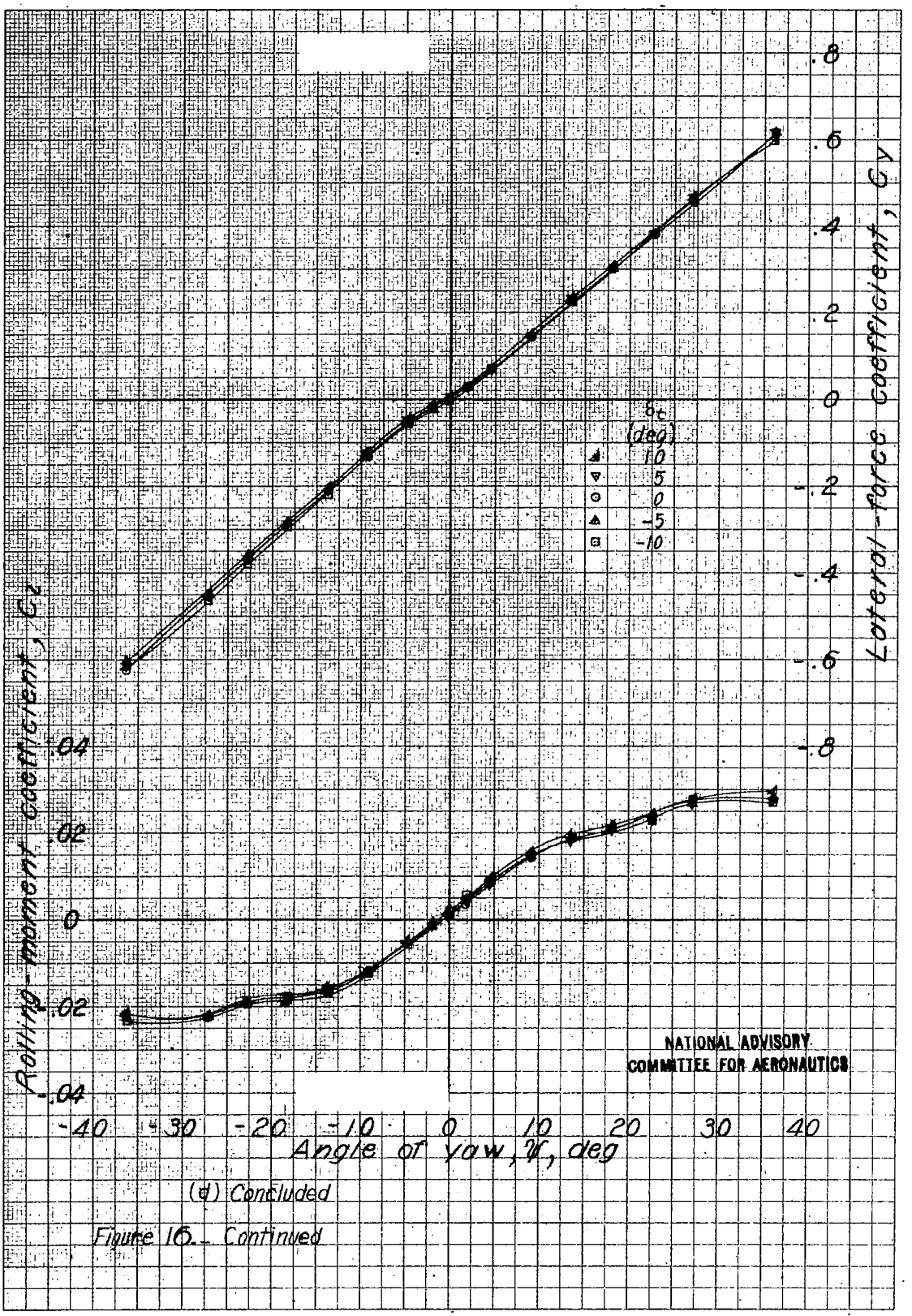

(d) Concluded

Figure 16.- Continued

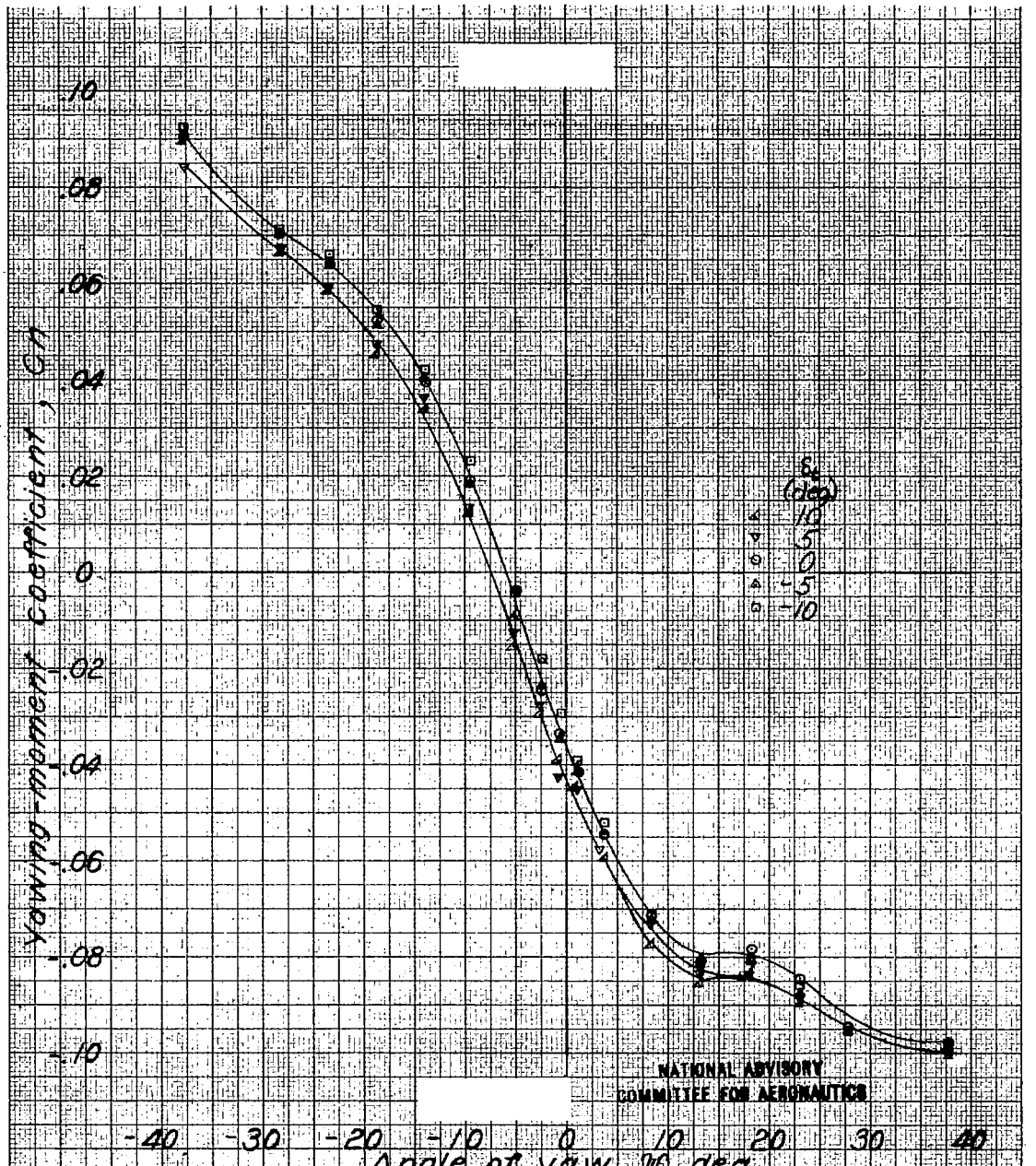

(e) Take-off power, landing configuration, $\alpha = 10.0$, $C_L = 2.06$

Figure 16.- continued

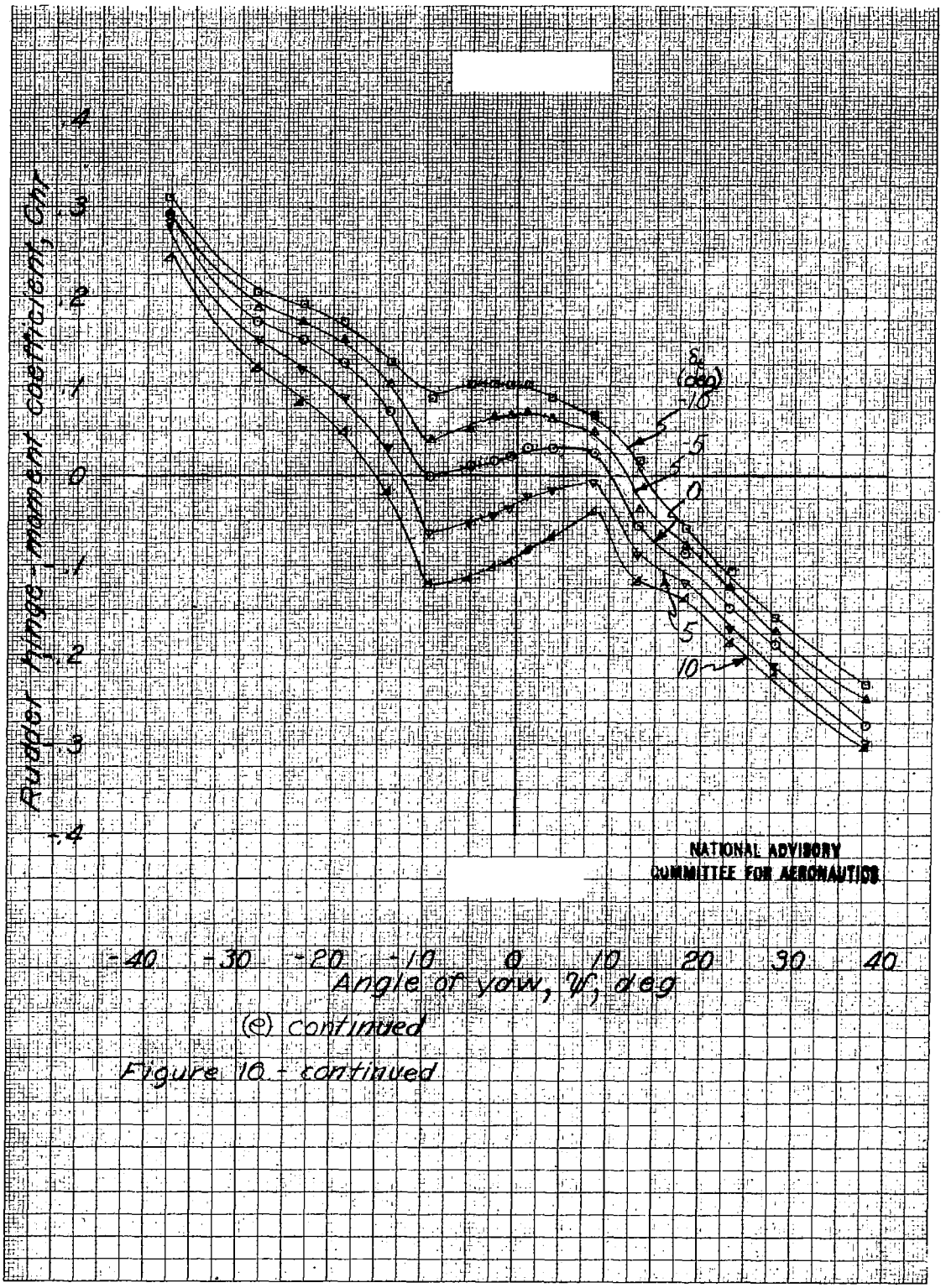

(e) continued

Figure 10 - continued

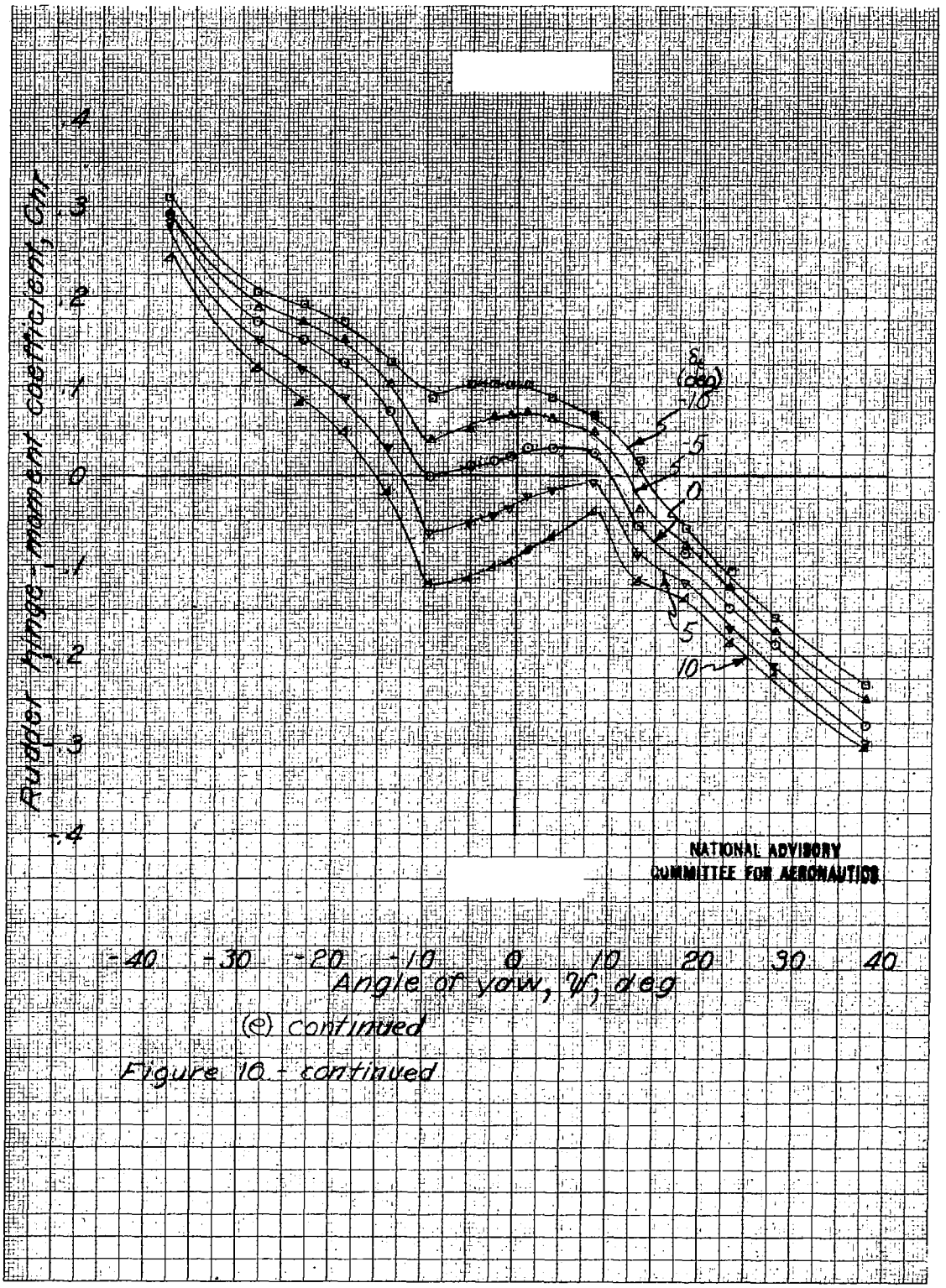

(e) continued

Figure 10 - continued

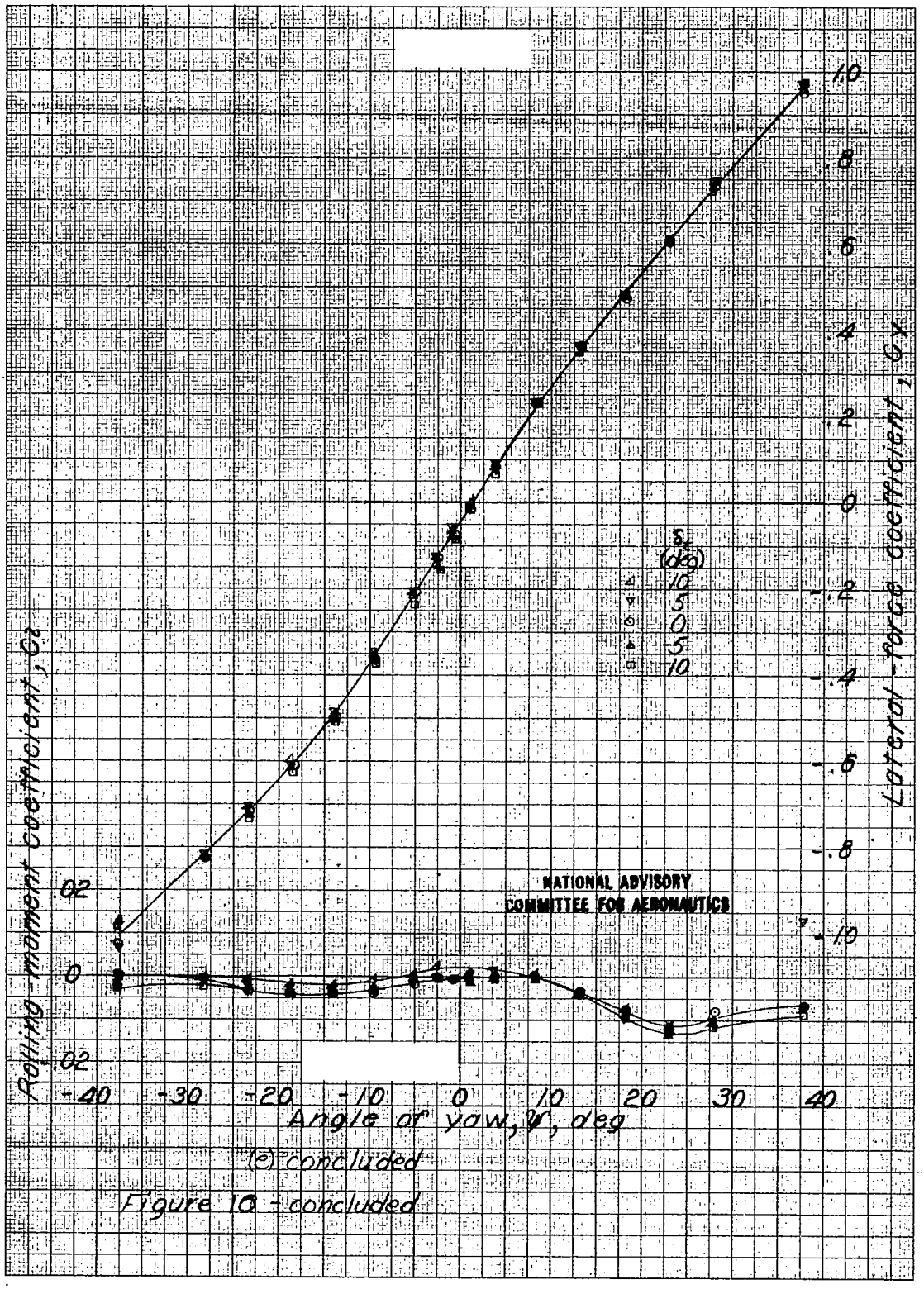

(e) concluded

Figure 10 - concluded

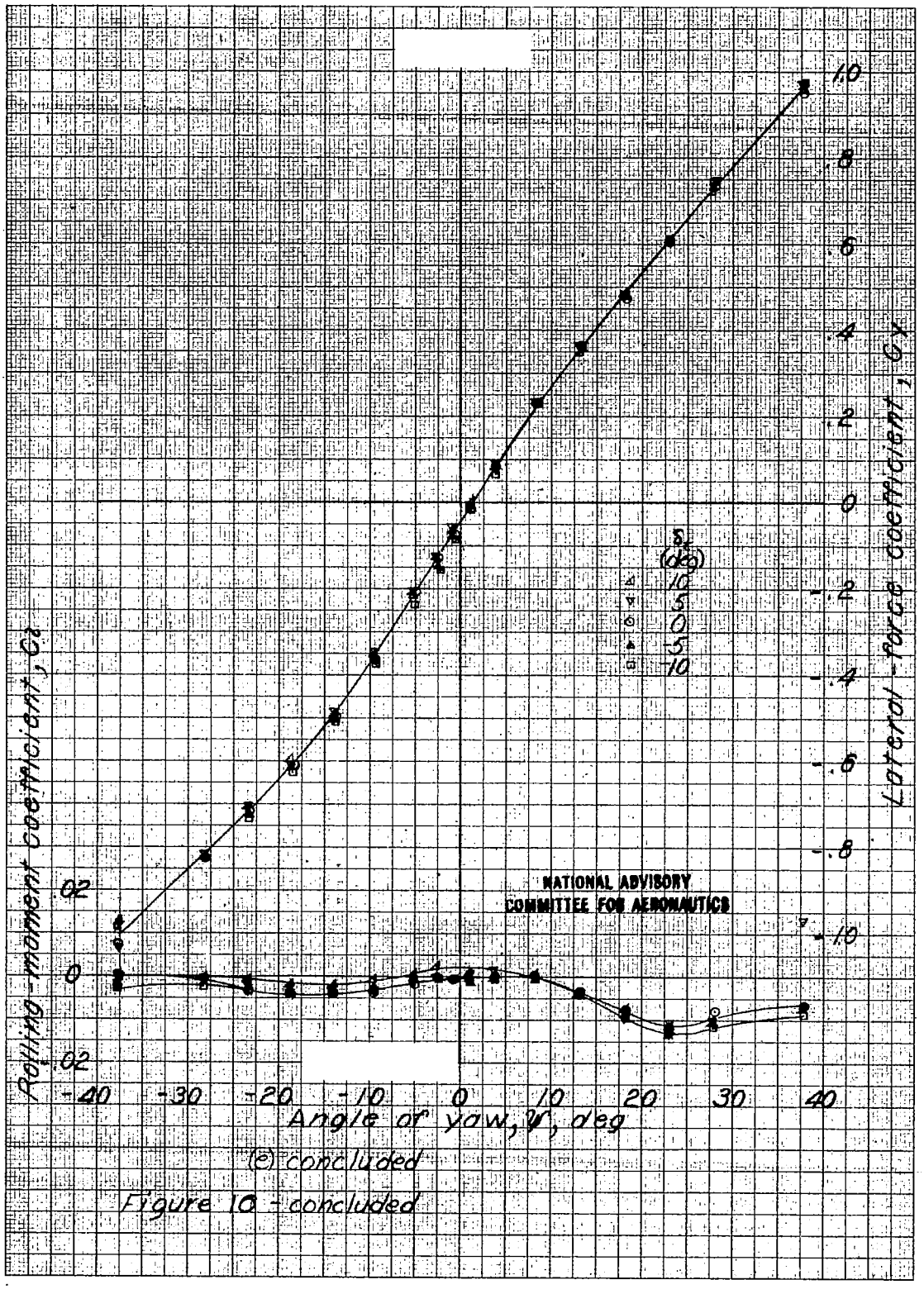

(e) concluded

Figure 10 - concluded

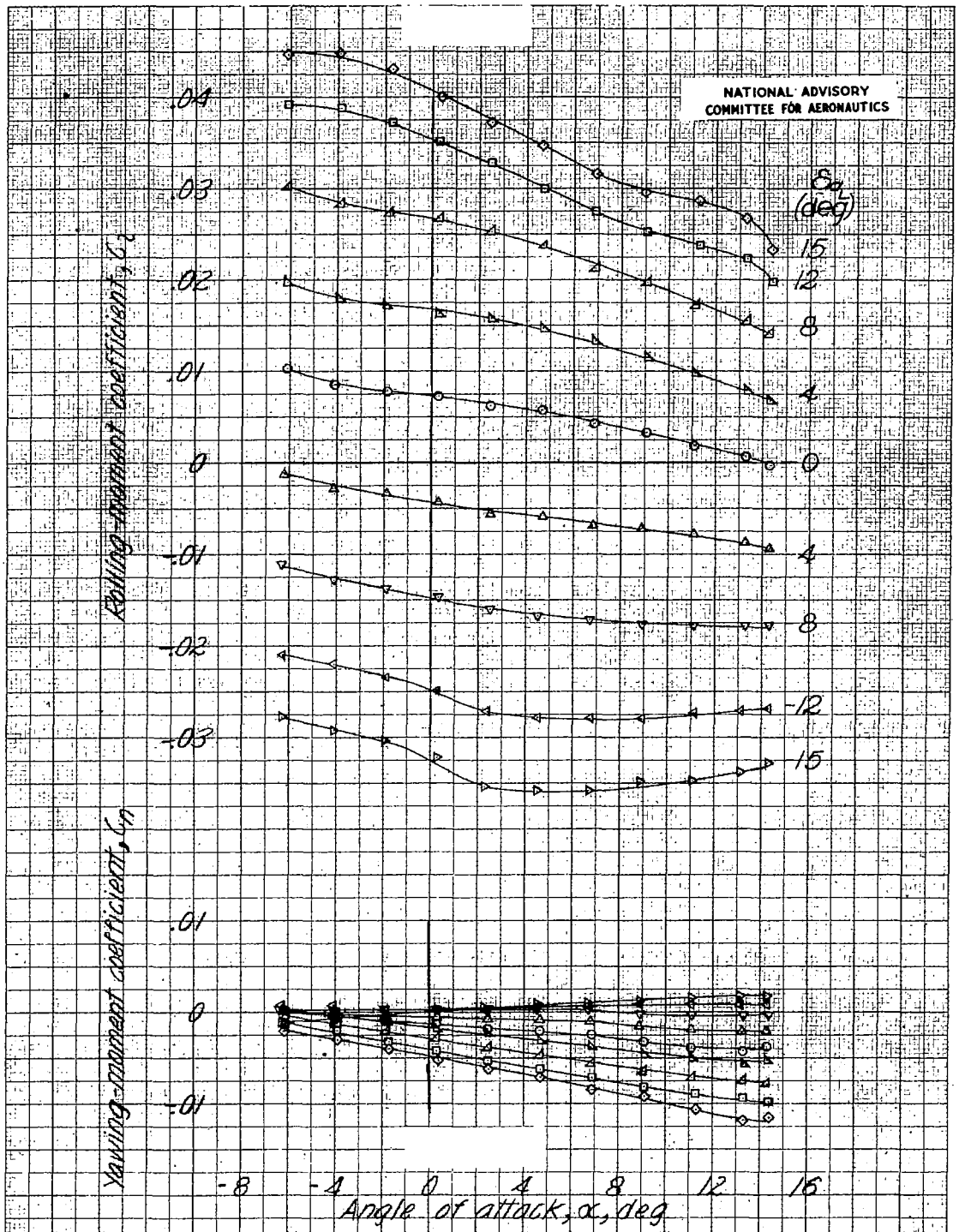

(a) Cruising configuration.

Figure 17.- Aileron characteristics of 0.15 scale model of the XBTK-1 airplane, propeller windmilling, tail off. $\delta_a = 0°$

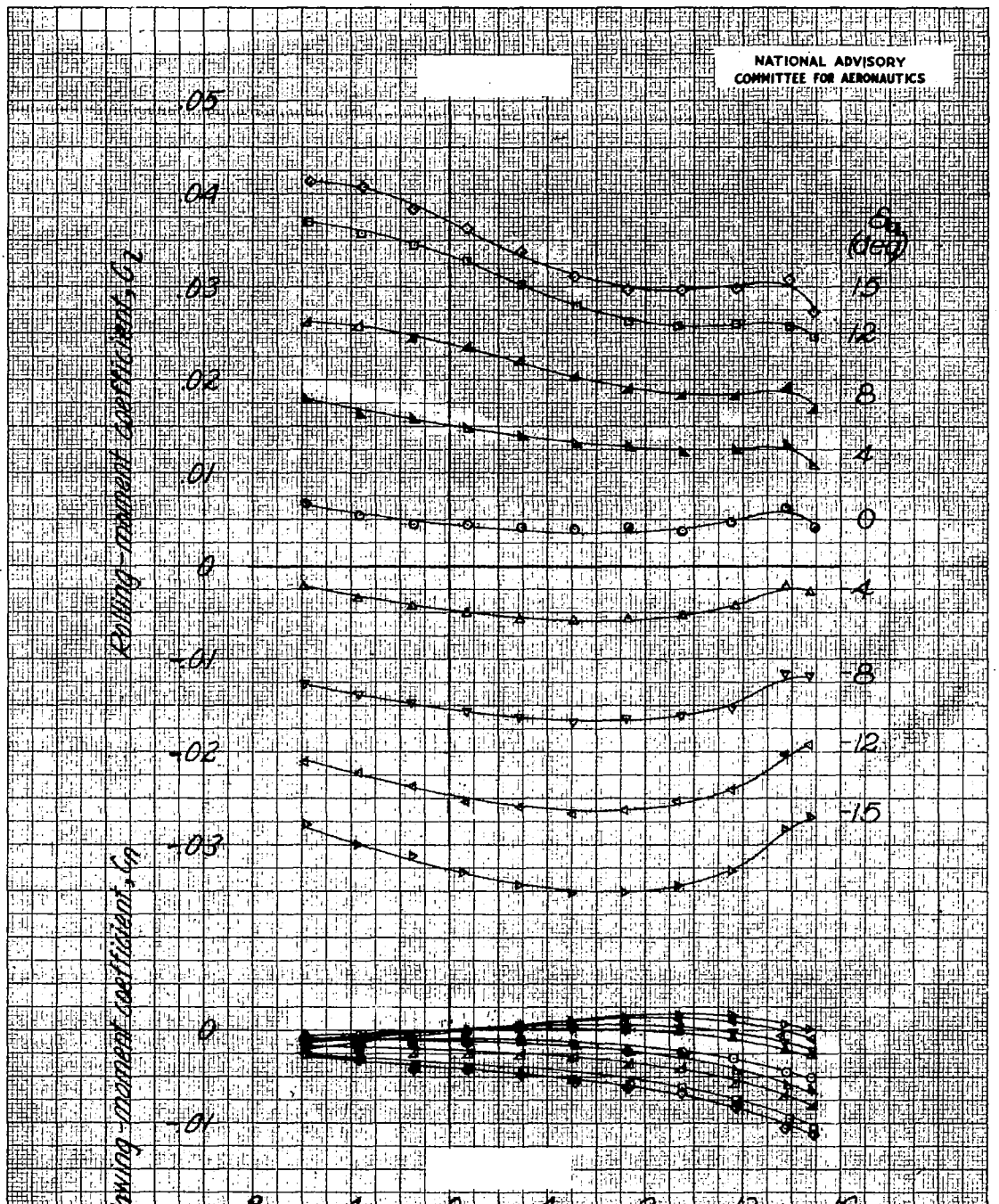

(b) Landing configuration.

Figure 17 Concluded.

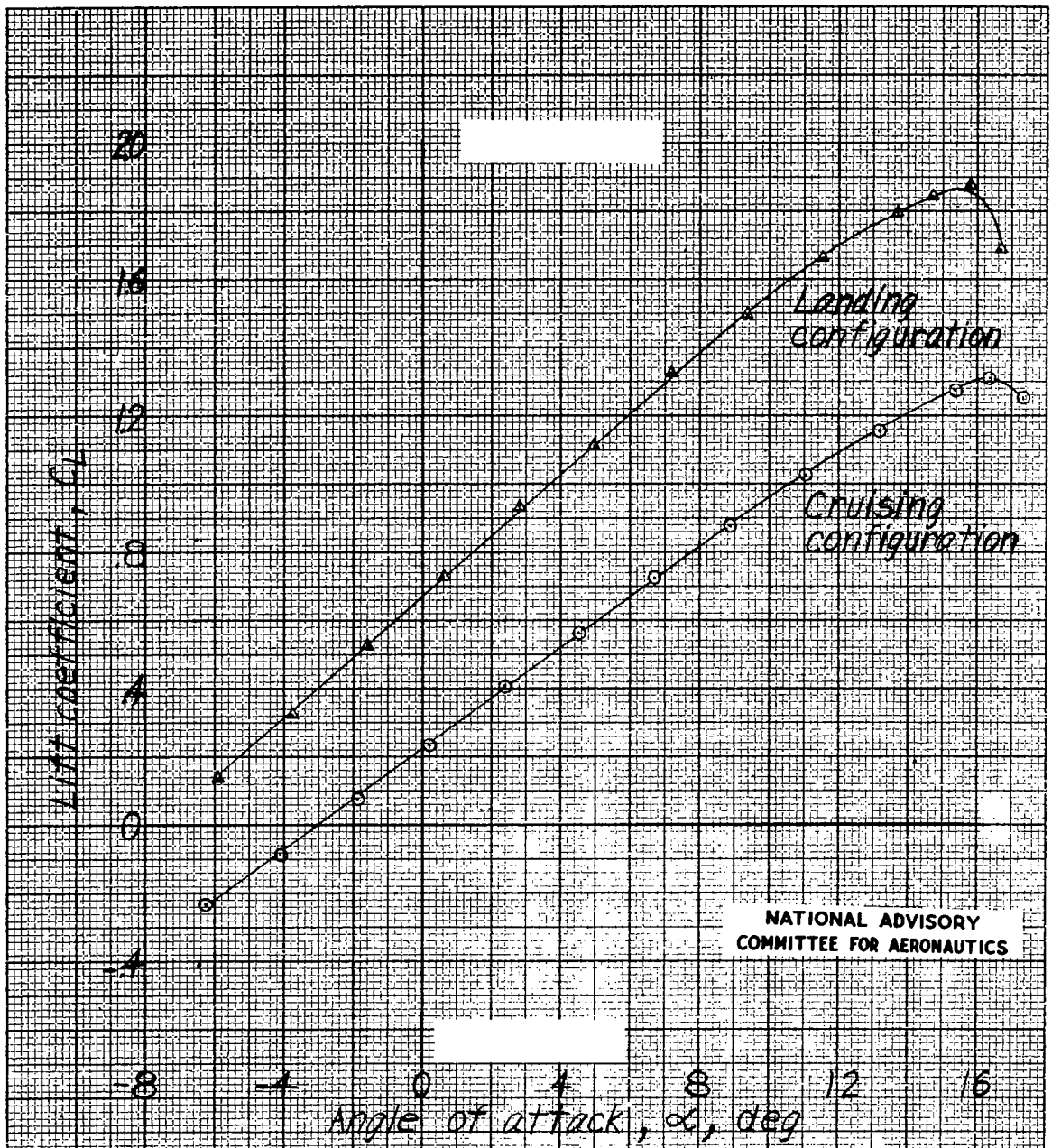

Figure 18.- Lift characteristics of 0.15 scale model of the XBTK-1 airplane, propeller windmilling, tail off. $\delta_{a_L} = \delta_{a_R} = 0$

LANGLEY RESEARCH CENTER
3 1176 01354 4375